

Molecular mechanisms of sonoporation in cancer therapy

Optimization of sonoporation parameters and investigations of intracellular signalling

Ragnhild Haugse

Thesis for the degree of Philosophiae Doctor (PhD)
University of Bergen, Norway
2020

UNIVERSITY OF BERGEN



Molecular mechanisms of sonoporation in cancer therapy

Optimization of sonoporation parameters and investigations of intracellular signalling

Ragnhild Hauge



Thesis for the degree of Philosophiae Doctor (PhD)
at the University of Bergen

Date of defense: 17.06.2020

© Copyright Ragnhild Hauge

The material in this publication is covered by the provisions of the Copyright Act.

Year: 2020

Title: Molecular mechanisms of sonoporation in cancer therapy

Name: Ragnhild Hauge

Print: Skipnes Kommunikasjon / University of Bergen

Scientific environment

This work was carried out between March 2016 and March 2020 with the Molecular Imaging in Cancer group headed by Professor Emmet McCormack in the Department of Clinical Science at the University of Bergen. This research group is a part of the Centre for Cancer Biomarkers (CCBIO) and the Centre for Pharmacy at the University of Bergen. My PhD project was supervised by Associate Professor Spiros Kotopoulos and Professor Emmet McCormack. The last half of the project was also supervised by Dr Anika Langer.

During my work for the PhD, I was employed at Sjukehusapoteka Vest. My PhD project was funded by Helse Vest. The project was further supported by the Norwegian Research Council, Kreftforeningen, the Norwegian Pharmacist Association (Nyegaards Legat) and a grant from the Norwegian Pharmaceutical Society.

During my work for this thesis, I was a member of the Norwegian PhD School of Pharmacy (NFIF), Norwegian PhD Network on Nanotechnology for Microsystems and the Norwegian Research School in Medical Imaging (MedIm).

Acknowledgements

First, I thank Spiros and Emmet, who were my supervisors even before I began my PhD project. It has been a long journey, which would not have happened without you and your support, enthusiasm, knowledge and expertise in this field. I am also grateful that you believed in me, and for the time and energy spent in pushing and helping me write the application for PhD funding; I hope to have gained at least a small piece of your excellent grant-writing skills. I also want to thank Anika, who came into the project at the right time (for me but perhaps not for you). Thank you for your support and for putting up with a very stressed version of me.

I also want to thank all my co-authors. In particular, I want to thank Bjørn Tore Gjertsen, who initially introduced me to this project and who came up with several of the ideas on which this thesis is based. Furthermore, you are an inspiration in clinical and translational research, and our discussions have given me valuable perspectives on my role as a pharmacist both in research and in the hospital. I also thank all the friendly past and present members of the Gjertsen group, particularly Stein-Erik and Jørn for patiently answering and discussing my seemingly endless questions about flow cytometry. For the same reasons, my gratitude also goes to Brith at the Core facility for flow cytometry. I also thank Odd Helge Gilja and the Medviz research consortium for the initiation of sonoporation in Bergen. The results of the first clinical trial on sonoporation in the world continue to motivate me to perform research in this field, and it is a privilege to belong to the research environment responsible for it.

I want to thank the past and present members of the McCormack group, particularly the SonoCURE team for both our scientific collaboration and our (most of the time) happy lab-life in “the seventh-floor lab”: Elisa, Tormod, Gorka, Silje Maria, Christina and Zeke in addition to Spiros, Emmet and Anika. I also want to thank the rest of the McCormack group, particularly Zina: we would all have been in a mess without you. Finally, I extend my gratitude to my fellow PhD students: Katrin, Tara, Elvira, Sam, Sabha and Calum, and to Pascal, Ida, May, Mireia, Mihaela, Constance and Geir.

I also thank the other PhD students, colleagues at the Centre for Pharmacy and all the nice people on the ninth floor in the laboratory building for making every day at work enjoyable. In particular, I thank the Herfindal group for being great company at lunch and in the lab and Lars Herfindal for his scientific insights and advice.

I thank my employer, Sjukehusapoteka Vest (SAV), for supporting me. The project started as a part-time research position funded by SAV. Neither this thesis nor the funding for it would have been a reality without this position or the support when I applied for Helse Vest funding. I am also very grateful for the support by and patience of my leaders, Christer, Roy and Aleksandra, and my friends and colleagues at the Hospital Pharmacy in Bergen. You were invaluable in supporting me through my endeavour to complete my PhD.

I am also very grateful for the financial support I have received to be able to do my research, in particular I thank Helse Vest, The Norwegian Pharmacist Association, the Norwegian Pharmaceutical Society and the Research Schools I have been a member of.

Finally, a huge thanks goes to friends and family. Thank you all for still being my friends, even when I spent all my time in the lab, and we did not meet for weeks and months. Thanks to my parents, Sigrid and Hans, for everything: from a good childhood to always being there when I need to go home to Haugse and take a break from work, science or Bergen in general. You have always encouraged me to seek knowledge, learn new things, make my own choices and think critically: all are important in becoming a scientist.

Ragnhild

Bergen, March 2020

Contents

Scientific environment.....	1
Acknowledgements.....	3
Contents.....	5
Abbreviations	7
Abstract	9
List of publications.....	11
1. Introduction.....	12
1.1 Cancer.....	12
1.1.1 Background.....	12
1.1.2 The tumour microenvironment	13
1.1.3 Aberrant intracellular signalling in cancer.....	14
1.1.4 Signalling from the tumour microenvironment.....	18
1.1.5 Current cancer therapy.....	18
1.2 Pancreatic ductal adenocarcinoma (PDAC).....	19
1.3 Drug delivery in cancer.....	20
1.3.1 Barriers to drug delivery.....	20
1.3.2 Drug delivery strategies in cancer.....	20
1.4 Sonoporation	21
1.4.1 Definition of sonoporation.....	21
1.4.2 Ultrasound (US)	22
1.4.3 Cavitation	24
1.4.4 Ultrasound used in sonoporation.....	25
1.4.5 Microbubbles (MB)	25
1.4.6 “Next-generation microbubbles”.....	27
1.5 Therapeutic uses of sonoporation.....	28
1.5.1 Enhancement of cancer therapy.....	28
1.5.2 Other therapeutic uses of sonoporation.....	31
1.6 Bioeffects of sonoporation	32
1.6.1 Cellular uptake: pore formation, endocytosis and membrane repair.....	33
1.6.2 Intracellular signalling responses of ultrasound ± microbubbles	35
1.6.3 Intracellular signalling responses of ultrasound.....	35

2. Aims of the study	37
3. Methodological considerations	38
3.1 Ultrasound treatment of cells	38
3.2 Microbubbles (MB)	40
3.3 Cell types and cell culture	42
3.3.1 Suspension cell types.....	42
3.3.2 Adherent cell types.....	42
3.3.3 Considerations related to cell culture.....	43
3.4 Assessment of cell viability	44
3.5 Flow cytometry	45
3.5.1 Flow cytometric measurements of cellular uptake.....	46
3.5.2 Analysis of intracellular phosphorylation events.....	47
3.5.3 Antibody selection.....	49
3.5.4 Flow cytometry controls and compensation.....	49
3.6 <i>In vivo</i> sonoporation in combination with paclitaxel	51
3.7 Statistical methods	51
Summary of publications	52
4. Discussion	55
4.1 Factors influencing sonoporation	56
4.1.1 Ultrasound parameters	56
4.1.2 Microbubbles, microbubble formulation and dose.....	57
4.1.3 Cell types, and properties of the cells	58
4.2 Intracellular signal transduction	59
4.2.1 MAPK – sonoporation membrane repair?.....	60
4.2.2 Translational control through Ribosomal protein S6, 4E-BP1 and eIF2 α	62
4.2.3 Therapeutic benefit from intracellular cell stress?.....	63
4.3 Suitability of methods and limitations of the studies	64
4.3.1 In vitro cell culture and ultrasound exposure	64
4.3.2 Uptake of cell impermeable dye	65
4.3.3 Phosphoflow cytometry.....	66
4.3.4 Preclinical study.....	67
5. Concluding remarks	68
6. Future perspectives	69
7. References	70

Abbreviations

AMPK – AMP-activated protein kinase	PDAC – Pancreatic ductal adenocarcinoma
BBB – Blood brain barrier	PEG – Polyethylene glycol
CAF – Cancer-associated fibroblast	PI3K – Phosphoinositide 3-kinase
CNS – Central nervous system	PKA – Protein kinase A
DC – Duty Cycle	PMA – Phorbol 12-myristate 13-acetate
ECM – Extracellular matrix	PMT – Photomultiplier tube
EGFR – Epidermal growth factor receptor	ROCK – Rho-associated protein kinase
eIF2 α – Eukaryotic initiation factor 2 alpha	SDT – Sonodynamic Therapy
EPR effect – Enhanced Permeability and Retention effect	SmPC – Summary of Product Characteristics
ER – Endoplasmatic reticulum	STAT – Signal transducer and activator of transcription
FAK – Focal adhesion kinase	TI – Thermal index
FDA – United States Food and Drug Administration	US – Ultrasound
HIFU – High intensity focused ultrasound	
JAK – Janus activated kinase	
KRAS – Kirsten rat sarcoma oncogene	
MAPK – Mitogen-activated protein kinase	
MB – Microbubbles	
MI – Mechanical Index	
MLC – Myosin light chain	
mTOR – Mammalian target of rapamycin	
mTORC1 – Mammalian target of rapamycin complex 1	
mTORC2 – Mammalian target of rapamycin complex 2	
NF-kB – Nuclear factor kappa B	
PBMC – Peripheral blood mononuclear cells	

"Du skal ikkje tru, du skal veta!"
(What my father used to tell me as a child)

Abstract

Background: Sonoporation, which is treatment with ultrasound (US) and microbubbles (MB), has shown great potential for enhancing the therapeutic efficacy of chemotherapy in cancer therapy. However, there is still very little consensus regarding the mechanism or optimal experimental and therapeutic parameters. The original assumption was that pore formation in the cell membrane was responsible for the increased uptake of drugs, but it is currently understood that the mechanisms are far more complex. The field combines US physics, MB formulation and physics, (cell) biology, pharmacology, pharmacokinetics and the biodistribution of both drugs and MBs. Hence, there is an almost endless range of experimental parameters and potential bioeffects. The current literature includes a plethora of experimental setups and parameters, which complicates the clinical translation of sonoporation.

Aims and methodology: In this thesis, the effects of low-intensity US and MB parameters were investigated *in vitro* using custom-made ultrasound chambers and correlating commonly used measures as uptakes of impermeable dye (*i.e.* flow cytometry) and viability to detect intracellular signalling responses to sonoporation in different cell types. Intracellular signalling responses to sonoporation are largely unknown, and their influence on key proteins in important signalling pathways have been elucidated using phosphoflow cytometry. To gain the understanding and translatability of US + MB parameters, three commercially available MB formulations were characterized, and important parameters, such as dose and formulation, were investigated *in vitro* and the *in vivo* enhancement of chemotherapy in a mural model of pancreatic ductal adenocarcinoma (PDAC).

Results and conclusions: Effective sonoporation was achieved using commercial microbubbles and low-intensity US in the diagnostic range, both *in vitro* and *in vivo*. In the low-intensity US regimen, effective sonoporation required MBs, and the efficacy increased as US intensity and MB concentrations increased. The choice of optimal MBs depended on the US parameters used, and must be carefully chosen based on the therapeutic context. The findings *in vivo* were correlated to those in the *in vitro* experiments and to simulations on MB behaviour. Sonoporation induced the immediate,

transient activation of intracellular signalling (MAPK-kinases; p38, ERK1/2, CREB, STAT3, Akt) as well as changes in the phosphorylation status of the proteins involved in protein translation (i.e. ribosomal protein S6, 4E-BP1 and eIF2 α).

The intracellular signalling response resembles cellular recovery after pore formation by electroporation and pore-forming toxins. Based on this observation, we hypothesize that sonoporation induces a cellular stress response that is related to the membrane repair and restoration of cellular homeostasis, and it may be exploited therapeutically. Varying responses in different cell types better represent the variability within a tumour, and they indicate that the effects on the tumour microenvironment may be important for sonoporation efficacy. In the present work, cellular stress was induced using low-intensity US below the intensity limit approved for diagnostic imaging, and healthy blood peripheral cells were minimally affected.

List of publications

Intracellular signalling in Key Pathways Is Induced by Treatment with Ultrasound and Microbubbles in a Leukemia Cell Line, but not in Healthy Peripheral Blood Mononuclear Cells *Pharmaceutics* 2019, 11(7), 319; <https://doi.org/10.3390/pharmaceutics11070319>

Haugse R, Langer A, Gullaksen S-E, Sundøy SM, Gjertsen BT, Kotopoulis S, McCormack E

Low-intensity sonoporation induced intracellular signalling of pancreatic cancer cells, fibroblasts and endothelial cells (*Manuscript*)

Haugse R, Langer A, Murvold ET, Costea DE, Gjertsen BT, Gilja OH, Kotopoulis S and McCormack E

SonoVue® vs Sonazoid™ vs Optison™:

Which bubble is best for low intensity sonoporation of pancreatic ductal adenocarcinoma? (*Manuscript*)

Kotopoulis S, Popa M, Safont MM, Murvold ET, Haugse R, Langer A, Dimcevski G, Lam C, Bjånes TK, Gilja OH, McCormack E

1. Introduction

Cancer is a leading cause of morbidity and mortality, resulting in 9.6 million deaths worldwide (2018) [1]. The incidence of cancer has been expected to increase from 17 million in 2018 to 26 million in 2040 [2]. Despite the advances in targeted therapies and immune therapy, a major treatment option is still chemotherapy. However, chemotherapy is known to have severe side effects, and it often fails because of toxicity and the development of drug resistance [3, 4].

Improved targeting of drug delivery would clearly be beneficial for increased efficacy and reduction of the side effects of chemotherapy. Over the last 20 years, the use of ultrasound (US) and microbubbles (MB) to increase the uptake of chemotherapeutics. This technique, which is often defined as “sonoporation”, has been shown to increase the efficacy of cancer therapy in both preclinical trials and clinical trials. However, the mechanisms leading to improved therapy are under debate, and they are not fully understood. These mechanisms are explored in this thesis.

1.1 Cancer

1.1.1 Background

The characteristics of cancer cells were defined by Hanahan and Weinberg in 2000 [5] and updated in 2011 [6]. Cancer cells have sustained proliferative signalling, leading cells to continuous cell growth. They evade growth suppressors, resist cell death and have unlimited replicative potential. Moreover, they activate invasion, metastasis and the reprogramming of the energy metabolism [6]. Furthermore, they have the ability to evade the immune system and induce tumour angiogenesis [6]. These properties are made possible by the following characteristics: genomic instability and mutations as well as the inflammatory state of premalignant and malignant lesions. In addition to disseminated cancers, such as leukaemia and lymphoma, the cancer cells form tumours. The tumours exhibit a further dimension of complexity in addition to cancer cells: in the

“tumour microenvironment” recruited normal cells form tumour-associated stroma and contribute to the acquisition of the hallmarks of cancer [6].

1.1.2 The tumour microenvironment

Solid tumours have increasingly been recognized as complex organs, and the biology can only be understood by studying both the individual cell types and the tumour microenvironment (Figure 1) [6]. In addition to cancer cells, the tumour consists of the extracellular matrix (ECM), adipocytes, stromal cells (*i.e.* fibroblasts, pericytes, and stellate cells), cancer-associated fibroblasts (CAFs), cancer-associated macrophages, mesenchymal stem cells (*i.e.* local or bone marrow derived), immune cells and vasculature/endothelial cells [7-9]. Adding to the complexity, late stage tumours are hypervascularized, hypoxic, have high interstitial pressure and abnormal blood flow [10]. The tumour microenvironment is involved in the progression of cancer through the complex interplay between the tumour cells, the surrounding non-neoplastic cells and the extracellular matrix (ECM) [11]. It also works as a biophysical barrier to drug delivery, making it an important a target in the improvement of drug therapy [8, 10, 12].

Tumour microenvironment

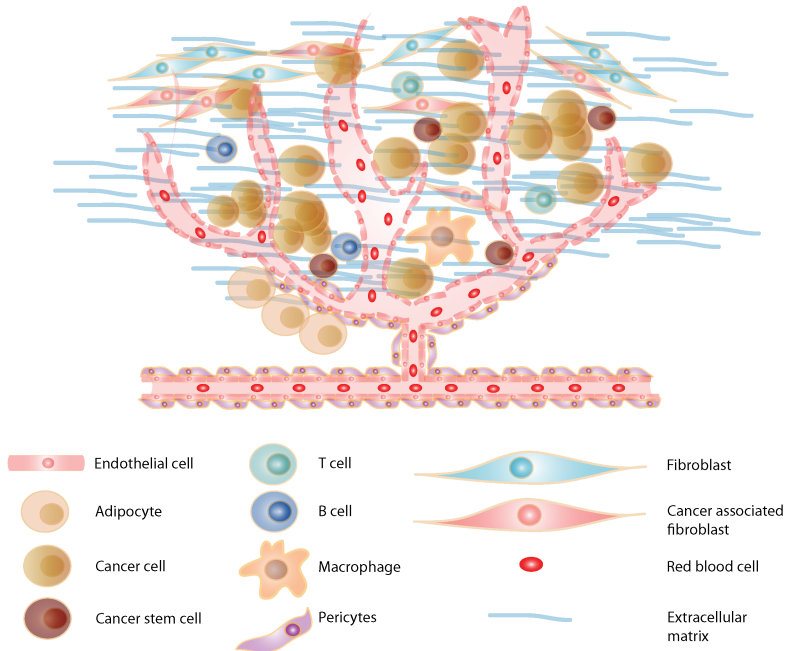


Figure 1: *The tumour microenvironment* (adapted from [9])

1.1.3 Aberrant intracellular signalling in cancer

Cell signal transduction is the cellular response to physical and chemical signals in the environment, resulting in a series of signals of which phosphorylation is the most common, leading to a cellular response [13]. Signal transduction is essential for the normal regulation of cells, and the alteration of the signalling networks is an important feature of cancer cells [6]. Many genetic and epigenetic alterations underlying uncontrolled cell growth and migration are linked to signalling pathways involved in cell growth, death, division and motility [11]. The pathways are often constitutively active, which is a result of oncogenic mutations, amplification or gene fusion involving tyrosine kinases and/or the deregulated synthesis of growth factors and their receptors [6, 11]. In a wider context, signalling that fuels cancer progression involves changes in the tumour microenvironment, angiogenesis and inflammation as well as the elimination of negative regulators of signalling by the inactivation of tumour suppressors [11].

For simplicity, signalling pathways are often described as a single series of events in the literature. However, these pathways form an elaborate network that includes cross-talk between pathways and intricate feedback mechanisms [13]. Several of the same cell receptor families activate the same downstream targets, and some common pathways are often activated in cancer, such as the PI3K/Akt, MAPK, mTOR and JAK/STAT pathways [11, 13]. Because of the importance of dysregulated signalling in tumorigenesis and cancer progression, the signalling pathways are targets in therapeutic intervention. Well-known examples are surface receptors, such as EGFR and HER2, and cytosolic signalling molecules, such as PI3K, ERK and mTOR [11, 13, 14]. Because the same pathways are often dysregulated in different cancers, targeting them constitutes a potential treatment option for different types of cancer [13, 14]. However, the commonality of downstream targets also represents a therapeutic challenge because when one pathway is inhibited, the signalling may be sent through another pathway to activate the substrate [13].

Mitogen-activated protein kinase (MAPK) pathway

The MAPK pathway is a highly conserved pathway that is involved in cellular processes, such as proliferation, growth, differentiation, cell movement/migration and apoptosis [15]. The pathway consists of extracellular signal-regulated kinase (ERK: 1/2, 3/4, 5 and 7/8), Jun-N terminal kinase (JNK) and p38. Abnormalities in MAPK signalling play a critical role in development of cancer and resistance to therapy [15, 16].

ERK signalling is commonly known to promote proliferation, but it is also involved in cell cycle regulation, cell adhesion, differentiation, survival, migration/cell movement, angiogenesis and chromatin remodelling [15, 16]. ERK is activated by numerous signals, including the Ras/Raf/MEK pathways, which are commonly activated in cancer by well-known mutations such as KRAS and BRAF [15].

In addition, p38 and JNK are typically activated by various cellular stresses, including hypoxia, oxidative stress, detachment from substrate, chemotherapy/DNA-damaging

agents, metabolic stress, radiation, osmotic shock and other environmental stresses [15, 17]. The role of these pathways in cancer is difficult to predict due to their dual role of the anti-proliferative and pro-apoptotic regulation of cell death, which leads to the suppression of tumorigenesis, and of cell survival, where adaptation to the microenvironment contributes to cancer progression and chemoresistance [15, 17].

PI3K/Akt/mTOR pathways

Another conserved pathway is the mTOR pathway, which is typically involved in the cellular processes related to cell survival, proliferation and growth in the response availability of nutrients, energy, growth factors and stress signals [18]. The pathway is a downstream effector of the PI3K/Akt pathway, but it is also activated downstream of MAPK and AMPK [18]. mTOR consists of mTORC1, regulating ribosomal protein S6 and 4E-BP1 involved in protein translation as well as mTORC2, which regulates actin cytoskeleton through PKC- α and Akt [18]. The activation of aberrant mTOR signalling in cancer contributes to cellular growth, angiogenesis and metastasis [18].

Elevated levels of phosphorylated ribosomal protein S6 are associated with a worsened prognosis in patients with solid tumours [19]. The canonical function of 4E-BP1 is considered a growth suppressor. However, paradoxically, high levels of 4E-BP1 phosphorylation and 4E-BP1 overexpression are common in cancer, and they are related to tumorigenesis and uncontrolled cell growth [20, 21].

ER stress, eIF2 α the unfolded protein response

Endoplasmic reticulum (ER) stress activates the unfolded protein response (UPR), resulting in the phosphorylation of eIF2 α and in some cases JNK [22, 23]. This activation is important in cell adaptation and survival under stressful conditions. This signalling inhibits global protein translation and the activation of the translation of proteins are important for cell survival, whilst cell apoptosis is initiated under prolonged stress [22]. This pathway is important for the adaptation of cancer to the stressful conditions in a tumour, such as hypoxia, nutrient deprivation and pH alterations. The

pathway also plays a role in tumour growth, metastasis, angiogenesis, immune suppression and chemoresistance [22, 23].

Other pathways involved in cancer development and progression

Because of its importance in many of the hallmarks of cancer, Ca^{2+} -signalling and calcium channels and pumps may be potential therapeutic targets in cancer [24]. The ion Ca^{2+} is the second messenger involved in a wide range of cellular processes, including the pathways involved in cancer progression [24].

Inappropriate activation of Janus kinase (JAK)/signal transducers and activators of transcription (STAT) signalling is present in haematological cancers and many solid tumours, contributing to oncogenesis [25]. The pathway is typically activated by growth factors, interleukins and cytokines through transmembrane receptors, leading primarily to regulation of transcription through the STATs – that represents a therapeutic target in cancer [25]. Mitochondrial activity of STAT3, by phosphorylation of the serine 727 epitope, has been found to be a critical substrate of Ras/MEK/ERK in cellular transformation [26].

The nuclear factor kappa-B (NF- κ B) has been found to be excessively activated in various tumour tissues, and the role of NF- κ B signalling has gained interest. NF- κ B signalling is activated by various extracellular signals, and is involved in cellular immunity, inflammation and stress [27]. NF- κ B inhibitors have developed, but their anti-cancer mechanism is not fully understood and they have not yet reached clinical use [27].

One of the most extensively studied proteins in cancer research is tumour suppressor p53, a transcription factor also known as “guardian of the genome” [28]. The activation of p53 induces antiproliferative processes such as apoptosis, cell cycle arrest and senescence in response to stress signals, including genotoxic stress and oncogene activation [28]. The TP53 gene is the most frequently mutated gene in cancer and the majority of cancers gain mutations that abrogate the p53 network [28, 29]. Mutated

TP53 is associated with poorer prognosis, cancer cell adaption to mechanical, metabolic, oxidative, proteotoxic and genotoxic stress in a tumour [29].

1.1.4 Signalling from the tumour microenvironment

Signalling from the tumour microenvironment is important in the progression of cancer [11] and in the development of drug resistance [30]. Mechanotransduction, which is the cellular translation of mechanical and physical forces in the environment to intracellular signalling responses [10, 31], is important because the abnormal mechanical properties of the tumour microenvironment, such as ECM stiffness, high interstitial pressure and abnormal fluid and blood flow, induce protein conformational changes that lead to the activation of classical tumorigenic signalling pathways [10]. A common route of activation is through integrin signalling and the activation of FAK and Src kinases, leading to the activation of the pro-survival and pro-mitogenic Ras/MAPK, PI3K/Akt and Yap/Taz pathways, resulting in hyperproliferation and cell motility [10, 11, 32]. Because many signalling pathways are involved, an extensive review is beyond the scope of this thesis [10]. In addition to mechanotransduction, the cellular adaptation to stress conditions in the tumour microenvironment, such as hypoxia and nutrient deprivation, which often take place by translation reprogramming that involves the eIF2 α , mTOR and eEF2K pathways, is important in tumour progression [33].

1.1.5 Current cancer therapy

The main current treatment options for cancer are surgery, radiotherapy and/or chemotherapy [1]. The cancer treatment may be local (*i.e.* surgery, radiation, cryotherapy or chemical/heat ablation), systemic (*i.e.* chemotherapy, hormonal therapy, immune therapy and targeted therapy), or a combination [4]. In recent decades, the improvement in cancer therapy has led to increased cancer survival. Moreover, advances have been made in targeted therapies, to attack specific proteins on cancer cells, which are important in cell growth (including signalling pathways) and in immune therapy, where the patient's immune system is stimulated to attack the cancer cells [4]. Despite these advances, chemotherapy is still the main drug treatment offered to patients.

However, the unspecific mechanism of action in traditional chemotherapy cause severe side effects, and this treatment often fails because of drug resistance and toxicity [3, 4].

1.2 Pancreatic ductal adenocarcinoma (PDAC)

The cancer receiving most attention in this thesis is Pancreatic ductal adenocarcinoma (PDAC). PDAC is one of the most lethal types of cancer, mainly because late diagnosis and chemoresistance developed during treatment. PDAC is the fourth most common cause of cancer-related death worldwide, and the incidence is expected to increase [34]. Currently, the treatment options are surgery, radiotherapy and traditional chemotherapy [34]. The chemotherapeutic regimens, including gemcitabine monotherapy or in combination with nab-paclitaxel, and FOLFIRINOX (*i.e.* fluorouracil, oxaliplatin, irinotecan and folinic acid), are associated with toxicity, and their application is limited in elderly patients and patients with poor performance status [34].

The disease is further characterized by desmoplasia and a complex tumour microenvironment, with hypoxia, minimal vasculature, a dense and rigid extracellular matrix (ECM) and high intratumoural pressure, all of which are major contributors to drug resistance [34, 35]. The desmoplastic stroma may constitute up to 90% of the tumour volume, and is thought to originate in cancer-associated fibroblasts (CAFs) [8, 34]. Hypoxia is another feature of the PDAC microenvironment supporting PDAC progression through the interference with immune cell infiltration and function [34].

The need for improved treatment of PDAC is urgent. Treatments that target the tumour microenvironment have been suggested as a promising strategy for combating PDAC because of its importance in PDAC progression and its role as a biophysical barrier against drug delivery [12]. Biologically targeted therapies targeting downstream effectors of the most common mutations in PDAC (KRAS, CDKN2A, TP53, and SMAD4), such as the MAPK pathway, are under investigation [34].

1.3 Drug delivery in cancer

1.3.1 Barriers to drug delivery

The accumulation of a sufficient amount of drug and uptake in cancerous tissue and cells is a prerequisite for effective chemotherapy, while toxicities in healthy tissue should be minimized or avoided. Many chemotherapeutics are administered as intravenous infusions, which by definition result in 100% bioavailability, but it also leads to severe systemic side effects. Nevertheless, to affect cancer cells, the drugs must reach their cellular target by extravasation across the endothelium of the blood vessels, the ECM, stroma and microenvironment of the tumour and then by distribution over the cell membrane of the cancer cells. Tumours are characterized by heterogenous and disorganized blood vessels, disrupted blood supply and high interstitial and osmotic pressure, all of which limit drug delivery [36]. Drugs with intracellular targets (*i.e.* most chemotherapeutics) are small molecules, which are taken up in cells either by passive diffusion (limited to small [> 500 Da], uncharged molecules of intermediate lipophilicity with limited hydrogen bonding capacity) or by active transportation through transporters in the cell membrane [37]. The ability to cross the cell membrane has thus been a limiting factor to which molecules were actually developed as drugs [37]. Furthermore, drug delivery is hindered by the uptake of drugs in the mononuclear phagocyte system before the drugs reach the tumour and by efflux pumps acting to remove the drugs taken up by the cancer cells [36]. Many cytotoxic agents, although they effectively kill cancer cells *in vitro*, have insufficient effects on tumour cell viability *in vivo*, where drug delivery is hindered [38].

1.3.2 Drug delivery strategies in cancer

The most extensive research to solve the drug delivery problem is being done to incorporate chemotherapeutic drugs in targeted formulations, which have the ability to deliver the drug exactly at the site of action, thus minimizing the side effects. Drug carriers, such as liposomes and nanoparticles, have been developed taking advantage of the fact that the blood vessels in tumours have enhanced permeability and impaired

lymphatic drainage, which is known as the enhanced permeability and retention effect (EPR effect) [39-41]. Although some nanoformulations are clinically approved and used in cancer therapy (*e.g.*, Caelyx[®], Daunoxome[®], Abraxane[®] etc.), this kind of targeted drug delivery has still not fully met expectations [40]. Their main advantage so far is the reduction of specific side effects; however, in general, they do not improve overall survival compared with free drug [39].

By passively relying on the EPR effect, the effectiveness of drug delivery is limited and heterogenous [40, 41]. To improve the efficiency and specificity of the EPR-effect, it has been suggested to apply vessel-modulating strategies by either pharmacological or physical methods [40], by targeted drug formulations that change from an inactive to an active form or by depositing the drug at a precise site of action [42], typically by physical stimuli [39]. A potential strategy is sonoporation, in which ultrasound (US) and microbubbles (MB) are used to increase the permeability of the blood vessels and the uptake of drugs [40]. In combination with US-sensitive drug carriers [39] or by the further development of MB drug carriers [43], the goals of specific and effective drug delivery may be achieved. Because it is known for the ability to form pores in the cell membrane, sonoporation also targets what has been named the “last major hurdle” in the development of cancer therapeutics—intracellular drug delivery, thus enabling the use of molecules previously considered un-druggable because of their low uptake in cells [44].

1.4 Sonoporation

1.4.1 Definition of sonoporation

Sonoporation was initially defined as the transient formation and resealing of pores in a cell membrane due to US alone or US in combination with MBs [45, 46]. These resulting pores allow for increased uptake and entrapment of drugs or genes. The term was derived from electroporation, a biological technique in which cells are placed in an electrical field to increase the permeability of cells [47]. Sonoporation was first used to

enhance gene transfection *in vitro* by Unger *et al.* [48], who found that transfection from liposomes was enhanced by US and by Greenleaf *et al.*, who found that US transfection was more efficient by the addition of Albunex[®] MBs [49]. It was later shown to increase the efficacy of chemotherapeutic drugs [50-53]. The definition of sonoporation is sometimes debated, probably because the mechanisms leading to enhanced therapeutic effect by the use of US and MBs are not yet fully understood. Nevertheless, the term “sonoporation” mainly refers to the formation of pores due to MBs and US exposure in cells in an *in vitro* context. However, the term “US + MB enhanced therapy” or similar terms are sometimes preferred because they are more generally descriptive. Recently, the term “sonopermeation” was suggested, which describes a mechanism that is probably more complex and includes endocytosis, the opening of intercellular junctions, improved tumour vessel perfusion and changes in the tumour microenvironment [54]. In this thesis, the term “sonoporation” is used because most of the work was done *in vitro*. However, it may also include uptake due to endocytosis [55] and other cellular bioeffects that may or may not be caused directly by pore formation.

1.4.2 Ultrasound (US)

Sound is the rapid vibration of molecules travelling as mechanical waves to transport energy from a transmitter to a receiver (*e.g.*, our ears) [56]. Depending on the frequency (*i.e.* the number of times a second that air vibrates to produce sound), sound can be classified as infrasound, audible sound or US. US consists of waves that propagate at frequencies higher than a human ear can detect (*i.e.*, above 20 kHz) [39, 56, 57]. US is used in medicine for diagnostic imaging, and therapeutic applications like tissue heating in physiotherapy; tissue ablation (*i.e.* high intensity focused US [HIFU] therapy) including tumours; lithotripsy; and low-intensity US for healing of bone fractures [58]. Recently, MB-based US has been used in drug delivery [39, 58].

Throughout the development of US, it has been known that US may be hazardous, and it may have dramatic effects on biological matter, depending on the US intensities used [56]. However, currently, the levels of US used diagnostically are generally considered safe within the limits recommended to avoid harmful bioeffects [58, 59]. The interaction

of US with biological materials is primarily separated into thermal and non-thermal effects [56]. Thermal effects may arise when ultrasonic energy is absorbed in tissue and converted into heat [39, 56]. Non-thermal mechanical effects have mainly been attributed to acoustically generated cavitation, particularly in the presence of MBs. However, effects have also been attributed to radiation force [39, 56].

The most commonly used measure for the quantification of US in studies on US bioeffects is US intensity, in which the amount of power in the US wave is divided by the surface to which it is applied (measured in W/cm^2) [39, 56]. US can be classified based on intensity, and low-intensity US ranging from 0.125 to 3 W/cm^2 [39]. In this thesis, the focus is on low-intensity US. The definitions of US intensity are based on the shape of the beam and the span of the pulse [39]: I_{SATA} = intensity averaged both on the pulse repetition period and on the cross-section of the beam; I_{SPTA} = maximum intensity occurring in an US beam averaged over the pulse repetition period; I_{SPPA} = the maximum intensity at in the ultrasound beam averaged over the duration of the pulse. I_{SPTA} , which is used the most frequently, is correlated to the thermal effects in biological tissue. I_{SPPA} is correlated to mechanical and cavitation effects [39]. The overall intensity limit for diagnostic applications is $I_{\text{SPTA}} = 720 \text{ mW}/\text{cm}^2$, which was introduced by the United States Food and Drug Administration (FDA) in 1993 [57, 60].

US waves may be either continuous or discontinuous (pulsed). However, continuous US may not be suitable for use in humans at higher acoustic amplitudes because of energy accumulation, which may cause tissue damage [39]. Therefore, US is broken down to pulses, where US is turned off and then repeated periodically [39, 56]. The percentage of time that US is applied (*i.e.* the proportion of time of effective US exposure) is called the duty cycle, and the frequency of the pulses is called the pulse repetition frequency [39]. There are no definite limits in the duty cycle, but this parameter must be set to fulfil the I_{SPTA} requirement.

1.4.3 Cavitation

Cavitation is the US-induced activation of bubbles or gas pockets (*i.e.* cavitation nuclei) in a liquid, in which the successive positive and negative peaks of the US waves lead to the successive growth (at peak-negative pressure) and shrinkage (at peak positive pressure) of (micro-)bubbles in the acoustic field [39, 56]. At low acoustic amplitudes, MBs pulsate stably, while at high amplitudes the expansion phase is elongated and is followed by a violent collapse, in which the bubbles may fragment into several smaller bubbles (*i.e.* inertial cavitation) (Figure 2) [39, 57]. The activation of bubbles depends on their size and frequency. The frequency at which bubbles oscillate stably is termed the resonance frequency. In shell-less bubbles $> 5 \mu\text{m}$, the resonance frequency is generally $< 1 \text{ MHz}$, which allows for a fairly good penetration depth for use in humans [39]. Very small bubbles ($\leq 1 \mu\text{m}$) require higher frequencies ($\geq 10 \text{ MHz}$), which results in poor tissue penetration depth [39].

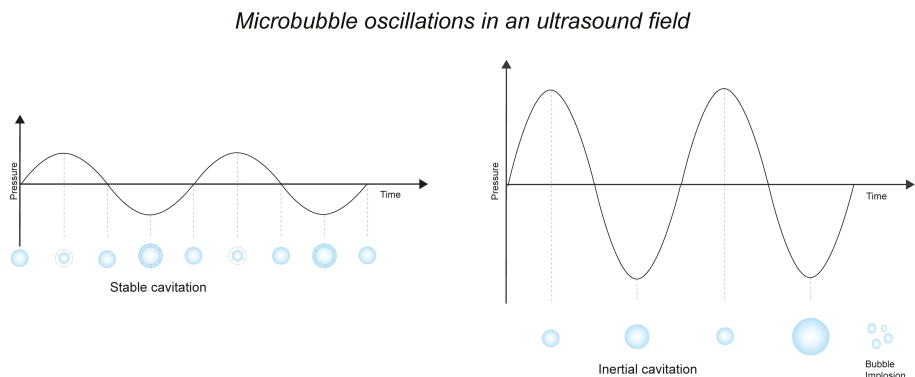


Figure 2: Stable versus inertial cavitation

The activity of bubbles in the US field (cavitation) increases the risk of adverse effects due to medical US, and inertial cavitation raises some safety concerns [59]. The risk of cavitation is lower in degassed tissue, and it increases when US contrast agents (MBs) are added to visualise blood vessels [39]. The mechanical index (MI) is a measure that was developed to indicate the risk of mechanical damage due to US, particularly inertial cavitation [56, 57, 59]. The MI is based on theoretical and *in vitro* experimentation by Apfel and Holland [61]. It is generally considered that without bubbles (*i.e.* US contrast

agents), US is safe at an $MI < 1$ and at $MI < 0.4$ in the presence of MBs [59]. In the guidelines of the British Medical US Society, $MI > 0.7$ is the threshold for cavitation. At $MI > 0.3$, there is a minor possibility of capillary bleeding in gas-containing organs, such as lungs or intestines, if US contrast agents (MBs) are used [57]. In medical imaging, MI is limited to 1.9 in commercial scanners when no bubbles are present [39, 57, 60]. Correspondingly, the thermal index (TI) was developed to assess possible adverse effects due to temperature elevation [57].

1.4.4 Ultrasound used in sonoporation

Currently, there are no guidelines for US exposure in therapeutic applications such as sonoporation [39]. In the first clinical trial [62] worldwide, the US exposure was limited to the level allowed for diagnostic imaging. Acoustic pressure, acoustic frequency, acoustic energy, acoustic phase, pulse bandwidth, pulse nonlinearity, duty cycle, pulse duration, pulse repetition frequency, pulse length, mechanical index (MI), insonation time and time interval after US exposure are all relevant parameters in sonoporation [63, 64]. As reviewed by Yu and Xu [63], almost all studies showed agreement that acoustic pressure was positively correlated with both transfer efficiency and therapeutic efficiency and negatively correlated with cell viability in both stable cavitation and inertial cavitation. The parameters that included acoustic energy, sonication time, duty cycle, mechanical index and cavitation index showed the same trend, while acoustic frequency showed somewhat variable effects [63]. However, the determination of the exact parameters is difficult because the formulation, size and dose of the MBs used must also be considered. To increase the efficiency of sonoporation, it has been shown that acoustic pressure should be kept below the inertial cavitation threshold to ensure linear or non-linear oscillations of the MBs [65, 66].

1.4.5 Microbubbles (MB)

MBs are gas-filled particles consisting of a gas core stabilized by a shell. They were first developed in the 1980s to enhance US contrast in humans [43, 67]. Currently, they are in clinical use for US imaging in cardiology [68] and the visualisation of cancerous lesions [69] and metastasis [70, 71]. The importance of MB addition in sonoporation

efficiency has been well-documented [63, 72-74] although sonoporation-induced drug delivery has been achieved without MBs [64, 75]. There are two main approaches to MB-assisted drug delivery: the co-administration of drugs and MBs (either the off-label use of commercially available MBs developed for imaging or MBs made for use in drug delivery); or drugs are entrapped or attached to the MBs and are released upon the activation of the bubbles by US [76, 77]. So far, the co-administration of commercially available MBs has been used primarily in sonoporation-induced drug delivery. The use of these MBs represents the fastest bench-to-bedside transition of sonoporation-enhanced therapies [62]. However, this therapy requires the systemic administration of MBs and drugs, which in chemotherapy result in systemic toxicities. As pointed out in [78] another strategy for inducing the contact of MBs with cancer cells may be the injection of higher concentrations of MBs intratumourally, which has been done in animal trials [50, 79, 80]. However, the suitability of intratumoural injections is limited to superficial tumours [81].

The first MB formulation was based on a protein shell filled with air (Albunex[®]), which was approved at the end of the previous century [82]. This formulation was followed by protein-based Optison[™] and lipid-based MBs Definity[®] and SonoVue[®] [67, 83, 84]. To date, MBs have been made using protein-, surfactant-, lipid- and polymer-based shells [67, 85, 86]. Four MB products have been clinically approved for imaging purposes in Europe and the United States: SonoVue[®]/Lumason[®] (Bracco); Optison[™] (GE Healthcare); Sonazoid[™] (GE Healthcare); and Luminity[®]/Definity[®], (Lantheus). Currently, the MBs are filled with dense gases of higher molecular weight, either sulphur hexafluoride or perfluorocarbon, which have less solubility in blood and lower diffusion from MBs compared with air. The use of these gases results in better *in vivo* MB stability and longer half-life in circulation; they also enhance echogenicity [87]. To prolong half-life in blood circulation the phospholipid MBs are PEGylated, *i.e.* polyethylene glycol (PEG) is covalently conjugated to phospholipids. However, but the MBs are still eliminated within minutes, and the lifetime may not be optimal for drug delivery [86].

The formulation, composition, size and dosage of MBs are important factors that may influence sonoporation efficiency. MB lipid shells are thinner and more flexible, while polymer- or protein shells are thicker and more rigid. In their review, Lentacker *et al.* [64] iterated that lipid MBs may be preferred at low acoustic pressure when small pores are required, whereas polymer- and protein-shelled MBs may produce stronger effects and larger pores although only above a certain threshold [64]. This effect can be explained by the fact that MBs with thick and rigid shells oscillate less than thin- and soft-shelled lipid MBs do [57, 86]; moreover, the stiffness of the shell increases resonance frequency [88]. The studies published so far have used different types of MBs, but few studies have compared different types of MBs [63]. Moreover, the optimal composition of MB has not yet been determined.

The size of the MBs is another important factor in the MB response to US. The MB size is limited to the range between 0.5–10 μm [67], typically 2–8 μm [86], to pass through the smallest microvessels and capillaries. Because the acoustic response is linked to the diameter of the MBs [88], the optimal sonoporation conditions occur at a specific acoustic frequency. Ideally, a single frequency could be used to excite homogeneously sized (monodispersed) MBs of a particular size. However, MBs have traditionally been manufactured by emulsification and/or sonification, which result in a polydisperse size distribution [89]. When polydisperse MBs are used, the challenge of optimising therapeutic sonication parameters is exacerbated because these MBs respond differently to the same frequency.

1.4.6 “Next-generation microbubbles”

Currently, a substantial amount of research is being conducted to develop “next-generation” MBs specifically for sonoporation targeted- and enhanced therapy; however, clinical use remains to be achieved. In the MB carrier research, several strategies have been attempted for the loading of drugs into MBs. In early research, the loading of hydrophobic drugs was attempted in hydrophobic MB shells or in a hydrophobic thickening oil layer via hydrophobic interaction, the attachment of drugs to shells with a modified surface charge via electrostatic interaction, or the covalent

linking of drugs to the MB shell [77, 86]. Other attempts included increasing the payload loading of drugs in liposomes attached to the shell surface and the encapsulation of MBs inside a liposome with the drug [86, 90]. In all these strategies, the amount of drug that could be loaded to MBs was limited. Therefore, so far, the loading of drugs to MBs has not been successful clinically [86, 91]. In addition, the loading of drugs into or in conjugation to the shell may inhibit acoustic sensitivity, thereby diminishing the efficacy of sonoporation [86].

Novel MB formulation strategies include but aren't limited to the following: echogenic "bubble liposomes" less than 2 μm in size that encapsulate tiny bubbles of perfluorocarbon gas, which induce cavitation upon exposure to US [92]; nanoliposomes (gas-filled particles in the nano-size range, which are expected to have enhanced penetration in tumour and better stability, less *in vivo* irritation and longer half-life [93, 94]); acoustic droplet vaporization (perfluorocarbon [PFC] nanodroplets vaporized by US to produce MBs *in vivo* [95], expectedly in tumour tissue due to their small size. The droplets may incorporate drugs that reside in the shell when converted to bubbles); and antibubbles, which are acoustically active [96] bubbles where the therapeutic is loaded in a liquid droplet in the gas core [97, 98]. A formulation concept of sonoporation that is in clinical trial is Acoustic Cluster Therapy (ACT[®]) [99-102]. In ACT[®], negatively charged, commercially available MBs (Sonazoid[™]) are combined with positively charged microdroplets. Upon sonication with diagnostic US, the volumetrically oscillating MBs transfer energy to the microdroplets and initiate a phase shift from liquid to gas. This deposits 20–30 μm transient MBs in a vasculature that occludes blood flow. The following US enhancement induces oscillations, thus increasing the permeability of the vasculature and allowing local enhanced drug permeability [101, 102].

1.5 Therapeutic uses of sonoporation

1.5.1 Enhancement of cancer therapy

In vitro research

The use of US and MBs has the great potential to improve drug delivery in cancer therapy. It is hypothesized that US + MB increases the intracellular concentrations of chemotherapeutics, which might allow the opportunity to administer lower doses and thereby reduce side effects. Many previous studies demonstrated that the use of MBs and US in combination with chemotherapeutic drugs reduced cell growth and increased cell death in cancer cells *in vitro* [50-53, 79, 80, 103-105]. However, it is not known whether the increase in therapeutic efficacy by sonoporation was solely due to pore formation and the increased cellular uptake of drugs. In *in vitro* research on sonoporation, the effect was often assessed by either the uptake of cell-impermeable dyes [50, 53, 103], which have no effect on the viability of cells, or by evaluating the viability of cells exposed to both sonoporation and drugs but without assessment of the actual uptake [50, 53, 79, 80, 103]. Only a few studies have measured the actual drug uptake or linking the increased uptake to the increased efficacy of sonoporation. These studies showed that sonoporation led to the increased uptake of cisplatin [104] and doxorubicin [51] as well as fluorescently labelled cisplatin and cetuximab [52]. However, a recent study by Mariglia *et al.* [105] found no increase in the uptake of a radio-labelled nucleoside analogue in pancreatic cancer cell lines. The cytotoxic efficacy was nevertheless increased in all these studies. In a recent study published by our research group [106], the higher drug uptake in sonoporated cells than in untreated cells was observed only when normal drug transporters (*i.e.* normal drug uptake) were inhibited and varied between cell lines. This result indicated that the benefit of sonoporation in enhancing cellular uptake varies between cell types and drugs, and it may be limited because the molecules developed as drugs are already taken up by the cells.

Preclinical trials

Several preclinical trials have shown that the use of MBs and low-intensity US could enhance tumour growth reduction by chemotherapy in animal models. This result has been shown in a range of cancer types and chemotherapeutics, such as the following: bleomycin in gingival squamous cell carcinoma [79, 107]; cisplatin in colon cancer [50];

melphalan in malignant melanoma [80]; epirubicin in a HL-60 (leukaemia) tumour model [108]; and paclitaxel in breast cancer [53]. In the treatment of PDAC, it was demonstrated that the combination of gemcitabine, commercial MBs (SonoVue[®]) and US, in which the parameters were kept within the safety limits for the clinical use of US and MBs, resulted in both reduced tumour volumes and moderately (but not significant) increased survival [109]. Reduced tumour growth and increased survival using sonoporation has also been shown in the ACT[®]-concept in different cancer models using different drugs [99, 100, 110] as well as in Nab-paclitaxel (nanoparticle formulation of paclitaxel) in PDAC using two microbubbles formulations made by Bracco Suisse S.A. [103]. The drug delivery of trastuzumab to the central nervous system (CNS) over the blood-brain barrier (BBB) using US and MBs has also been demonstrated [111].

Because the effect of intracellular drug delivery *in vitro* has been questioned, there has been an increased focus on the effects of sonoporation in drug delivery at the tumour level. Although the studies discussed above did not demonstrate that the enhancement of therapy was the result of increased drug delivery, the increased accumulation of quantum dot nanoparticles in a tumour [112] and the extravasation of nanoparticles into extracellular matrix [113] have been demonstrated *in vivo*. The increased accumulation of the drug and reduced tumour growth were further demonstrated in mice by sonoporation + PEGylated liposomal doxorubicin [114]. Sonoporation was also used to enhance the extravasation of fluorescent liposomes in tumours characterized by low EPR [115].

Clinical trials

Currently, there is great interest in the clinical use of sonoporation. The first phase I clinical trial showed that US+MB enhanced therapy in combination with chemotherapy was safe. The results also indicated that this therapy may increase the survival of patients suffering from PDAC [62]. However, a recent search of the PubMed database using the search term “sonoporation” and filtering for clinical trials yielded only the first clinical trial, which was published in 2016 [62]. A limited safety study from China on cancers in the digestive system also concluded that sonoporation is safe at $MI < 1$ [116]. Further

studies were initiated (*i.e.* registered in www.clinicaltrials.gov) in breast and colorectal cancer [117, 118] and colorectal cancer and hepatic metastasis [119].

1.5.2 Other therapeutic uses of sonoporation

In cancer therapy, the use of US \pm MBs has benefits in addition to increased drug perfusion and uptake. In sonodynamic therapy (SDT), sonosensitizers are used in combination with US to generate cytotoxic levels of reactive oxygen species (ROS), which is used in combination with chemotherapy [120, 121]. In addition to the above-mentioned vascular effects of US \pm MBs, US \pm MBs may also have anti-vascular effects on disrupting the tumour vasculature [121] to increase the EPR effect and drug diffusion from the vasculature.

The delivery of drugs and genes to the central nervous system (CNS) is challenging. It is generally limited to small lipophilic molecules that are able to cross the blood brain barrier (BBB). The BBB consists of endothelial cells connected by tight junctions in a thick basement membrane and a layer of astrocyte end-feet, which prevent the majority of drugs from entering the CNS [122]. Sonoporation has shown great promise in enhancing the delivery of molecules to the brain. So far, sonoporation has been tested preclinically in brain cancer, Alzheimer's disease and Huntington's disease [122]. Permeabilization of the BBB by sonoporation has been shown to be efficient, non-invasive and safe in pigs and non-human primates [122], and drug delivery across BBB has reached clinical trials in Alzheimer's disease [123, 124]. Several studies on US + MB enhanced drug delivery across the blood brain barrier (BBB) to treat glioblastoma are also initiated and/or published [122, 125, 126].

In gene therapy, the lack of specificity has resulted in a narrow therapeutic index, which has hampered efficacy at the target site [127]. The therapeutic use of small interfering RNA (siRNA), micro RNA (miRNA) and plasmid DNA (pDNA) has been challenging because of inefficient delivery. However, the incorporation in bubble liposomes and US exposure constitute a potential delivery system [128-130]. Furthermore, the loading of nucleic acids in MBs may also protect nucleic acids from degradation by nucleases [77].

MBs and US also have shown potential in treating cardiovascular disease and in the use of sonothrombolysis to dissolve blood clots in acute ischemic stroke and acute myocardial infarction, which has reached clinical trials [91, 131]. In addition, sonoporation has therapeutic potential in delivering genes and oxygen to treat diseases in the cardiovascular system [91].

1.6 Bioeffects of sonoporation

Sonoporation is accompanied by many bioeffects, and the mechanisms that it influences are complex. It has been suggested that bioeffects, which cause cellular stress, also contribute to the efficacy of sonoporation [132]. The effects of sonoporation are caused by acoustic phenomena, such as microstreaming, microjets, stable cavitation and inertial cavitation, all of which are induced by the oscillation or destruction of MBs activated by US waves [133]. Most of the current literature on bioeffects consists of *in vitro* studies, particularly the effects induced on the cellular level, including pore formation [134, 135], endocytosis [55, 136, 137], delays in cell cycle [132, 138], membrane shrinkage [132], generation of reactive oxygen species and free radicals [139, 140], apoptosis [139, 141-143], cytoskeleton disassembly [144] and rearrangement [140], endoplasmic reticulum stress [141] and increases in intracellular $[Ca^{2+}]$ [139, 140, 145, 146], most of which are depicted in Figure 3. Furthermore, most of the *in vitro* studies were performed on cancer cell lines. Some studies were focused on endothelial cells under static [147, 148] and physiologically relevant flow conditions [149]. Their findings indicated that multiple mechanisms seem to occur simultaneously with respect to uptake and the biophysical effects of sonoporation on cells. In tissues, these interactions are even more complex, but there is a limited amount of published data on the bioeffects generated in living tissues. Sonoporation has been shown to form pores between confluent endothelial cells [150].

Sonoporation bioeffects

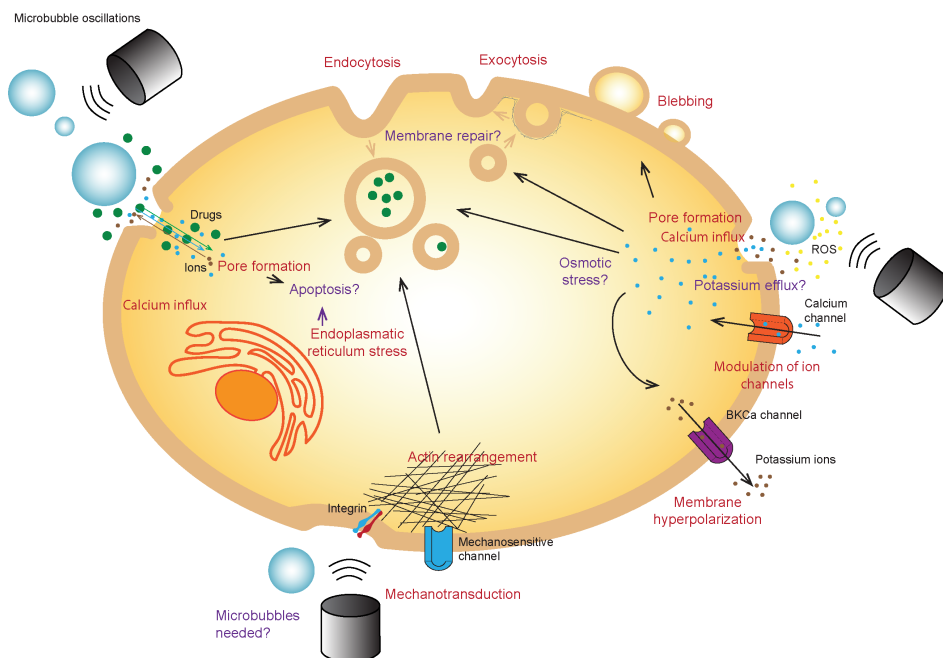


Figure 3: Known cellular bioeffects of sonoporation (adapted from [64, 141, 151])

1.6.1 Cellular uptake: pore formation, endocytosis and membrane repair

According to the original definition of sonoporation, the most well-known bioeffect of sonoporation is the transient formation and resealing of pores in the cell membrane. A few reports showed direct evidence of pore formation [134, 135, 152], which was supported by indirect evidence in numerous *in vitro* studies that showed the increased uptake of various dyes *in vitro* [46, 105, 135, 141, 153-162] and by measurements of changes in the transmembrane current of *Xenopus* oocytes [163] and cells [164]. Structural changes of the membrane observed by electron microscopy were correlated to the uptake of a cell-impermeable dye (SYTOX green) [160]. Delalande *et al.* [127] summarized six mechanistic effects related to pore formation in cells: push, pull, shearing, translation, jetting and inertial cavitation. Jetting and inertial cavitation occur only at higher acoustic amplitudes, which may surpass the current safety guidelines for

US with MBs [165]. In efficient sonoporation, keeping the acoustic pressure below the inertial cavitation threshold was shown to increase the uptake of cell-impermeable dye, which was hypothesized to be caused by microstreaming induced by oscillating MBs [65, 66]. However, the increased uptake in cells may be a result of sonoporation-induced endocytosis, particularly for larger molecules [55, 72-74, 166]. Electron microscopy immediately after sonoporation revealed both pore formation and the formation of membrane structures, which were concluded to be uncoated and clathrin-coated pits, supporting the hypothesis that the increased cellular uptake by sonoporation is the result of both pore formation and endocytosis [160].

It has been argued that the US parameters determine the mechanism of the uptake. It was further suggested that pore formation and endocytosis are not separate events in drug uptake; instead, endocytosis is a consequence of the preceding pore formation by either enhanced Ca^{2+} influx or the enhanced polymerization of microtubules [166]. Sonoporation induces the activation of ion channels, the formation of hydrogen peroxide, the influx of Ca^{2+} and membrane polarization [167], all of which may be related to endocytosis [133]. Endocytosis and patching/exocytosis are important in membrane repair [64, 168], and the cellular mechanisms in membrane repair may be the reason that exocytosis and endocytosis are observed during or after sonoporation. Furthermore, the restoration of the cell membrane includes blebbing; which depends on Ca^{2+} [151], but the mechanism for pore re-sealing and membrane repair is not yet fully known.

The duration of pore opening and resealing (*i.e.* “temporal window”) in the cell membrane influences the extent of the increased uptake of molecules and cell viability after sonoporation. Several studies indicated the different timing of pore resealing from seconds [134, 152, 161, 163, 164, 169] to hours [78, 160]. The differences in these results may have been due to the methods used to measure pore openings [78], different cell lines [78], US parameters [160] and pore sizes [152, 160]. Extracellular Ca^{2+} is known to be important in pore re-sealing/membrane repair after sonoporation [151, 152, 163, 170].

1.6.2 Intracellular signalling responses of ultrasound \pm microbubbles

There is little published work on signal transduction in response to sonoporation although some intracellular signalling mechanisms can be anticipated based on known intracellular responses, such as endocytosis [137], ER stress [141] and apoptosis [138]. Knowledge about the intracellular mechanisms may contribute to explaining and optimising the timing of formation and re-sealing of pores in the cell membrane or intracellular gaps, the timing of other bioeffects, and whether these could be exploited therapeutically or used to assess the safety of sonoporation. Based on the knowledge about cytoskeleton disassembly and membrane deformation, a review by Qin *et al.* [168] suggested that mechanosensors, such as integrins and stretch-activated ion channels, may activate intracellular signalling pathways related to endocytic and exocytic activities. The authors also suggested that the underlying mechanisms in the opening and resealing of gaps (*i.e.* adherens junctions and tight junctions) and the restoration of endothelial integrity could involve myosin light chain (MLC) kinase, RhoA signalling, focal adhesion kinase (FAK) and the activation of cAMP-dependant protein kinase A (PKA) [168]. Whether these pathways are relevant for sonoporation remains to be proven experimentally, but theoretically at least, intercellular permeability and restoration may be regulated by mechanotransduction pathways.

1.6.3 Intracellular signalling responses of ultrasound

Intracellular signalling responses to low intensity US have been more investigated, particularly in the context of bone and joint healing. The activation of integrin/mechanotransduction signalling, including p38, ERK1/2 and JNK (*i.e.* the mitogen-activated protein [MAP]-kinase pathway) and focal adhesion kinase (FAK) was found in chondrocytes [171] and synovial cells [172]. Additionally, the stimulation of cell growth through the integrin/FAK/phosphoinositide-3-kinase-protein kinase (PI3K) pathway, including Akt in chondrocytes [173] and osteoblasts [174], was described. The PI3K/Akt pathway was found to be important in cell proliferation in human bone marrow mesenchymal stem cells [175]. US also activated ERK1/2 in fibroblasts, depending on the Rho/ROCK and Src pathway, promoting cell proliferation

in human fibroblasts in wound healing [176]. Relevant in cancer therapy and angiogenesis, the pro-apoptotic effect on endothelial cells was recently found [177]. This mechanism involved the phosphorylation of p38 and ER-stress proteins eIF2 α and ATF4 and the dephosphorylation of ERK. The importance of p38, eIF2 α and ATF4 phosphorylation in LIPUS-induced apoptosis was confirmed in human omental adipose-derived mesenchymal stem cells by the same research group [178]. The observed involvement of both mechanotransduction pathways and of cell stress pathways (p38, ER-stress) is reasonable because US, depending on parameters such as intensity [178] and duration [175], induces both increases and decreases in viability. Moreover, the underlying molecular mechanisms are most likely different.

2. Aims of the study

The main aim of this study was to gain a better understanding of the mechanisms underlying sonoporation and the optimisation of sonoporation parameters for its translation into clinical use. To achieve this aim, the following objectives were met:

- 1) Investigate MB formulations and US parameters for sonoporation efficacy *in vitro* and *in vivo*.
- 2) Investigate whether and how sonoporation activates intracellular signalling in the context of cell permeabilization/uptake (pore formation) and cell viability.
 - a. Non-adherent cancer cells and healthy blood cells
 - b. Adherent pancreatic cancer cell types and cell types relevant in the tumour microenvironment in pancreatic cancer

3. Methodological considerations

3.1 Ultrasound treatment of cells

In these studies, custom-made US treatment chambers were used to expose cells to US. The chamber used to treat suspension cells on 24-well cell culture plates in Paper I was described in detail in [179] (Figure 4). A new US treatment chamber was developed to treat adherent cells, which was first published in [106] and used in Paper II and III (Figure 5). The chamber consisted of 128 US transducers and the US was non-focused, allowing for the treatment of cells across the entire surface of the treatment chamber. Increasing the intensity was achieved by increasing both the number of cycles (*i.e.* the duty cycle) and the peak-negative acoustic pressure.

In Paper I, the highest intensity (I_{SPTA}) used was above the maximum acoustic output allowed by the FDA in US imaging (720 mW/cm^2) [57, 60]. In Papers II and III, the highest intensity (I_{SPTA}) was below this limit. In all experiments, the Mechanical Index (MI) was kept ≤ 0.4 , which is generally considered safe [59]. In general, low-intensity US within the limits approved for diagnostic use combined with commercially available MB is the fastest translation to clinical use [62, 180].

The parameter ranges chosen in Paper I were based on the parameters used in the first preclinical study, which was executed at the University of Bergen [109]: 1 MHz, DC = 40%, MI = 0.2, $I_{SPTA} = 688 \text{ mW/cm}^2$. The parameters used in Papers II and III relate to the parameters used preclinically in Paper III: 1.8 MHz, DC = 1.1 %, MI = 0.2, $I_{SPTA} = 16 \text{ mW/cm}^2$, and attempted to match the settings for the clinical trial executed at Haukeland University Hospital, Bergen [62]: 1.9 MHz, DC = 0.3 %, MI = 0.2, $I_{SPTA} = 0.25 \text{ mW/cm}^2$. In Paper II, only Medium US (50 mW/cm^2) and High US (358 mW/cm^2) were used (Table 2) based on the low permeabilization rate at Low US (3 mW/cm^2) + MB in Paper III (Table 2) and the weak intracellular signalling response in applying the lowest US intensity to suspension cells (74 mW/cm^2) (Table 1).

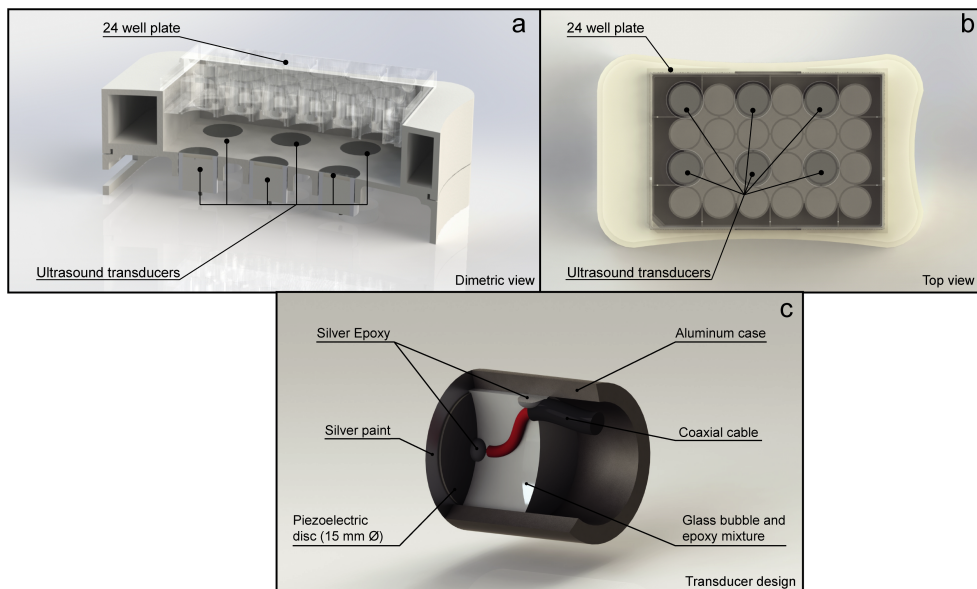


Figure 4: US treatment chamber made for suspension cells (CC BY 4.0 (Paper I))

Table 1: US parameters for suspension cells (10 min sonication) – Paper I

Name	Frequency (MHz)	No. of cycles	Duty cycle (%)	Pulse repetition frequency (kHz)	MI	Intensity	
						I _{SPTA} (mW/cm ²)	I _{SPPA} (W/cm ²)
Low	1.108	4	4	10	0.2	74	0.66
Medium	1.108	18	16	10	0.3	501	2.31
High	1.108	41	37	10	0.4	2079	5.0

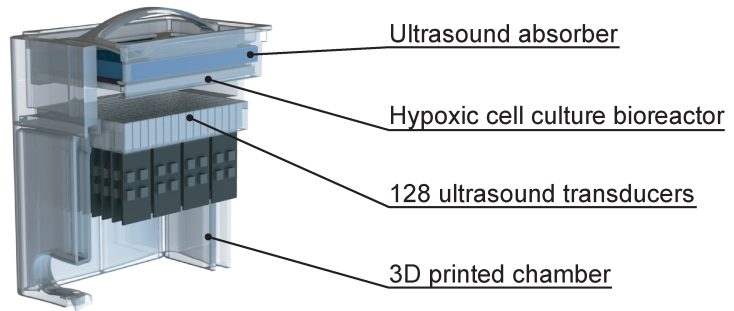


Figure 5: US treatment chamber made for adherent cells (adapted from Paper II)

Table 2: US parameters for adherent cells (5 min sonication) – Papers II–III

Name	Frequency (MHz)	No. of cycles	Duty cycle (%)	Pulse repetition frequency (kHz)	MI	Intensity	
						I _{SPTA} (mW/cm ²)	I _{SPPA} (W/cm ²)
Low	2	20	0.4	22	0.1	3	1
Medium	2	80	1.8	22	0.2	50	2.7
High	2	160	3.6	22	0.378	358	9.64

3.2 Microbubbles (MB)

The MBs used in these studies were SonoVue[®], Sonazoid[™] and Optison[™] (Table 3). SonoVue[®] and Sonazoid[™] are lipid-based MBs where the shell is made of phospholipids, whereas in Optison[™], the protein shell is made of albumin. The importance of MB formulation in sonoporation was explored in Papers I and III.

MBs have limited stability both *in vitro* and *in vivo*. To ensure the consistency of experimental results, it is important to use the MBs within a timeframe during which

their physiochemical properties are unchanged, particularly the size (diameter) and concentration of the MBs. SonoVue[®] was used within 20–30 minutes after reconstitution, and Sonazoid[™] was used within one hour after reconstitution. This timeframe was shorter than the use-by times recommended by the manufacturer (Table 3). Optison[™] was used within 20 minutes after perforation of the vial rubber stopper.

In Paper III, to ensure reproducible exposure of MBs, the size, concentration and polydispersity of the MB formulations were characterized by optical microscopy.

Table 3: Characteristics of the commercial MBs used in the studies (adopted from the Summary of Product Characteristics (SmPC) approved in Norway unless other references are stated)

MB formulation	Mean Diameter	Concentration (MB/ml)	In-use storage*	Recommended dose (adults)	Calculated MB-concentration** (MB/ml)
SonoVue[®] Phospholipid shell	2.5 μm [181]	1-5 x 10 ⁸ [181]	6 hours	Max 2.4 ml	0.048 – 0.24 x 10 ⁶
Sonazoid[™] Phospholipid shell	2.1 μm [182]	12 x 10 ⁸ [182]	2 hours	0.015 ml/kg body weight (example 1.2 ml for 80kg)	0.29 x 10 ⁶
Optison[™] Albumin shell	2.5 – 4.5 μm	5-8 x 10 ⁸	30 min	Normal: 3ml Max: 8.7ml	0.30 – 0.48 x 10 ⁶ 0.87 – 1.39 x 10 ⁶

* SonoVue[®] and Sonazoid[™]: after reconstitution; Optison[™]: after perforation of vial rubber stopper ** Calculation based on 5 litre blood in the human body, not taking elimination into consideration

In Paper I, the dose of MBs was 0.4×10^6 MB/mL, which was above the recommendations of the manufacturers of SonoVue[®] and Sonazoid[™] for use in clinical imaging and diagnostics. Correspondingly, the concentration of MOLM-13 cells was 0.4×10^6 cells/mL (*i.e.* the minimum concentration of cells recommended from the supplier for cell culturing of MOLM-13), resulting in a 1:1 ratio of cell and MBs [155, 183]. Because PBMCs are substantially smaller than MOLM-13 the cell concentration was increased to 3.2×10^6 cell/mL, to achieve approximately the same likelihood of interaction between cells and MBs, (*i.e.* MOLM-13 and PBMCs occupied the same

volume per ml cell culture medium), which was in the range of concentrations of PBMCs commonly found in human blood [184].

The concentration used in a cell culture well or chamber is difficult to translate to an *in vivo* situation when MBs are circulating and being continuously eliminated from the blood. In Paper III, relevant MB concentrations in mice, based on injected dose of MBs and their pharmacokinetics, were calculated. The importance of the MB concentration (0.28×10^6 , 2.8×10^6 , 4.6×10^6 and 6.5×10^6 MB/ml) were evaluated *in vitro*, based on the cellular uptake of calcein. In Paper II, the dose of MBs ($60 \mu\text{l} = 2.8 \times 10^6$ MBs/ml) and formulation (SonazoidTM) were chosen based on the results in Paper III.

3.3 Cell types and cell culture

3.3.1 Suspension cell types

In Paper I, a leukemic cell line (MOLM-13; wild-type p53 [185]) was chosen as the model of cancer cells because suspension cells allowed for high-throughput US treatment in our validated US treatment chamber [179] as well as the rapid and reliable sample preparation for flow cytometry (Figure 7) [186]. Suspension cells were used in a range of sonoporation studies [132, 141, 159]. In addition to blood cancer cells, healthy peripheral blood mononuclear cells (PBMCs) donated by healthy individuals were isolated and sonoporated to assess the effects on healthy blood cells, which are inevitably exposed during sonoporation.

3.3.2 Adherent cell types

The following adherent PDAC cell lines were used: MIA PaCa-2, PANC-1 and BxPC-3. Both MIA PaCa-2 and PANC-1 has KRAS and p53 mutations [187] are major genetic alterations commonly found in PDAC [187-189] and associated with aggressive cancer growth. KRAS mutational status is relevant in signalling studies because it activates the Raf/MAP kinase pathway and the Akt/PKB pathway [188]. BxPC-3 does not have a

KRAS mutation, but it does have a SMAD4 mutation, which is another common mutation in pancreatic cancer; it has been found in approximately half of pancreatic cancers [188].

Non-cancerous cells used in Paper II were primary human vascular endothelial cells derived from umbilical cord veins (HUVEC) and BJ fibroblasts from human foreskin. These are commercially available and further allow for the easy culturing of large numbers of cells. The main findings were repeated in a more relevant model: Cancer-associated fibroblasts (CAF) isolated from patient material. The use of patient material was approved from the regional ethical committee.

3.3.3 Considerations related to cell culture

In the sonoporation literature, a range of different cell types have been used, including both suspension cells and adherent cells. Adherent cell lines detached and suspended before US treatment were also frequently used in *in vitro* sonoporation studies [53, 105, 153, 154, 190]. However, adherent cells are “trapped” in a monolayer and are exposed to MBs in a more reproducible manner compared with cell suspensions when the exposure time is short and the chance that the cells are in the vicinity of MBs is random because both cells and MBs move freely [59]. Kinoshita and Hynynen (2007) found that the method of cell culturing (suspension vs. adherent) could influence studies on uptake and viability [156]. Furthermore, studies on cell signalling indicated that cell adhesion may be important in the signalling responses in certain pathways [191]. Hence, adherent cell lines in suspension were not treated in Paper II and III, and an US treatment chamber was custom-made for experiments with adherent cells.

Adherent cells were cultured and sonoporated in low oxygen transfer cell culture chambers (Petaka G3 LOT®). The use of cell culture chambers was necessary for the US exposure of cells in the treatment chamber, allowing for the cells to be treated upside-down in close contact with floating MBs. Furthermore, the Petaka G3 LOT® mimics the hypoxic intratumoural conditions in pancreatic tumours, which are known

to be very hypoxic [34, 192]. This hypoxia is particularly relevant for intracellular signalling, because hypoxia influences several pathways, such as ER-stress/eIF2 α [22], PI3K [192] and MAPK [192].

The flow cytometric analysis of adherent cells is more challenging compared with blood cells, where flow cytometry is well established. The reason is that adherent cells have to be detached and suspended before the analysis [193]. The detachment process is an experimental factor that may influence the results, so the method must be chosen carefully. Trypsin is a commonly used detachment reagent, but is an activator of cell signalling pathways such as MAPkinase [194] and may interfere with and obscure the signalling induced by sonoporation. To avoid this effect, we used cold ($\approx 0^{\circ}\text{C}$) trypsin, a method that was developed to address this problem in cell signalling studies [193]. At low temperatures, intracellular kinases and phosphatases are inactive, whereas trypsin retains 50% of its activity [193]. Furthermore, the signalling events induced by US application may be transient and decay rapidly after the US is turned off (referred to as 5 min in Paper I and 0 hours in Paper II), which may be preserved better when the cells are put on ice and cooled as soon as possible after sonication. In all experiments, to preserve transient signalling events, the cells were fixed by adding paraformaldehyde. In previous viability studies, Accutase[®] was used for the detachment of cells because it is more gentle than trypsin, and it does not require inactivation and centrifugation after detachment [195].

3.4 Assessment of cell viability

US is known to cause cell lysis [46], depending on the US parameters and cavitation (*i.e.* the addition of MBs). In Paper I, the cell count and concentration were measured immediately after sonoporation and compared with the concentration seeded before sonication. In Paper II, the cell concentration was measured after sonoporation and detachment from the Petaka[™] system. Because the cells were seeded three days before sonoporation and cultured using the Petaka[™], the cell counts could not be directly

compared with counts before sonoporation. The cell counts were therefore compared with the untreated controls in the Petaka™.

The viability of the suspension cells after treatment was assessed by microscopy of cells stained with the cell death marker Hoechst 33342 and by a colony forming assay. Because of the limitations of cell culturing using Petaka™, viability assays were performed after detachment of the cells treated in this system. Microscopy (Trypan Blue) and flow cytometry (Annexin V/PI)-based assays were used to assess cell death. In these assays, the cells were analysed in suspension shortly after detachment. In viability assays requiring longer incubation or analysis on a cell culture plate, the cells were re-seeded on cell culture plates.

3.5 Flow cytometry

Flow cytometry was the main method of cellular analysis used in this thesis. Flow cytometry is used to measure the fluorescence emitted from excited fluorochromes in single cells [196]. Modern flow cytometers allow detection of up to 27 parameters [197], enabling the simultaneous analyses of several extra- and intracellular effectors that participate in cellular processes in different cell types in one sample. Hence, the method is suitable in screening for effects of drugs and other treatments [198, 199]. A LSRII Fortessa was used in multiparameter flow cytometry, and a C6 Accuri was used for a simpler flow analysis with one or two fluorochromes. These instruments were located in the Flow cytometry Core Facility at the University of Bergen.

Flow cytometry allows for the analysis of single cells and subpopulations in the sample, which is an important feature in assessing the population of cells affected by sonoporation. In Papers I-III, we used flow cytometry for three reasons: 1) the assessment of uptake of dyes in single cells; 2) the assessment of cell death; and 3) the investigation of intracellular signal transduction induced by sonoporation in single cells.

3.5.1 Flow cytometric measurements of cellular uptake

In a flow cytometer, the fluorochromes are excited by light of a certain wavelength. They then emit light of a different wavelength, which is detected in the photon multiplier tube (PMT) [200]. In choosing the dyes, it is important to select molecules with the ability to be excited and to emit light (*i.e.* fluorescent molecules). Although the detection of the uptake of real drugs using flow cytometry is of interest, it is limited to only a few fluorescent drugs that are available, which is one reason that fluorescent dyes are often used.

Assessment of uptake of dyes in sonoporated cells, by flow cytometry, is depicted in Figure 6. The dyes that are commonly used in sonoporation research, such as calcein [50, 53, 141, 153-156], FITC-dextran [46, 105, 157-159], SYTOX Green [160] and propidium iodide (PI) [161, 162], are cell-impermeable. Their uptake has been used as a measure of cell permeabilization and successful drug uptake. Their relevance as a measure of drug uptake can be debated (see section 1.5.1). In general, drugs are taken up by cells, whereas these dyes are cell impermeable without the aid of sonoporation. However, because of the latter property, they are well suited as a measure of the permeabilization of the cell membrane.

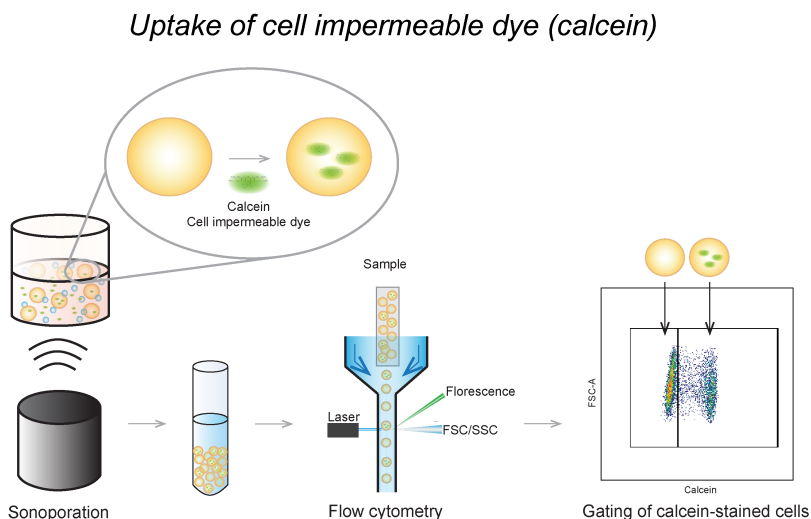


Figure 6: Assessment of uptake of cell impermeable dye, calcein, using flow cytometry (Suspension cells are used as examples)

3.5.2 Analysis of intracellular phosphorylation events

Phospho-specific flow cytometry simultaneously quantifies the phosphorylation levels of intracellular signalling proteins on a single cell level and provides insights into the complex treatment effects in multiple pathway components in signalling networks [198]. The technique requires antibodies that are specific to the phosphorylated form of a protein, which also have sufficient specificity to detect different phospho-epitopes on the same signalling protein [199]. In Papers I and II, intracellular phospho-specific flow cytometry was used to screen several signalling pathways that might be linked to the bioeffects of sonoporation. The use of our US treatment chambers in combination with the barcoding technique [201] allowed for the cell treatment, analysis and comparison of samples treated at variable US intensities both with and without the addition of MBs. Because phosphorylation events are transient and reversible [199], and the kinetics of sonoporation signalling were unknown, samples were taken at two (Paper II) and three (Paper I) timepoints after sonoporation.

Barcoding involves staining the cell samples using succinimidyl esters of Pacific Blue and Pacific Orange [201], prior to the analysis. Individual cell samples are stained with specific concentrations of each dye, which gives them a unique signature that can be identified later using flow cytometry software. This technique increases the speed of acquisition, decreases antibody consumption and lowers or eliminates variability in antibody staining. In Paper I, a 3x3 matrix was used (Figure 7), in which each barcode consisted of the samples harvested at a certain timepoint post-sonoporation (*i.e.* untreated cells, low US, medium US, high US, untreated cells + MB, low US + MB, medium US + MB, high US + MB, and a positive control). The antibody staining of the treated samples was the same as the untreated control to which they were normalized. Varying cell types often require different titrations of Pacific Blue and Orange. In Paper II, the barcodes were reduced to a 2x3 matrix for MIA PaCa-2/HUVEC/fibroblast (Figure 7) (*i.e.*, untreated cells, medium US, high US, medium US + MB, high US + MB, and a positive control) and 2x2 matrix for CAFs (*i.e.*, untreated cells, high US, high

US + MB, and a positive control), to avoid the overlap of the population of the larger cells used in this study. Some smaller optimisations of the concentrations of dyes was also required.

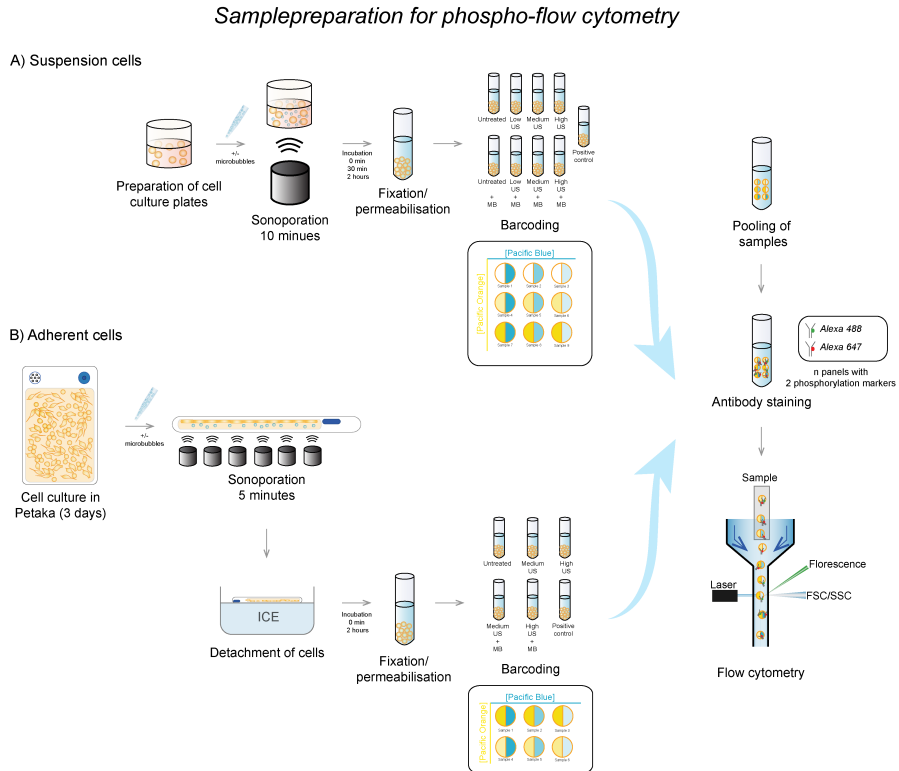


Figure 7: Sample preparation for phosphoflow cytometry

The access to intracellular epitopes requires fixation and permeabilization of the cell membrane [197]. In Paper I and II, methanol was used for permeabilization, which is generally recommended for phosphoflow cytometry [186, 199]. Methanol gives better access to proteins in the cell, including nuclear antigens, but it is also a harsh detergent that can damage surface epitopes. Although it is not required, permeabilization is also advantageous in barcode staining, as there are more targets for the dye to bind inside the cells, leading to reduced dye concentrations and increased signal intensity [202].

The data collected using LSR Fortessa on barcoded samples were de-barcoded and gated using either FlowJo® or DIVA software, as shown in Figure 8. The arcsinh ratio (arcsinh[treated/cofactor]- arcsinh [control/cofactor]) was used to calculate the changes in phosphorylation.

Gating/data analysis for phospho-flow cytometry

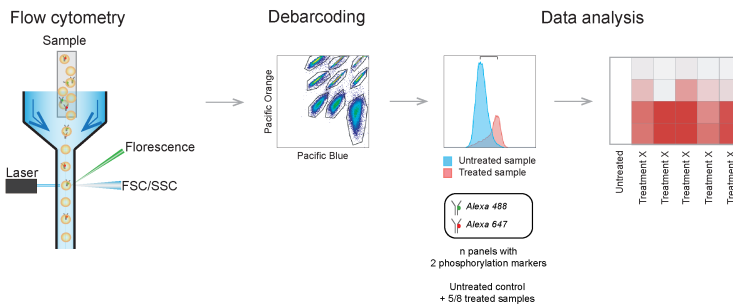


Figure 8: Gating strategy and data analysis of phosphoflow cytometry

3.5.3 Antibody selection

Because the intracellular signalling responses to sonoporation were unknown before this study, antibodies that targeted key proteins in several signalling pathways were selected: p38 and ERK1/2 (MAPK), Akt (PI3K), S6 and 4E-BP1 (mTOR), FAK and Src (Mechanotransduction), CREB and PKA (Ca²⁺ signalling), STAT3 and STAT5 (JAK/STAT), p53 (genotoxic damage) and NF-kB (NF-kB signalling). The panel used in Paper II was revised based on the results in Paper I. However, the limited availability of antibodies suitable for flow cytometry restricted the proteins that were included in the study.

3.5.4 Flow cytometry controls and compensation

In flow cytometry, particularly in phosphoflow, it is recommended to use positive controls to assess antibody affinity and specificity by treating cells with stimuli that elicit a well-known response [199]. There are several reasons why flow cytometric

analysis of certain phospho-proteins is not possible: low affinity to antibodies; buried epitopes within the fixed cellular structure; and unfavourable intracellular localization [199]. In addition, proteins with low abundance may be difficult to detect because of low signal-to-noise ratios [199]. In this work, the flow cytometry of p-eIF2 α (S51) was attempted, but it was unsuccessful. In testing the only available pre-conjugated antibody for flow cytometry, an unacceptably low signal-to-noise ratio was observed. To analyse this protein, we used Western Blot, where increasing the amount of protein loaded on the gel and using super-sensitive chemiluminescent detection (SuperSignal West Femto Maximum sensitivity substrate) allowed us to study the effects of signalling on this protein.

Before the sonoporated cells were analysed, the antibody panels were tested on each cell line/type by examining a barcode of cells treated with various stimuli known to influence the phosphorylation status in cells. In the barcoding and analysis of the sonoporated cells, a sample of the same cell type was treated with a positive control and included in the barcode to show that the barcoded cell sample had been appropriately stained with antibodies. A stimulus that activated several of the proteins in question was used for this purpose (PMA + A23187).

In detecting fluorescence emitted from the fluorochromes, the emission spectra sometimes overlap, and fluorescence from more than one fluorochrome is detected by the PMT. Compensation is needed to correct for the spectral overlap/spill over [197]. In Papers I and II, the cells (in Pacific Blue or Pacific Orange controls) or compensation beads (in antibody controls) that were stained with the fluorochromes used in the study were used as compensation controls to calculate the compensation matrix. The Pacific Blue and Pacific Orange controls were stained by the highest concentration of dye used in the barcode. Because the Accuri C6 instrument has only one laser, compensation was also required for Annexin V (Alexa 488) and PI. Cells stained separately with Annexin V antibody (Alexa 488) and PI were used for the compensation. On the LSRII Fortessa Cytometer Setup and tracking (CST) beads were used to daily check the performance of the instrument.

3.6 *In vivo* sonoporation in combination with paclitaxel

The enhancement of paclitaxel efficacy using SonoVue[®] vs. Sonazoid[™] vs. Optison[™] and low-intensity US was further investigated preclinically in a murine PDAC model.

An orthotopic xenograft model of MIA PaCa-2^{luc} cells in NOD-scid IL2r^{null} mice was used [109]. An orthotopic model is considered the most relevant because tumours are located at a relevant site in the body, and blood flow and vascularisation closely resemble the human cancer that it models [109, 203]. These features may be highly relevant in drug delivery using sonoporation.

Mice receiving no treatment, or paclitaxel alone were used as controls. The treatment groups were paclitaxel + US, paclitaxel + US + SonoVue[®], paclitaxel + US + Sonazoid[™] and paclitaxel + US + Optison[™]. Mice were injected intraperitoneally with 8 mg/mg paclitaxel. Thirty minutes after the injection of paclitaxel, the MB infusion was started with 1–5 x 10⁸ MB/ml (concentration of undiluted SonoVue[®]). Sonazoid[™] and Optison[™] were diluted in glucose (50 mg/ml) to achieve a similar concentration. The tumours were exposed to US (1.8 MHz, DC = 1.1 %, MI = 0.2, I_{SPTA} = 16 mW/cm²) and MB for 10 minutes. Tumour volume and vascularisation were determined using 3D US imaging using a small animal ultrasound imaging system (Vevo 2100, FJIFILM Visualsonics Inc, Ontario Canada).

The experiments using animals were conducted according to The European Convention for the Protection of Vertebrates Used for Scientific Purposes, and approved by The Norwegian Animal Research Authority.

3.7 Statistical methods

In Paper I, unpaired two-tailed t-tests were used for statistical comparisons. An ANOVA was used to assess the significance of the results in Papers II and III. The significance level was set at $p = 0.05$.

Summary of publications

Paper I: Intracellular signalling in Key Pathways Is Induced by Treatment with Ultrasound and Microbubbles in a Leukemia Cell Line, but not in Healthy Peripheral Blood Mononuclear Cells *Pharmaceutics*, 2019

Haugse R, Langer A, Gullaksen S-E, Sundøy SM, Gjertsen BT, Kotopoulis S, McCormack E

The aims of this study was to detect of intracellular signalling responses to sonoporation in two different cell types (*i.e.* leukemic cells and healthy peripheral blood mononuclear cells), and how it was influenced by US intensity and the presence of MBs. This study was complemented by studies on the uptake of a cell-impermeable dye and investigations of cell viability.

The results showed that treatment with US and MBs affected the viability and intracellular signalling in the cells, which may be relevant for the efficacy of sonoporation in enhancing cancer therapy. The cancerous MOLM-13 cells were more susceptible to sonoporation compared with the healthy blood cells.

US alone under clinical diagnostic conditions had no significant effects on cell permeabilization, cell viability, or intracellular protein phosphorylation. The addition of MBs and the surpassing of clinical diagnostic intensities resulted in increased permeabilization efficiency, reduced cell viability and change in phosphorylation status of key proteins in the cancer cells. US + MBs resulted in both early changes (p38, ERK1/2, CREB, STAT3 and Akt) and late changes (ribosomal protein S6 and eIF2 α in protein phosphorylation). The changes observed in protein phosphorylation corresponded to changes in sonoporation efficiency and viability, predominantly in cancer cells. The sonoporation induced changes in protein phosphorylation in healthy cells was less pronounced.

Paper II: Low-intensity sonoporation induced intracellular signalling of pancreatic cancer cells, fibroblasts and endothelial cells (*Manuscript*)

Haugse R, Langer A, Murvold ET, Costea DE, Gjertsen BT, Gilja OH, Kotopoulos S and McCormack E

In this study, the aim was to investigate sonoporation-induced permeabilization (*i.e.* the uptake of cell impermeable dye; calcein), changes in intracellular signalling and viability in a PDAC cancer cell line (MIA PaCa-2), and in cells relevant for the tumour microenvironment (*i.e.* fibroblasts, cancer-associated fibroblasts [CAF] and endothelial cells [HUVEC]).

Different cell types responded differently to US and MBs in the uptake of cell impermeable dye, reduction in viability and intracellular signalling. Sonoporation induced the immediate, transient activation of MAPK-kinases (p38, ERK1/2) and an increase in the phosphorylation of ribosomal protein S6 combined with dephosphorylation of 4E-BP1. The sonoporation stress response resembled cellular responses to electroporation and pore-forming toxins in membrane repair and cellular homeostasis restoration, which may be exploited therapeutically. Moreover, the cells of the tumour microenvironment were more sensitive to sonoporation. Further efforts in optimising sonoporation-enhanced therapy should target the microenvironment.

Paper III: SonoVue® vs Sonazoid™ vs Optison™:

Which bubble is best for low intensity sonoporation of pancreatic ductal adenocarcinoma? (*Manuscript*)

Kotopoulos S, Popa M, Safont MM, Murvold ET, Haugse R, Langer A, Dimcevski G, Lam C, Bjånes TK, Gilja OH, McCormack E

The fastest bench-to-bedside translation of sonoporation involves the use of MBs commercially available for diagnostic purposes. Despite the substantial amount of research in this field, it is currently unknown, which of the different microbubbles available results in the greatest enhancement of therapy.

Three microbubble formulations — lipid-shell SonoVue®, Sonazoid™ and protein-shell Optison™ — were characterized physiochemically (*i.e.* size, concentration and polydispersity) and acoustically (*i.e.* attenuation and cavitation). The *in vitro* comparison of the permeabilization of the cells (*i.e.* the uptake of the cell impermeable dye calcein) indicated that SonoVue® was the best microbubble at lower US intensities, whereas Sonazoid™ performed better at higher intensities. SonoVue® was confirmed to be the best at low US intensity in an PDAC orthotopic murine model. The results of the preclinical study indicated that any commercial ultrasound contrast agent and diagnostic ultrasound imaging system could be used to significantly enhance the therapeutic efficacy of chemotherapy (*i.e.* paclitaxel).

4. Discussion

Understanding the phenomenon and optimising all relevant parameters is a complex task, as sonoporation is governed by many experimental parameters and bioeffects and comprises diverse scientific fields [39, 63]. Recent review papers [63, 64, 168] attempted to summarize and clarify the effects of the experimental parameters used in *in vitro* sonoporation. However, it is difficult to draw any final conclusions regarding optimal sonoporation parameters based on the existing literature because of the variety of experimental set-ups and parameters that have been used. For this reason, an extensive discussion of the experimental US and MB parameters used in the context of the current literature is beyond the scope of this thesis.

The effects of US and MB parameters were investigated using our experimental platforms by correlating commonly used measures, such as the uptake of impermeable dye (*i.e.* calcein) [104, 153-155, 157, 160] and cell viability [141, 153, 156, 157, 160], to the previously largely unknown intracellular signalling induced by sonoporation. The experiments were performed using a range of cell types, both suspension and adherent. Overall, the same trends in uptake and intracellular mechanisms were observed in the different cell types but of different magnitudes and timing. Intracellular signalling was generally activated in cells that were permeabilized, predominantly in cell types that had the highest percentage of permeabilized cells. The downstream effects on viability could be related to US intensity above a certain threshold, and they varied between the cell types, indicating that their biological and molecular characteristics properties also affected sonoporation outcomes. The studies on intracellular signalling were conducted at a higher US intensity than that used in the preclinical trial. Further studies are required to establish its clinical relevance.

The translation of the *in vitro* results to *in vivo* sonoporation is limited, as described in section 4.3. However, in Paper III the effects of MB formulation found *in vitro* and also in simulations were confirmed *in vivo*.

4.1 Factors influencing sonoporation

4.1.1 Ultrasound parameters

As expected based on the literature reviews [63, 168], the permeabilization of cells (*i.e.* calcein uptake) relied on the presence of MB. Therefore, the discussion of US parameters is mainly in the context of MBs. Furthermore, because of the chosen settings, the discussion of the US parameters is focused on US intensity (I_{SPTA}). To aid the readability in the different manuscripts, the terms Low US, Medium US and High US refer to different parameters in Paper I (suspension cells), Paper II and Paper III (adherent cells) (see Table 1 and Table 2). Increased intensity was achieved by increasing the duty cycle (*i.e.* the number of cycles) and MI, and the importance of these parameters was not investigated separately. In particular, MI is a parameter that influences sonoporation [53, 113], which should be investigated independently in future research.

In all three papers, increasing the US intensity increased the cellular responses, which is in agreement with previous studies [63]. Increased permeabilization (*i.e.* calcein uptake) at increasing US intensity was reproduced in all three papers until this effect plateaued. In the literature, increasing intensity is also linked to reduced viability [63]. The US parameters used in these studies only had minor and predominantly non-significant influences on cell viability, which was expected at an $MI \leq 0.4$ [59]. The viability of MOLM-13 (Paper I) was reduced when the intensity was raised above the recommended limit (FDA; 720 mW/cm^2 [57, 60]), but as reduced cell counts/colony forming ability after incubation and not as immediate cell lysis. The reduced growth of cancer cells could potentially have a therapeutic application. The viability of PBMCs was not reduced, even when the 10-minute sonication in a cell culture plate was worse than in an *in vivo* setting where these cells were circulating. However, these results are insufficient to conclude whether the upper FDA intensity limit is appropriate for therapeutic sonoporation.

Permeabilization measured as calcein uptake seemed to correlate with activation of the signalling pathways. In terms of signalling, US intensity was not a major factor, as long

as it was high enough to induce the permeabilization of the cells. Regarding clinical translatability, investigations at a lower mW/cm^2 would have been of interest due to the current acoustic output from commercial diagnostic ultrasound systems when emitting long pulses.

The preclinical study demonstrated that sonoporation improved survival and inhibited tumour growth at a very low ultrasound intensity close to $15 \text{ mW}/\text{cm}^2$ (I_{SPTA}). SonoVue[®]+US significantly increased paclitaxel efficacy on mouse survival, which was not observed in the previous study using the same murine model and SonoVue[®] but higher US intensity ($688 \text{ mW}/\text{cm}^2$) [109]. This may possibly demonstrate the need to optimize MB formulation and US parameters in relation to each other. However, the use of a different drug (gemcitabine) with different pharmacokinetics may also be the reason for this observation. In general, the comparison with previously published studies is difficult because most were performed in subcutaneous models and often at higher intensities ($1\text{--}3 \text{ mW}/\text{cm}^2$), although it is not always stated if intensity is I_{SPTA} , I_{SPPA} or I_{SATA} [31, 50, 79, 81, 107, 108].

4.1.2 Microbubbles, microbubble formulation and dose

The physiochemical characterization of MBs confirmed the concentration and size of MBs in the SmPC literature (Table 3). However, shorter in-use storage times after reconstitution is recommended to assure reproducibility in the experiments, particularly in SonoVue[®], where the MB diameter increased and the concentration decreased after 30 minutes, indicating the coalescence of MBs.

In Paper I, the results indicated that Sonazoid[™] MBs were more effective than SonoVue[®] MBs in this limited experimental set up. In Paper III, the results also showed that Sonazoid[™] was more efficient when the US intensity was above $15 \text{ mW}/\text{cm}^2$. In Paper I, US intensities below $15 \text{ mW}/\text{cm}^2$ were not explored. However, as mentioned above, the results for the suspension cells and the adherent cells cannot be compared directly. In Paper III, SonoVue[®] and Optison[™] were better than Sonazoid[™] below $15 \text{ mW}/\text{cm}^2$. The *in vivo* study demonstrated that at the preclinically relevant US parameters ($16 \text{ mW}/\text{cm}^2$), SonoVue[®] was the preferable MB. This study suggests that

the *in vitro* assessment of permeabilization rate may be indicative of *in vivo* outcome, but this may depend on the MBs and US used [103].

In Paper III, permeabilization (*i.e.* calcein uptake) increased with increasing MB concentrations in the adherent cells until it plateaued at higher concentrations. Contrary to expectations, the concentration of MB in MOLM-13 did not have a significant effect on the calcein uptake.

4.1.3 Cell types, and properties of the cells

The sensitivity of and responses to sonoporation differed among all the cell types used in this study, and indicate that variability can be expected among the cells in a tumour. The uptake of the cell-impermeable dye calcein varied from 26 % to approximately 90% even with the addition of the same MB and the same US parameters (SonazoidTM + high US used as example). Although the percentage of the suspension cells that took up calcein could not be directly compared to the adherent cells (see section 3.3.3), lower percentages of suspension cells than adherent cells were permeabilized. This was expected because of the reduced chance and shorter duration of interaction between the suspension cells and the MBs [59], and is primarily relevant for the evaluation of the methodological aspects of *in vitro* sonoporation experiments.

In Paper I, the calcein uptake, reduction in viability and activation of intracellular signalling was higher in the larger MOLM 13 than in the smaller, healthy PBMCs. In previous studies, cancer cells were observed to be susceptible to sonoporation [204, 205], potentially because of the different cell size, morphology or faster growth rates of cancer cells. In Paper II, the results showed that healthy HUVECs and fibroblast cells experienced higher calcein uptake as well as greater influence on viability and intracellular signalling than the cancer cells, which indicates that cancer cells vs. healthy cells are not a determining factor in sonoporation sensitivity. Furthermore, in Paper III, the results demonstrated substantial variations between PDAC cancer cell lines, which aligns with previous comparisons of leukemic cell lines and breast cancer cell lines [183, 206]. Cell size is suggested to influence sonoporation sensitivity [205], but this was not confirmed in Paper II based on the calcein uptake in small HUVECs vs. large HUV-EC-

C cells (*i.e.* the HUVEC cell line). Because sonoporation directly influences the cell membrane, we hypothesize that the properties, such as composition and fluidity, of the cell membrane are important factors in the differences observed between the cell lines. Differences in membrane stiffness, resulting from different phases in the cell cycle, has been found to influence sonoporation efficiency [207].

The influence on healthy cells inevitably exposed to US + MB is relevant for the safety assessment of sonoporation even when low-intensity US is used. Chromosome aberrations in human lymphocytes in response to low-intensity US were reported in the 1970s [208]. However, these results could not be reproduced [56, 57]. In Paper I, US intensity above the current FDA limitations did not have negative effects on PBMCs despite the long exposure to US (*i.e.* 10 minutes).

Only the primary CAFs were extensively lysed in the US and MB conditions used. This effect on CAF viability is interesting because of their crucial role in the formation of the desmoplastic stroma in PDAC and their vital role in supporting and promoting tumour growth and induction in chemoresistance [8, 9].

4.2 Intracellular signal transduction

Prior to the studies conducted for this thesis, the signalling responses to sonoporation were largely unknown although some effects were anticipated based on the bioeffects described in section 1.6. However, signalling induced by US (without MBs) has received attention, particularly in relation to mechanotransduction involving integrin/FAK [171, 172] and Rho/ROCK/Src [176]. In the studies conducted for this thesis, the mechanotransduction pathways were not significantly activated by sonoporation although minor increases in phosphorylation were observed in adherent cells treated with US without MBs. With the addition of MBs, the trend was to the deactivation of the pathways.

As mentioned above, the presence of MBs was important for the activation of intracellular signalling in these studies, and there was a possible correlation between the

extent of calcein uptake (representing permeabilization) and the magnitude of the activation of MAPK signalling (p38, ERK1/2, CREB, STAT3). Overall, in Papers I and II, the same pathways were activated in the different cell types although the extent and timing of the activation differed, which suggests that these were general mechanisms generated by sonoporation. Because of the possible correlation to uptake calcein, we hypothesize that this activation of intracellular signalling is a result of membrane permeabilization.

In addition to the differences in permeabilization (as discussed above), the molecular characteristics of each cell type may also explain differences in magnitude and timing of signalling events. For example, the reasons for the low activation of MAPK in MIA PaCa-2 may have been both low level of sonoporation and the insensitivity to MAPK activation because of constitutive activation of this pathway downstream of the KRAS mutation in this cell line [187].

4.2.1 MAPK – sonoporation membrane repair?

The immediate increase of p38 phosphorylation was observed in all the cell lines used in both Paper I and II. In MOLM-13, MIA PaCa-2 and fibroblasts sonoporation caused the immediate activation of ERK1/2 as well as Akt in MOLM-13. In previous studies on US, the activation of p38, ERK1/2 and Akt in other cell types was observed (without MBs) [171, 172, 174] and US increased cell growth. In our studies, the responses did not lead to major changes in viability with the exception at high US intensity (MI = 0.4, DC = 37 %, $I_{SPPA} = 5 \text{ W/cm}^2$ and $I_{SPTA} = 2079 \text{ mW/cm}^2$) + MB in MOLM-13. The immediate activation of p38 and ERK1/2 observed in the fibroblasts, MIA PaCa-2 and MOLM-13 was more likely due to cellular signalling to initiate membrane repair following pore formation. This activation resembled the transient activation of MAP-kinases p38, ERK1/2 shown in cells exposed to pore-forming toxins as a part of membrane repair following pore formation and osmotic stress [209, 210] in response to electroporation [211]. In HUVECs p38 and ERK1/2, the activation was delayed or weak.

The hypothesis on membrane repair is further supported in Paper I by the pronounced activation of the transcription factor CREB in MOLM-13. PKA/PKC and p38 signalling, PKA and CREB signalling and Ca^{2+} -influx were part of the general mechanism in stimulating cell membrane recovery [212], and CREB was involved in the recovery of cells after pore formation by pore-forming toxins [209]. Previous studies also showed that sonoporation increased intracellular $[\text{Ca}^{2+}]$ [139, 140, 145, 146] and that extracellular Ca^{2+} was important for pore re-sealing and membrane repair after sonoporation [152, 163].

The repair of pores in the cell membrane is required for cells to maintain viability after transient sonoporation, which is referred to as repairable sonoporation [169]. As mentioned in section 1.6.1, the repair mechanism is still not fully known but has been suggested to involve Ca^{2+} -influx, shear stress, endocytosis and the exocytosis of lysosomes and to resemble membrane repair in cells exposed to pore-forming toxins [64, 169]. The mechanism includes blebbing, depending on Ca^{2+} , which was suggested to be a part of cells' anti-stress machinery [151]. The activation of intracellular signalling found in Papers I and II provided further insights into cells' stress response and recovery from sonoporation in a repair mechanism similar to other pore-forming actions on the cell membrane. Furthermore, it is important to note that the sensitivity of this sonoporation-induced stress is different in different cell types.

Pore size has been shown to be an important factor in repairable sonoporation, where cells with large pores have less ability to repair the cell membrane [160, 169]. Pore duration and the kinetics of re-sealing are also important, and they are influenced by the US parameters and presence of MBs [160]. Because Ca^{2+} -influx is an universal trigger of membrane repair [212], its role may potentially explain the different responses in different cell types. The sensitivity to intracellular Ca^{2+} -increase that stimulates membrane repair and survival differs among cell types [212], and furthermore the magnitude of $[\text{Ca}^{2+}]$ -increase after membrane damage has been shown to determine the fate of the cells [213]. The role of Ca^{2+} -influx in sonoporation signalling that leads to membrane repair should be further investigated.

4.2.2 Translational control through Ribosomal protein S6, 4E-BP1 and eIF2 α

As expected, based on existing knowledge about sonoporation and ER-stress [141], eIF2 α was activated by high US + MB (beyond the recommendations for US imaging [57, 60]). In Paper I, the relationship between phosphorylation of eIF2 α and ribosomal protein S6 showed an inverse trend. The activation of ribosomal protein S6 was absent under US \pm MB conditions where cellular viability was decreased although the role of S6 activation in this context is not yet known. S6 can be activated downstream of ERK [18], but under conditions of reduced viability, ERK was activated whereas S6 was not.

Ribosomal protein S6 is typically linked to an increase in cell growth while the phosphorylation of eIF2 α and dephosphorylation of 4E-BP1 may reduce cell growth, through their roles in protein translation – the final step on expression of genes into proteins and an important part of biosynthesis [20, 21, 214]. Under stressful conditions, the dephosphorylation of 4E-BP1 has been found to be a part of protein synthesis suppression through the unfolded protein response (UPR) to restoring cellular homeostasis combined with the well-known phosphorylation of eIF2 α [215]. In the cellular response to pore-forming toxins, the full activation of UPR to restore cellular homeostasis further depended on the activation of p38 [216]. Similar to MAPK signalling, as discussed above, a similar response was activated by electroporation (pore formation), where the dephosphorylation of 4E-BP1 and the phosphorylation of eIF2 α suppressed protein synthesis [217]. Based on these results, we hypothesize that cellular recovery after pore formation by sonoporation involves the suppression of protein translation through 4E-BP1 and eIF2 α , perhaps involving UPR and MAPK (Figure 9). Under severe or prolonged stress, this signalling causes cells to go into apoptosis, which was observed in response to ER stress [141].

Sonoporation stress-response

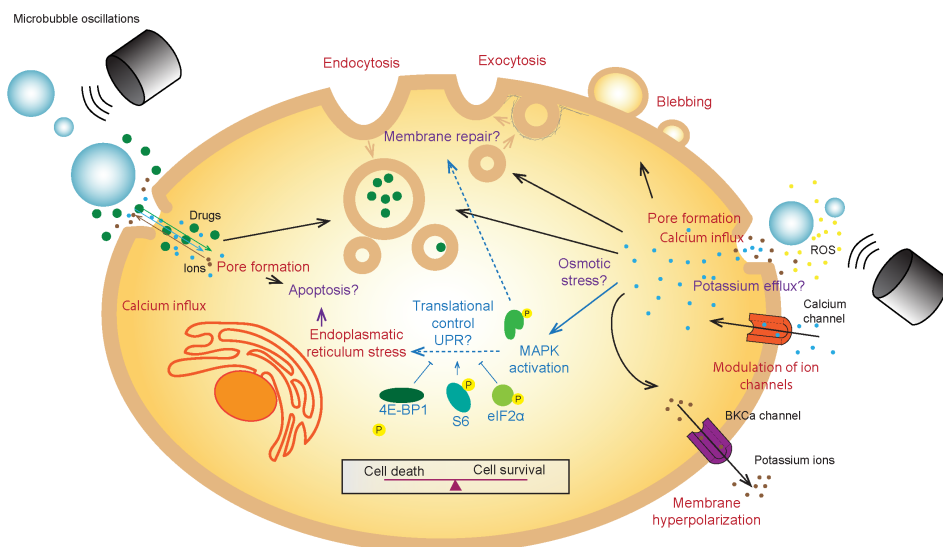


Figure 9: Sonoporation-induced intracellular signalling (blue) is a part of the cellular stress response, which is likely involved in membrane repair and translational control to restore cellular homeostasis

4.2.3 Therapeutic benefit from intracellular cell stress?

Cell stress has been suggested to contribute to the enhanced therapeutic efficacy of sonoporation [132, 218]. The pathways we found to be activated by sonoporation are a part of cell survival and the restoration of cellular homeostasis after sonoporation. Under prolonged stress, they induce apoptosis [215, 219], which can be exploited to enhance the efficacy of cancer therapy. In Paper I, this enhancement was achieved by using MB + high US ($MI = 0.4$, $DC = 37\%$, $I_{SPPA} = 5 \text{ W/cm}^2$ and $I_{SPTA} = 2079 \text{ mW/cm}^2$). In Paper II, it was achieved by treatment with a MEK/ERK-inhibitor prior to sonoporation, which was previously hypothesized to inhibit cell recovery [209]. Similarly, chemotherapeutics induces various cellular stress that may be enhanced by the addition of sonoporation in therapy. A further approach used to inhibit signalling pathways by sonoporation was delivery of transcription factor STAT3 decoy [220], a concept that can be further potentiated in the context of sonoporation-induced signalling.

Some sonoporation-induced signalling may contribute to the anti-cancer effects of sonoporation. For example, the inhibition of 4E-BP1 in CAFs was found to repress the secretion of proteins involved in chemoresistance and enhance the efficacy of chemotherapy (gemcitabine) in PDAC therapy [221]. In Paper II, CAFs were mechanically damaged by sonoporation, and 4E-BP1 was dephosphorylated in the remaining cells. If these effects occur *in vivo*, they may at least partially explain the increased efficacy of gemcitabine by the addition of sonoporation in PDAC [62, 109].

4.3 Suitability of methods and limitations of the studies

4.3.1 In vitro cell culture and ultrasound exposure

In this thesis, a limitation of all the *in vitro* experiments is that the cells were cultured under static conditions without the regulation of liquid flow, temperature or gas saturation. HUVECs cultured under shear stress were shown to experience less membrane disruption and change in intracellular Ca^{2+} concentration upon sonoporation [148], indicating that sonoporation may be less damaging *in vivo*. Neither treatment of cells in suspension nor attachment to a plastic surface represented realistic conditions of for neither *in vivo* US nor MB exposure. The MB circulated *in vivo*, and the parameters inducing MB oscillations in cell culture medium were not directly transferrable to MB behaviour in blood, which has a different composition, different viscosity and different gas saturation. Furthermore, each cell type was studied separately, and the results did not reveal interaction between the same cells and/or different cell types. The application of US on plastic can lead to acoustic aberrations in the cell culture plates in Paper I and in the Petakas™ system in Papers II and III. Generally, all cell culture experiments using US may have limited US transmission through the plastic in culture wells and chambers, resulting in the conversion of mode, the generation of heat and the potential formation of standing waves [222].

Predominantly commercially available cell lines were used in the experiments. Although they are useful in biomedical research because of their convenience, they do not replicate the properties of primary cells; therefore, clinical relevance and translation

may be limited [223]. In this work, particularly in using Petakas™, it was necessary to obtain a large number of cells. The pancreatic cancer lines are used extensively, and they represent the most common mutations found in PDAC [188]. BJ fibroblasts obtained from human foreskin are the least representative of tumour cells, so the study was supplemented by primary cancer-associated fibroblasts. The use of primary cancer-associated fibroblasts substantially limited the study parameters and the replication of the experiments. In addition, the cells were extensively detached from the plastic surface in Petaka™, and they were lysed by sonoporation. It cannot be ruled out that this effect was caused by the conditions under which the cells were cultured. Because of the interesting observations of the fibroblasts and CAFs, and the importance of these cells in tumour microenvironments and drug resistance, these cells should be prioritized in future studies.

The use of the Petaka™ cell culture chambers caused specific limitations, as many cell culture assays were designed for the use of cell culture plates. The choice of assays, including viability assays and protein translation assays, that could be performed was limited to either assays that could be performed in Petaka™ or that could tolerate the detachment and re-seeding of cells. The use Petakas™ resulted in an additional limitation regarding the HUVEC cells. The manufacturer recommends changing the cell culture medium for these cells every second day, which was not possible because it would have disturbed the hypoxic conditions. To ensure consistency, the setup and similar culturing conditions were the same for all adherent cell types.

4.3.2 Uptake of cell impermeable dye

The uptake of impermeable dyes does not distinguish between uptakes resulting from pore formation and those from other mechanisms, such as endocytosis. However, it may not be problematic because endocytosis is suggested to be a consequence of pore formation, not separate events [166]. However, it was difficult to determine because the assay did not yield any information about the mechanism of the uptake.

4.3.3 Phosphoflow cytometry

In studies on intracellular signalling, the number of replicates is low and the variability is rather high, particularly in adherent cells. In our experiments, we prioritized the screening of intracellular signalling pathways. Further studies may prioritize an increased number of replicates to validate these initial findings. Mechanotransduction signalling cannot be completely ruled out, and the lack of significant results may be due to the combination of low numbers of replicates and the transience and absence of signalling when the US is turned off. The research on mechanotransduction should await the development of better models. It is widely accepted that studies on the mechanical stimuli, such as US, of cells are more realistic using a 3D scaffold with the multicellular complexity and ECM of an organ [222].

To the best of our knowledge, phosphoflow cytometry has not been used previously to study intracellular signalling induced by sonoporation. A main advantage of this method is that it could be used to design panels where several pathways could be screened simultaneously, which allowed us to screen key proteins in important signalling pathways. Furthermore, the rapid sample preparation by fixation in paraformaldehyde may have been an advantage because the activation of some proteins was very transient. However, some proteins were found to be activated in Paper I (*i.e.* CREB and weak STAT3 phosphorylation) but not in Paper II. In particular, in Paper II, CREB and PKA were not activated as expected by the positive control, and we could not conclude that these proteins were not activated by sonoporation. Limited access to intracellular targets or low abundance could have produced false negatives.

The full potential of flow cytometry was not exploited in the study on PBMC, as the subpopulations (*i.e.* T-cells, B-cells, NK-cells, monocytes and dendritic cells) were not separated using surface markers. The expected MeOH damage to relevant epitopes limited the availability surface markers [224], and it would have been difficult to relate the results to calcein uptake and viability assays. Although no major signalling events were observed, the effects on small subpopulations may have been obscured. In future studies on PBMCs, gentler permeabilization may allow for staining a range of

subpopulations, particularly if methods such as mass cytometry were used, which would allow for the detection of over 40 cellular markers [225].

4.3.4 Preclinical study

Even though an orthotopic model was used, it is still a xenograft of a cell line (MIA PaCa-2) without a humanized tumour microenvironment nor an immune system. Hence, this model does not fully represent the cellular complexity or tumour microenvironment in a human tumour, which we hypothesize to be important for sonoporation efficacy based on the findings in Papers II and III. Development of patient derived xenografts with a human immune system [226] would improve the translatability of preclinical optimizations of sonoporation parameters. A role of sonoporation in cancer immunotherapy has been suggested but is so far largely unknown [227].

Furthermore, in this preclinical study therapy started when the tumours were very small. This makes it more difficult to target the tumours accurately. The concentrations of MBs used were much higher than what has been used in humans [62], but this is nevertheless difficult to compare because of different biodistribution, pharmacokinetics and elimination in mice and humans.

5. Concluding remarks

The studies comprising this thesis revealed new insights into intracellular signalling and cell stress mechanisms caused by sonoporation. It is intriguing to note that these mechanisms seemed to be related to pore formation, which was originally hypothesized as the mechanism of sonoporation. However, our results extend to cell stress, which may be exploited therapeutically instead of just diffusion of drugs across the cell membrane. However, because of the limitations in the experimental setup and the US and MB parameters used, the clinical relevance of our results must be confirmed in more appropriate models. The fact that intracellular stress signalling was activated at US intensities below the current diagnostic limitations in healthy cells, such as fibroblasts and HUVECs, may also affect what is considered appropriate and safe in clinical diagnostic use.

Although there is increasing understanding that the efficacy of sonoporation in the enhancement of cancer therapy is beyond the diffusion of drugs through pores created in the cell membrane, the findings *in vivo* were correlated to the *in vitro* results for the permeabilization of cells, indicating that the permeabilization rate may be indicative of sonoporation efficiency. It is not possible to provide absolute recommendations for the best US parameters or MB formulations because the studies showed that they are highly interdependent. However, the results of the studies included in this thesis support that sonoporation using very low-intensity US and commercial MBs could improve cancer therapy.

6. Future perspectives

Better models, such as a 3D organoid with relevant cell types and connective tissue mimicking a tumour microenvironment, are needed to determine the sonoporation mechanism. Such models should take into account the relevance and interplay of different cell types and the relevance of mechanical effects (*e.g.*, damage and cell lysis) compared with intracellular stress responses, taking into account blood flow and tissue perfusion. Our research group is developing a fully vascularised and perfused PDAC organoid model which may be an optimal mid-point between *in vitro* and *in vivo* experimentation. Repeating the work in in paper II using this model could increase the clinical translatability of the results of the observed intracellular signalling.

Papers I and II contribute to the knowledge about how cells respond to the stress induced by sonoporation and potentially to the understanding of the membrane repair mechanisms following pore formation. However, our methodology did not allow for direct evidence of membrane repair initiation by MAPK and eIF2 α /UPR/mTOR signalling; therefore, better evidence should be provided. The therapeutic benefit of cell stress and the inhibition of membrane repair, such as by ERK inhibition, should be further explored, particularly in combination with chemotherapeutics.

Because different effects on protein translation may be required in different sonoporation applications, such as the enhancement of chemotherapy vs. gene delivery, the sonoporation parameters should be optimised according to each purpose. The mechanism of translational control should be further investigated using assays to quantitate protein translation in relation to sonoporation parameters.

7. References

1. WHO Cancer Fact Sheet. February 2015 [cited 2018; Available from: <https://www.who.int/en/news-room/fact-sheets/detail/cancer>.
2. Wilson, B.E., et al., Estimates of global chemotherapy demands and corresponding physician workforce requirements for 2018 and 2040: a population-based study. *Lancet Oncol*, **2019**. DOI: 10.1016/S1470-2045(19)30163-9.
3. Vasan, N., J. Baselga, and D.M. Hyman, A view on drug resistance in cancer. *Nature*, **2019**. 575(7782): p. 299-309. DOI: 10.1038/s41586-019-1730-1.
4. *Cancer Treatment & Survivorship Facts & Figures 2019-2021*. 2019, American Cancer Society: Atlanta.
5. Hanahan, D. and R.A. Weinberg, The hallmarks of cancer. *Cell*, **2000**. 100(1): p. 57-70.
6. Hanahan, D. and R.A. Weinberg, Hallmarks of cancer: the next generation. *Cell*, **2011**. 144(5): p. 646-74. DOI: 10.1016/j.cell.2011.02.013.
7. Thomas, D. and P. Radhakrishnan, Tumor-stromal crosstalk in pancreatic cancer and tissue fibrosis. *Mol Cancer*, **2019**. 18(1): p. 14. DOI: 10.1186/s12943-018-0927-5.
8. Sun, Q., et al., The impact of cancer-associated fibroblasts on major hallmarks of pancreatic cancer. *Theranostics*, **2018**. 8(18): p. 5072-5087. DOI: 10.7150/thno.26546.
9. Huang, W., et al., New Insights into the Tumor Microenvironment Utilizing Protein Array Technology. *Int J Mol Sci*, **2018**. 19(2). DOI: 10.3390/ijms19020559.
10. Broders-Bondon, F., et al., Mechanotransduction in tumor progression: The dark side of the force. *J Cell Biol*, **2018**. 217(5): p. 1571-1587. DOI: 10.1083/jcb.201701039.
11. Sever, R. and J.S. Brugge, Signal transduction in cancer. *Cold Spring Harb Perspect Med*, **2015**. 5(4). DOI: 10.1101/cshperspect.a006098.
12. Cannon, A., et al., Desmoplasia in pancreatic ductal adenocarcinoma: insight into pathological function and therapeutic potential. *Genes Cancer*, **2018**. 9(3-4): p. 78-86. DOI: 10.18632/genesandcancer.171.
13. Harvey, A., Overview of Cell Signaling Pathways in Cancer, in *Predictive Biomarkers in Oncology*, K.G. Badve S., Editor. 2019, Springer, Cham.
14. Bianco, R., et al., Key cancer cell signal transduction pathways as therapeutic targets. *Eur J Cancer*, **2006**. 42(3): p. 290-4. DOI: 10.1016/j.ejca.2005.07.034.
15. Dhillon, A.S., et al., MAP kinase signalling pathways in cancer. *Oncogene*, **2007**. 26(22): p. 3279-90. DOI: 10.1038/sj.onc.1210421.
16. Burotto, M., et al., The MAPK pathway across different malignancies: a new perspective. *Cancer*, **2014**. 120(22): p. 3446-56. DOI: 10.1002/cncr.28864.
17. Zou, X. and M. Blank, Targeting p38 MAP kinase signaling in cancer through post-translational modifications. *Cancer Lett*, **2017**. 384: p. 19-26. DOI: 10.1016/j.canlet.2016.10.008.
18. Populo, H., J.M. Lopes, and P. Soares, The mTOR signalling pathway in human cancer. *Int J Mol Sci*, **2012**. 13(2): p. 1886-918. DOI: 10.3390/ijms13021886.
19. Zhang, S., et al., The Prognostic Role of Ribosomal Protein S6 Kinase 1 Pathway in Patients With Solid Tumors: A Meta-Analysis. *Front Oncol*, **2019**. 9: p. 390. DOI: 10.3389/fonc.2019.00390.
20. Qin, X., B. Jiang, and Y. Zhang, 4E-BP1, a multifactor regulated multifunctional protein. *Cell Cycle*, **2016**. 15(6): p. 781-6. DOI: 10.1080/15384101.2016.1151581.
21. Wang, R., S. Ganesan, and X.F. Zheng, Yin and yang of 4E-BP1 in cancer. *Cell Cycle*, **2016**. 15(11): p. 1401-2. DOI: 10.1080/15384101.2016.1168200.
22. Rozpedek, W., et al., The Role of the PERK/eIF2alpha/ATF4/CHOP Signaling Pathway in Tumor Progression During Endoplasmic Reticulum Stress. *Curr Mol Med*, **2016**. 16(6): p. 533-44.
23. Madden, E., et al., The role of the unfolded protein response in cancer progression: From oncogenesis to chemoresistance. *Biol Cell*, **2019**. 111(1): p. 1-17. DOI: 10.1111/boc.201800050.

24. Bong, A.H.L. and G.R. Monteith, Calcium signaling and the therapeutic targeting of cancer cells. *Biochim Biophys Acta Mol Cell Res*, **2018**. 1865(11 Pt B): p. 1786-1794. DOI: 10.1016/j.bbamcr.2018.05.015.
25. Thomas, S.J., et al., The role of JAK/STAT signalling in the pathogenesis, prognosis and treatment of solid tumours. *Br J Cancer*, **2015**. 113(3): p. 365-71. DOI: 10.1038/bjc.2015.233.
26. Gough, D.J., L. Koetz, and D.E. Levy, The MEK-ERK pathway is necessary for serine phosphorylation of mitochondrial STAT3 and Ras-mediated transformation. *PLoS One*, **2013**. 8(11): p. e83395. DOI: 10.1371/journal.pone.0083395.
27. Xia, L., et al., Role of the NFkappaB-signaling pathway in cancer. *Onco Targets Ther*, **2018**. 11: p. 2063-2073. DOI: 10.2147/OTT.S161109.
28. Zilfou, J.T. and S.W. Lowe, Tumor suppressive functions of p53. *Cold Spring Harb Perspect Biol*, **2009**. 1(5): p. a001883. DOI: 10.1101/cshperspect.a001883.
29. Mantovani, F., L. Collavin, and G. Del Sal, Mutant p53 as a guardian of the cancer cell. *Cell Death Differ*, **2019**. 26(2): p. 199-212. DOI: 10.1038/s41418-018-0246-9.
30. Qu, Y., et al., Tumor microenvironment-driven non-cell-autonomous resistance to antineoplastic treatment. *Mol Cancer*, **2019**. 18(1): p. 69. DOI: 10.1186/s12943-019-0992-4.
31. BurrIDGE, K., E. Monaghan-Benson, and D.M. Graham, Mechanotransduction: from the cell surface to the nucleus via RhoA. *Philos Trans R Soc Lond B Biol Sci*, **2019**. 374(1779): p. 20180229. DOI: 10.1098/rstb.2018.0229.
32. Cooper, J. and F.G. Giancotti, Integrin Signaling in Cancer: Mechanotransduction, Stemness, Epithelial Plasticity, and Therapeutic Resistance. *Cancer Cell*, **2019**. 35(3): p. 347-367. DOI: 10.1016/j.ccell.2019.01.007.
33. Leprivier, G., et al., Stress-mediated translational control in cancer cells. *Biochim Biophys Acta*, **2015**. 1849(7): p. 845-60. DOI: 10.1016/j.bbagr.2014.11.002.
34. Orth, M., et al., Pancreatic ductal adenocarcinoma: biological hallmarks, current status, and future perspectives of combined modality treatment approaches. *Radiat Oncol*, **2019**. 14(1): p. 141. DOI: 10.1186/s13014-019-1345-6.
35. Grasso, C., G. Jansen, and E. Giovannetti, Drug resistance in pancreatic cancer: Impact of altered energy metabolism. *Crit Rev Oncol Hematol*, **2017**. 114: p. 139-152. DOI: 10.1016/j.critrevonc.2017.03.026.
36. Nizzero, S., A. Ziemys, and M. Ferrari, Transport Barriers and Oncophysics in Cancer Treatment. *Trends Cancer*, **2018**. 4(4): p. 277-280. DOI: 10.1016/j.trecan.2018.02.008.
37. Stewart, M.P., R. Langer, and K.F. Jensen, Intracellular Delivery by Membrane Disruption: Mechanisms, Strategies, and Concepts. *Chem Rev*, **2018**. 118(16): p. 7409-7531. DOI: 10.1021/acs.chemrev.7b00678.
38. Park, K., Focused ultrasound for targeted nanoparticle delivery to tumors. *J Control Release*, **2010**. 146(3): p. 263. DOI: 10.1016/j.jconrel.2010.08.001.
39. Boissenot, T., et al., Ultrasound-triggered drug delivery for cancer treatment using drug delivery systems: From theoretical considerations to practical applications. *J Control Release*, **2016**. 241: p. 144-163. DOI: 10.1016/j.jconrel.2016.09.026.
40. Ojha, T., et al., Pharmacological and physical vessel modulation strategies to improve EPR-mediated drug targeting to tumors. *Adv Drug Deliv Rev*, **2017**. 119: p. 44-60. DOI: 10.1016/j.addr.2017.07.007.
41. Prabhakar, U., et al., Challenges and key considerations of the enhanced permeability and retention effect for nanomedicine drug delivery in oncology. *Cancer Res*, **2013**. 73(8): p. 2412-7. DOI: 10.1158/0008-5472.CAN-12-4561.
42. Jhaveri, A., P. Deshpande, and V. Torchilin, Stimuli-sensitive nanopreparations for combination cancer therapy. *J Control Release*, **2014**. 190: p. 352-70. DOI: 10.1016/j.jconrel.2014.05.002.
43. Kirn, T.F., Microbubbles show promise for enhancing ultrasound signal, image, other applications. *JAMA*, **1989**. 261(11): p. 1542.
44. Luginbuehl, V., et al., Intracellular drug delivery: Potential usefulness of engineered Shiga toxin subunit B for targeted cancer therapy. *Biotechnol Adv*, **2018**. 36(3): p. 613-623. DOI: 10.1016/j.biotechadv.2018.02.005.

45. Bao, S., B.D. Thrall, and D.L. Miller, Transfection of a reporter plasmid into cultured cells by sonoporation in vitro. *Ultrasound Med Biol*, **1997**. 23(6): p. 953-9.
46. Ward, M., J. Wu, and J.F. Chiu, Ultrasound-induced cell lysis and sonoporation enhanced by contrast agents. *J Acoust Soc Am*, **1999**. 105(5): p. 2951-7.
47. Gehl, J., Electroporation: theory and methods, perspectives for drug delivery, gene therapy and research. *Acta Physiol Scand*, **2003**. 177(4): p. 437-47. DOI: 10.1046/j.1365-201X.2003.01093.x.
48. Unger, E.C., T.P. McCreery, and R.H. Sweitzer, Ultrasound enhances gene expression of liposomal transfection. *Invest Radiol*, **1997**. 32(12): p. 723-7.
49. Greenleaf, W.J., et al., Artificial cavitation nuclei significantly enhance acoustically induced cell transfection. *Ultrasound Med Biol*, **1998**. 24(4): p. 587-95.
50. Watanabe, Y., et al., Low-intensity ultrasound and microbubbles enhance the antitumor effect of cisplatin. *Cancer Sci*, **2008**. 99(12): p. 2525-31. DOI: 10.1111/j.1349-7006.2008.00989.x.
51. Escoffre, J.M., et al., Doxorubicin delivery into tumor cells with ultrasound and microbubbles. *Mol Pharm*, **2011**. 8(3): p. 799-806. DOI: 10.1021/mp100397p.
52. Heath, C.H., et al., Microbubble therapy enhances anti-tumor properties of cisplatin and cetuximab in vitro and in vivo. *Otolaryngol Head Neck Surg*, **2012**. 146(6): p. 938-45. DOI: 10.1177/0194599812436648.
53. Sorace, A.G., et al., Microbubble-mediated ultrasonic techniques for improved chemotherapeutic delivery in cancer. *J Drug Target*, **2012**. 20(1): p. 43-54. DOI: 10.3109/1061186X.2011.622397.
54. Snipstad, S., et al., Sonopermeation to improve drug delivery to tumors: from fundamental understanding to clinical translation. *Expert Opin Drug Deliv*, **2018**: p. 1-13. DOI: 10.1080/17425247.2018.1547279.
55. Meijering, B.D., et al., Ultrasound and microbubble-targeted delivery of macromolecules is regulated by induction of endocytosis and pore formation. *Circ Res*, **2009**. 104(5): p. 679-87. DOI: 10.1161/CIRCRESAHA.108.183806.
56. O'Brien, W.D., Jr., Ultrasound-biophysics mechanisms. *Prog Biophys Mol Biol*, **2007**. 93(1-3): p. 212-55. DOI: 10.1016/j.pbiomolbio.2006.07.010.
57. Postema, M., Fundamentals of Medical Ultrasonics. 2011: Taylor & Francis Group.
58. Miller, D.L., et al., Overview of therapeutic ultrasound applications and safety considerations. *J Ultrasound Med*, **2012**. 31(4): p. 623-34. DOI: 10.7863/jum.2012.31.4.623.
59. ter Haar, G., Safety and bio-effects of ultrasound contrast agents. *Med Biol Eng Comput*, **2009**. 47(8): p. 893-900. DOI: 10.1007/s11517-009-0507-3.
60. *Marketing Clearance of Diagnostic Ultrasound Systems and Transducers*. 2019: <https://www.fda.gov/media/71100/download>.
61. Apfel, R.E. and C.K. Holland, Gauging the likelihood of cavitation from short-pulse, low-duty cycle diagnostic ultrasound. *Ultrasound Med Biol*, **1991**. 17(2): p. 179-85.
62. Dimcevski, G., et al., A human clinical trial using ultrasound and microbubbles to enhance gemcitabine treatment of inoperable pancreatic cancer. *J Control Release*, **2016**. 243: p. 172-181. DOI: 10.1016/j.jconrel.2016.10.007.
63. Yu, H. and L. Xu, Cell experimental studies on sonoporation: state of the art and remaining problems. *J Control Release*, **2014**. 174: p. 151-60. DOI: 10.1016/j.jconrel.2013.11.010.
64. Lentacker, I., et al., Understanding ultrasound induced sonoporation: definitions and underlying mechanisms. *Adv Drug Deliv Rev*, **2014**. 72: p. 49-64. DOI: 10.1016/j.addr.2013.11.008.
65. Forbes, M.M., R.L. Steinberg, and W.D. O'Brien, Jr., Examination of inertial cavitation of Optison in producing sonoporation of chinese hamster ovary cells. *Ultrasound Med Biol*, **2008**. 34(12): p. 2009-18. DOI: 10.1016/j.ultrasmedbio.2008.05.003.
66. Forbes, M.M., R.L. Steinberg, and W.D. O'Brien, Jr., Frequency-dependent evaluation of the role of definity in producing sonoporation of Chinese hamster ovary cells. *J Ultrasound Med*, **2011**. 30(1): p. 61-9. DOI: 10.7863/jum.2011.30.1.61.
67. Sirsi, S. and M. Borden, Microbubble Compositions, Properties and Biomedical Applications. *Bubble Sci Eng Technol*, **2009**. 1(1-2): p. 3-17. DOI: 10.1179/175889709X446507.

68. Senior, R., et al., Comparison of sulfur hexafluoride microbubble (SonoVue)-enhanced myocardial contrast echocardiography with gated single-photon emission computed tomography for detection of significant coronary artery disease: a large European multicenter study. *J Am Coll Cardiol*, **2013**. 62(15): p. 1353-61. DOI: 10.1016/j.jacc.2013.04.082.
69. Uemura, H., et al., Usefulness of perflubutane microbubble-enhanced ultrasound in imaging and detection of prostate cancer: phase II multicenter clinical trial. *World J Urol*, **2013**. 31(5): p. 1123-8. DOI: 10.1007/s00345-012-0833-1.
70. Takahashi, M., et al., Contrast-enhanced intraoperative ultrasonography using perfluorobutane microbubbles for the enumeration of colorectal liver metastases. *Br J Surg*, **2012**. 99(9): p. 1271-7. DOI: 10.1002/bjs.8844.
71. Correas, J.M., et al., Contrast enhanced ultrasound in the detection of liver metastases: a prospective multi-centre dose testing study using a perfluorobutane microbubble contrast agent (NC100100). *Eur Radiol*, **2011**. 21(8): p. 1739-46. DOI: 10.1007/s00330-011-2114-6.
72. Afadzi, M., et al., Mechanisms of the ultrasound-mediated intracellular delivery of liposomes and dextrans. *IEEE Trans Ultrason Ferroelectr Freq Control*, **2013**. 60(1): p. 21-33. DOI: 10.1109/TUFFC.2013.2534.
73. Paula, D.M., et al., Therapeutic ultrasound promotes plasmid DNA uptake by clathrin-mediated endocytosis. *J Gene Med*, **2011**. 13(7-8): p. 392-401. DOI: 10.1002/jgm.1586.
74. Lionetti, V., et al., Enhanced caveolae-mediated endocytosis by diagnostic ultrasound in vitro. *Ultrasound Med Biol*, **2009**. 35(1): p. 136-43. DOI: 10.1016/j.ultrasmedbio.2008.07.011.
75. Tomizawa, M., et al., Irradiation with ultrasound of low output intensity increased chemosensitivity of subcutaneous solid tumors to an anti-cancer agent. *Cancer Lett*, **2001**. 173(1): p. 31-5.
76. Escoffre, J.-M. and A. Bouakaz, *Therapeutic Ultrasound*. 2016, Springer International Publishing : Imprint: Springer: Cham.
77. Suzuki, R. and A.L. Klibanov, Co-administration of Microbubbles and Drugs in Ultrasound-Assisted Drug Delivery: Comparison with Drug-Carrying Particles. *Adv Exp Med Biol*, **2016**. 880: p. 205-20. DOI: 10.1007/978-3-319-22536-4_12.
78. Lammertink, B., et al., Duration of ultrasound-mediated enhanced plasma membrane permeability. *Int J Pharm*, **2015**. 482(1-2): p. 92-8. DOI: 10.1016/j.ijpharm.2014.12.013.
79. Iwanaga, K., et al., Local delivery system of cytotoxic agents to tumors by focused sonoporation. *Cancer Gene Ther*, **2007**. 14(4): p. 354-63. DOI: 10.1038/sj.cgt.7701026.
80. Matsuo, M., et al., Synergistic inhibition of malignant melanoma proliferation by melphalan combined with ultrasound and microbubbles. *Ultrason Sonochem*, **2011**. 18(5): p. 1218-24. DOI: 10.1016/j.ulsonch.2011.03.005.
81. Lammertink, B.H., et al., Sonochemotherapy: from bench to bedside. *Front Pharmacol*, **2015**. 6: p. 138. DOI: 10.3389/fphar.2015.00138.
82. Christiansen, C., et al., Physical and biochemical characterization of Albutex, a new ultrasound contrast agent consisting of air-filled albumin microspheres suspended in a solution of human albumin. *Biotechnol Appl Biochem*, **1994**. 19 (Pt 3): p. 307-20.
83. Bokor, D., et al., Clinical safety of SonoVue, a new contrast agent for ultrasound imaging, in healthy volunteers and in patients with chronic obstructive pulmonary disease. *Invest Radiol*, **2001**. 36(2): p. 104-9.
84. Morel, D.R., et al., Human pharmacokinetics and safety evaluation of SonoVue, a new contrast agent for ultrasound imaging. *Invest Radiol*, **2000**. 35(1): p. 80-5.
85. Kendall, M.R., et al., Scaled-Up Production of Monodisperse, Dual Layer Microbubbles Using Multi-Array Microfluidic Module for Medical Imaging and Drug Delivery. *Bubble Sci Eng Technol*, **2012**. 4(1): p. 12-20. DOI: 10.1179/1758897912Y.0000000004.
86. Bettinger, T. and F. Tranquart, Design of Microbubbles for Gene/Drug Delivery. *Adv Exp Med Biol*, **2016**. 880: p. 191-204. DOI: 10.1007/978-3-319-22536-4_11.
87. Wible, J., Jr., et al., Effects of inhaled gases on the ultrasound contrast produced by microspheres containing air or perfluoropropane in anesthetized dogs. *Invest Radiol*, **1998**. 33(12): p. 871-9.

88. Parrales, M.A., et al., Acoustic characterization of monodisperse lipid-coated microbubbles: relationship between size and shell viscoelastic properties. *J Acoust Soc Am*, **2014**. *136*(3): p. 1077. DOI: 10.1121/1.4890643.
89. Martin, K.H. and P.A. Dayton, Current status and prospects for microbubbles in ultrasound theranostics. *Wiley Interdiscip Rev Nanomed Nanobiotechnol*, **2013**. *5*(4): p. 329-45. DOI: 10.1002/wnan.1219.
90. Ibsen, S., et al., A novel nested liposome drug delivery vehicle capable of ultrasound triggered release of its payload. *J Control Release*, **2011**. *155*(3): p. 358-66. DOI: 10.1016/j.jconrel.2011.06.032.
91. Unger, E., et al., Cardiovascular drug delivery with ultrasound and microbubbles. *Adv Drug Deliv Rev*, **2014**. *72*: p. 110-26. DOI: 10.1016/j.addr.2014.01.012.
92. Suzuki, R., et al., Effective gene delivery with novel liposomal bubbles and ultrasonic destruction technology. *Int J Pharm*, **2008**. *354*(1-2): p. 49-55. DOI: 10.1016/j.ijpharm.2007.10.034.
93. Fan, X., et al., Inhibition of prostate cancer growth using doxorubicin assisted by ultrasound-targeted nanobubble destruction. *Int J Nanomedicine*, **2016**. *11*: p. 3585-96. DOI: 10.2147/IJN.S111808.
94. Wheatley, M.A., et al., Surfactant-stabilized contrast agent on the nanoscale for diagnostic ultrasound imaging. *Ultrasound Med Biol*, **2006**. *32*(1): p. 83-93. DOI: 10.1016/j.ultrasmedbio.2005.08.009.
95. Seo, M., R. Williams, and N. Matsuura, Size reduction of cosolvent-infused microbubbles to form acoustically responsive monodisperse perfluorocarbon nanodroplets. *Lab Chip*, **2015**. *15*(17): p. 3581-90. DOI: 10.1039/c5lc00315f.
96. Kotopoulos, S., et al., Acoustically Active Antibubbles. *Acta Physica Polonica A*, **2015**. *127*(1): p. 99-102.
97. Poortinga, A.T., Long-lived antibubbles: stable antibubbles through Pickering stabilization. *Langmuir*, **2011**. *27*(6): p. 2138-41. DOI: 10.1021/la1048419.
98. Silpe, J.E., et al., Generation of Antibubbles from Core-Shell Double Emulsion Templates Produced by Microfluidics. *Langmuir*, **2013**. *29*(28): p. 8782-8787. DOI: 10.1021/la4009015.
99. Kotopoulos, S., et al., Sonoporation with Acoustic Cluster Therapy (ACT(R)) induces transient tumour volume reduction in a subcutaneous xenograft model of pancreatic ductal adenocarcinoma. *J Control Release*, **2017**. *245*: p. 70-80. DOI: 10.1016/j.jconrel.2016.11.019.
100. van Wamel, A., et al., Acoustic Cluster Therapy (ACT) enhances the therapeutic efficacy of paclitaxel and Abraxane(R) for treatment of human prostate adenocarcinoma in mice. *J Control Release*, **2016**. *236*: p. 15-21. DOI: 10.1016/j.jconrel.2016.06.018.
101. Wamel, A., et al., Acoustic Cluster Therapy (ACT) - pre-clinical proof of principle for local drug delivery and enhanced uptake. *J Control Release*, **2016**. *224*: p. 158-64. DOI: 10.1016/j.jconrel.2016.01.023.
102. Sontum, P., et al., Acoustic Cluster Therapy (ACT)--A novel concept for ultrasound mediated, targeted drug delivery. *Int J Pharm*, **2015**. *495*(2): p. 1019-27. DOI: 10.1016/j.ijpharm.2015.09.047.
103. Bressand, D., et al., Enhancing Nab-Paclitaxel Delivery Using Microbubble-Assisted Ultrasound in a Pancreatic Cancer Model. *Mol Pharm*, **2019**. DOI: 10.1021/acs.molpharmaceut.9b00416.
104. Lammertink, B.H.A., et al., Increase of intracellular cisplatin levels and radiosensitization by ultrasound in combination with microbubbles. *J Control Release*, **2016**. *238*: p. 157-165. DOI: 10.1016/j.jconrel.2016.07.049.
105. Mariglia, J., et al., Analysis of the cytotoxic effects of combined ultrasound, microbubble and nucleoside analog combinations on pancreatic cells in vitro. *Ultrasonics*, **2018**. *89*: p. 110-117. DOI: 10.1016/j.ultras.2018.05.002.
106. Bjanec, T., et al., Ultrasound- and Microbubble-Assisted Gemcitabine Delivery to Pancreatic Cancer Cells. *Pharmaceutics*, **2020**. *12*(2). DOI: 10.3390/pharmaceutics12020141.
107. Hirabayashi, F., et al., Epidermal growth factor receptor-targeted sonoporation with microbubbles enhances therapeutic efficacy in a squamous cell carcinoma model. *PLoS One*, **2017**. *12*(9): p. e0185293. DOI: 10.1371/journal.pone.0185293.

108. Zhao, Y.Z., et al., Enhancing chemotherapeutic drug inhibition on tumor growth by ultrasound: an in vivo experiment. *J Drug Target*, **2011**. 19(2): p. 154-60. DOI: 10.3109/10611861003801834.
109. Kotopoulis, S., et al., Sonoporation-enhanced chemotherapy significantly reduces primary tumour burden in an orthotopic pancreatic cancer xenograft. *Mol Imaging Biol*, **2014**. 16(1): p. 53-62. DOI: 10.1007/s11307-013-0672-5.
110. Bush, N., et al., Therapeutic Dose Response of Acoustic Cluster Therapy in Combination With Irinotecan for the Treatment of Human Colon Cancer in Mice. *Front Pharmacol*, **2019**. 10: p. 1299. DOI: 10.3389/fphar.2019.01299.
111. Kinoshita, M., et al., Noninvasive localized delivery of Herceptin to the mouse brain by MRI-guided focused ultrasound-induced blood-brain barrier disruption. *Proc Natl Acad Sci U S A*, **2006**. 103(31): p. 11719-23. DOI: 10.1073/pnas.0604318103.
112. Lin, C.Y., et al., Quantitative and qualitative investigation into the impact of focused ultrasound with microbubbles on the triggered release of nanoparticles from vasculature in mouse tumors. *J Control Release*, **2010**. 146(3): p. 291-8. DOI: 10.1016/j.jconrel.2010.05.033.
113. Yemane, P.T., et al., Effect of Ultrasound on the Vasculature and Extravasation of Nanoscale Particles Imaged in Real Time. *Ultrasound Med Biol*, **2019**. 45(11): p. 3028-3041. DOI: 10.1016/j.ultrasmedbio.2019.07.683.
114. Lin, C.Y., et al., Enhancement of focused ultrasound with microbubbles on the treatments of anticancer nanodrug in mouse tumors. *Nanomedicine*, **2012**. 8(6): p. 900-7. DOI: 10.1016/j.nano.2011.10.005.
115. Theek, B., et al., Sonoporation enhances liposome accumulation and penetration in tumors with low EPR. *J Control Release*, **2016**. 231: p. 77-85. DOI: 10.1016/j.jconrel.2016.02.021.
116. Wang, Y., et al., Clinical study of ultrasound and microbubbles for enhancing chemotherapeutic sensitivity of malignant tumors in digestive system. *Chin J Cancer Res*, **2018**. 30(5): p. 553-563. DOI: 10.21147/j.issn.1000-9604.2018.05.09.
117. Ultrasound-enhanced Delivery of Chemotherapy to Patients With Liver Metastasis From Breast- and Colorectal Cancer. [Internet] 2018 November 14 [cited 2019 May 21]; Available from: <https://ClinicalTrials.gov/show/NCT03477019>.
118. KVUS at Neoadjuvant CTx of Breast Cancer. [Internet] 2017 December 28 [cited 2019 May 21]; Available from: <https://ClinicalTrials.gov/show/NCT03385200>.
119. Targeted Delivery of Chemotherapy With Ultrasound and Microbubbles. [Internet] 2018 March 29 [cited 2019 May 21]; Available from: <https://ClinicalTrials.gov/show/NCT03458975>.
120. Logan, K., et al., Targeted chemo-sonodynamic therapy treatment of breast tumours using ultrasound responsive microbubbles loaded with paclitaxel, doxorubicin and Rose Bengal. *Eur J Pharm Biopharm*, **2019**. 139: p. 224-231. DOI: 10.1016/j.ejpb.2019.04.003.
121. Wood, A.K. and C.M. Sehgal, A review of low-intensity ultrasound for cancer therapy. *Ultrasound Med Biol*, **2015**. 41(4): p. 905-28. DOI: 10.1016/j.ultrasmedbio.2014.11.019.
122. Dasgupta, A., et al., Ultrasound-mediated drug delivery to the brain: principles, progress and prospects. *Drug Discov Today Technol*, **2016**. 20: p. 41-48. DOI: 10.1016/j.ddtec.2016.07.007.
123. Lipsman, N., et al., Blood-brain barrier opening in Alzheimer's disease using MR-guided focused ultrasound. *Nat Commun*, **2018**. 9(1): p. 2336. DOI: 10.1038/s41467-018-04529-6.
124. Non-invasive Blood-brain Barrier Opening in Alzheimer's Disease Patients Using Focused Ultrasound. [Internet] February 18, 2020 [cited 2020 March 8]; Available from: <https://clinicaltrials.gov/ct2/show/NCT04118764>.
125. Carpentier, A., et al., Clinical trial of blood-brain barrier disruption by pulsed ultrasound. *Sci Transl Med*, **2016**. 8(343): p. 343re2. DOI: 10.1126/scitranslmed.aaf6086.
126. NN, R., *World first: blood-brain barrier opened non-invasively to deliver chemotherapy – Sunnybrook Hospital*. 2015: Sunnybrook Canada.
127. Delalande, A., et al., Sonoporation: mechanistic insights and ongoing challenges for gene transfer. *Gene*, **2013**. 525(2): p. 191-9. DOI: 10.1016/j.gene.2013.03.095.

128. Endo-Takahashi, Y., et al., Efficient siRNA delivery using novel siRNA-loaded Bubble liposomes and ultrasound. *Int J Pharm*, **2012**. 422(1-2): p. 504-9. DOI: 10.1016/j.ijpharm.2011.11.023.
129. Endo-Takahashi, Y., et al., Systemic delivery of miR-126 by miRNA-loaded Bubble liposomes for the treatment of hindlimb ischemia. *Sci Rep*, **2014**. 4: p. 3883. DOI: 10.1038/srep03883.
130. Endo-Takahashi, Y., et al., pDNA-loaded Bubble liposomes as potential ultrasound imaging and gene delivery agents. *Biomaterials*, **2013**. 34(11): p. 2807-13. DOI: 10.1016/j.biomaterials.2012.12.018.
131. Kvistad, C.E., et al., Contrast-enhanced sonothrombolysis in acute ischemic stroke patients without intracranial large-vessel occlusion. *Acta Neurol Scand*, **2018**. 137(2): p. 256-261. DOI: 10.1111/ane.12861.
132. Chen, X., J.M. Wan, and A.C. Yu, Sonoporation as a cellular stress: induction of morphological repression and developmental delays. *Ultrasound Med Biol*, **2013**. 39(6): p. 1075-86. DOI: 10.1016/j.ultrasmedbio.2013.01.008.
133. Bouakaz, A., A. Zeghimi, and A.A. Doinikov, Sonoporation: Concept and Mechanisms. *Adv Exp Med Biol*, **2016**. 880: p. 175-89. DOI: 10.1007/978-3-319-22536-4_10.
134. Mehier-Humbert, S., et al., Plasma membrane poration induced by ultrasound exposure: implication for drug delivery. *J Control Release*, **2005**. 104(1): p. 213-22. DOI: 10.1016/j.jconrel.2005.01.007.
135. Schlicher, R.K., et al., Mechanism of intracellular delivery by acoustic cavitation. *Ultrasound Med Biol*, **2006**. 32(6): p. 915-24. DOI: 10.1016/j.ultrasmedbio.2006.02.1416.
136. De Cock, I., et al., Ultrasound and microbubble mediated drug delivery: acoustic pressure as determinant for uptake via membrane pores or endocytosis. *J Control Release*, **2015**. 197: p. 20-8. DOI: 10.1016/j.jconrel.2014.10.031.
137. Delalande, A., et al., Efficient Gene Delivery by Sonoporation Is Associated with Microbubble Entry into Cells and the Clathrin-Dependent Endocytosis Pathway. *Ultrasound Med Biol*, **2015**. 41(7): p. 1913-26. DOI: 10.1016/j.ultrasmedbio.2015.03.010.
138. Zhong, W., et al., Sonoporation induces apoptosis and cell cycle arrest in human promyelocytic leukemia cells. *Ultrasound Med Biol*, **2011**. 37(12): p. 2149-59. DOI: 10.1016/j.ultrasmedbio.2011.09.012.
139. Honda, H., et al., Role of intracellular calcium ions and reactive oxygen species in apoptosis induced by ultrasound. *Ultrasound Med Biol*, **2004**. 30(5): p. 683-92. DOI: 10.1016/j.ultrasmedbio.2004.02.008.
140. Juffermans, L.J., et al., Ultrasound and microbubble-induced intra- and intercellular bioeffects in primary endothelial cells. *Ultrasound Med Biol*, **2009**. 35(11): p. 1917-27. DOI: 10.1016/j.ultrasmedbio.2009.06.1091.
141. Zhong, W., et al., Induction of endoplasmic reticulum stress by sonoporation: linkage to mitochondria-mediated apoptosis initiation. *Ultrasound Med Biol*, **2013**. 39(12): p. 2382-92. DOI: 10.1016/j.ultrasmedbio.2013.08.005.
142. Ando, H., et al., An echo-contrast agent, Levovist, lowers the ultrasound intensity required to induce apoptosis of human leukemia cells. *Cancer Lett*, **2006**. 242(1): p. 37-45. DOI: 10.1016/j.canlet.2005.10.032.
143. Feril, L.B., Jr., et al., Apoptosis induced by the sonomechanical effects of low intensity pulsed ultrasound in a human leukemia cell line. *Cancer Lett*, **2005**. 221(2): p. 145-52. DOI: 10.1016/j.canlet.2004.08.034.
144. Wang, M., et al., Sonoporation-induced cell membrane permeabilization and cytoskeleton disassembly at varied acoustic and microbubble-cell parameters. *Sci Rep*, **2018**. 8(1): p. 3885. DOI: 10.1038/s41598-018-22056-8.
145. Kumon, R.E., et al., Spatiotemporal effects of sonoporation measured by real-time calcium imaging. *Ultrasound Med Biol*, **2009**. 35(3): p. 494-506. DOI: 10.1016/j.ultrasmedbio.2008.09.003.
146. Fan, Z., et al., Intracellular delivery and calcium transients generated in sonoporation facilitated by microbubbles. *J Control Release*, **2010**. 142(1): p. 31-9. DOI: 10.1016/j.jconrel.2009.09.031.

147. van Rooij, T., et al., Viability of endothelial cells after ultrasound-mediated sonoporation: Influence of targeting, oscillation, and displacement of microbubbles. *J Control Release*, **2016**. 238: p. 197-211. DOI: 10.1016/j.jconrel.2016.07.037.
148. Park, J., Z. Fan, and C.X. Deng, Effects of shear stress cultivation on cell membrane disruption and intracellular calcium concentration in sonoporation of endothelial cells. *J Biomech*, **2011**. 44(1): p. 164-9. DOI: 10.1016/j.jbiomech.2010.09.003.
149. Shamout, F.E., et al., Enhancement of non-invasive trans-membrane drug delivery using ultrasound and microbubbles during physiologically relevant flow. *Ultrasound Med Biol*, **2015**. 41(9): p. 2435-48. DOI: 10.1016/j.ultrasmedbio.2015.05.003.
150. Helfield, B., et al., Biophysical insight into mechanisms of sonoporation. *Proc Natl Acad Sci U S A*, **2016**. 113(36): p. 9983-8. DOI: 10.1073/pnas.1606915113.
151. Leow, R.S., J.M. Wan, and A.C. Yu, Membrane blebbing as a recovery manoeuvre in site-specific sonoporation mediated by targeted microbubbles. *J R Soc Interface*, **2015**. 12(105). DOI: 10.1098/rsif.2015.0029.
152. Hu, Y., J.M. Wan, and A.C. Yu, Membrane perforation and recovery dynamics in microbubble-mediated sonoporation. *Ultrasound Med Biol*, **2013**. 39(12): p. 2393-405. DOI: 10.1016/j.ultrasmedbio.2013.08.003.
153. Guzman, H.R., et al., Ultrasound-mediated disruption of cell membranes. I. Quantification of molecular uptake and cell viability. *J Acoust Soc Am*, **2001**. 110(1): p. 588-96.
154. Guzman, H.R., et al., Ultrasound-mediated disruption of cell membranes. II. Heterogeneous effects on cells. *J Acoust Soc Am*, **2001**. 110(1): p. 597-606.
155. Guzman, H.R., et al., Bioeffects caused by changes in acoustic cavitation bubble density and cell concentration: a unified explanation based on cell-to-bubble ratio and blast radius. *Ultrasound Med Biol*, **2003**. 29(8): p. 1211-22.
156. Kinoshita, M. and K. Hynynen, Key factors that affect sonoporation efficiency in in vitro settings: the importance of standing wave in sonoporation. *Biochem Biophys Res Commun*, **2007**. 359(4): p. 860-5. DOI: 10.1016/j.bbrc.2007.05.153.
157. Karshafian, R., et al., Sonoporation by ultrasound-activated microbubble contrast agents: effect of acoustic exposure parameters on cell membrane permeability and cell viability. *Ultrasound Med Biol*, **2009**. 35(5): p. 847-60. DOI: 10.1016/j.ultrasmedbio.2008.10.013.
158. Karshafian, R., et al., Microbubble mediated sonoporation of cells in suspension: clonogenic viability and influence of molecular size on uptake. *Ultrasonics*, **2010**. 50(7): p. 691-7. DOI: 10.1016/j.ultras.2010.01.009.
159. Ward, M., J. Wu, and J.F. Chiu, Experimental study of the effects of Optison concentration on sonoporation in vitro. *Ultrasound Med Biol*, **2000**. 26(7): p. 1169-75.
160. Zeghimi, A., J.M. Escoffre, and A. Bouakaz, Role of endocytosis in sonoporation-mediated membrane permeabilization and uptake of small molecules: a electron microscopy study. *Phys Biol*, **2015**. 12(6): p. 066007. DOI: 10.1088/1478-3975/12/6/066007.
161. van Wamel, A., et al., Vibrating microbubbles poking individual cells: drug transfer into cells via sonoporation. *J Control Release*, **2006**. 112(2): p. 149-55. DOI: 10.1016/j.jconrel.2006.02.007.
162. Kooiman, K., et al., Sonoporation of endothelial cells by vibrating targeted microbubbles. *J Control Release*, **2011**. 154(1): p. 35-41. DOI: 10.1016/j.jconrel.2011.04.008.
163. Deng, C.X., et al., Ultrasound-induced cell membrane porosity. *Ultrasound Med Biol*, **2004**. 30(4): p. 519-26. DOI: 10.1016/j.ultrasmedbio.2004.01.005.
164. Fan, Z., et al., Spatiotemporally controlled single cell sonoporation. *Proc Natl Acad Sci U S A*, **2012**. 109(41): p. 16486-91. DOI: 10.1073/pnas.1208198109.
165. Piscaglia, F., et al., The EFSUMB Guidelines and Recommendations on the Clinical Practice of Contrast Enhanced Ultrasound (CEUS): update 2011 on non-hepatic applications. *Ultraschall Med*, **2012**. 33(1): p. 33-59. DOI: 10.1055/s-0031-1281676.
166. Hauser, J., et al., Ultrasound enhanced endocytotic activity of human fibroblasts. *Ultrasound Med Biol*, **2009**. 35(12): p. 2084-92. DOI: 10.1016/j.ultrasmedbio.2009.06.1090.
167. Juffermans, L.J., et al., Transient permeabilization of cell membranes by ultrasound-exposed microbubbles is related to formation of hydrogen peroxide. *Am J Physiol Heart Circ Physiol*, **2006**. 291(4): p. H1595-601. DOI: 10.1152/ajpheart.01120.2005.

168. Qin, P., et al., Mechanistic understanding the bioeffects of ultrasound-driven microbubbles to enhance macromolecule delivery. *J Control Release*, **2018**. 272: p. 169-181. DOI: 10.1016/j.jconrel.2018.01.001.
169. Yang, F., et al., Experimental study on cell self-sealing during sonoporation. *J Control Release*, **2008**. 131(3): p. 205-10. DOI: 10.1016/j.jconrel.2008.07.038.
170. Zhou, Y., et al., Effects of extracellular calcium on cell membrane resealing in sonoporation. *J Control Release*, **2008**. 126(1): p. 34-43. DOI: 10.1016/j.jconrel.2007.11.007.
171. Whitney, N.P., et al., Integrin-mediated mechanotransduction pathway of low-intensity continuous ultrasound in human chondrocytes. *Ultrasound Med Biol*, **2012**. 38(10): p. 1734-43. DOI: 10.1016/j.ultrasmedbio.2012.06.002.
172. Sato, M., et al., Low-intensity pulsed ultrasound activates integrin-mediated mechanotransduction pathway in synovial cells. *Ann Biomed Eng*, **2014**. 42(10): p. 2156-63. DOI: 10.1007/s10439-014-1081-x.
173. Takeuchi, R., et al., Low-intensity pulsed ultrasound activates the phosphatidylinositol 3 kinase/Akt pathway and stimulates the growth of chondrocytes in three-dimensional cultures: a basic science study. *Arthritis Res Ther*, **2008**. 10(4): p. R77. DOI: 10.1186/ar2451.
174. Tang, C.H., et al., Ultrasound stimulates cyclooxygenase-2 expression and increases bone formation through integrin, focal adhesion kinase, phosphatidylinositol 3-kinase, and Akt pathway in osteoblasts. *Mol Pharmacol*, **2006**. 69(6): p. 2047-57. DOI: 10.1124/mol.105.022160.
175. Xie, S., et al., Low-intensity pulsed ultrasound promotes the proliferation of human bone mesenchymal stem cells by activating PI3K/Akt signaling pathways. *J Cell Biochem*, **2019**. 120(9): p. 15823-15833. DOI: 10.1002/jcb.28853.
176. Zhou, S., et al., Molecular mechanisms of low intensity pulsed ultrasound in human skin fibroblasts. *J Biol Chem*, **2004**. 279(52): p. 54463-9. DOI: 10.1074/jbc.M404786200.
177. Su, Z., et al., Lowintensity pulsed ultrasound promotes apoptosis and inhibits angiogenesis via p38 signalingmediated endoplasmic reticulum stress in human endothelial cells. *Mol Med Rep*, **2019**. 19(6): p. 4645-4654. DOI: 10.3892/mmr.2019.10136.
178. Wang, Y., et al., p38 MAPK signaling is a key mediator for low-intensity pulsed ultrasound (LIPUS) in cultured human omental adipose-derived mesenchymal stem cells. *Am J Transl Res*, **2019**. 11(1): p. 418-429.
179. Yddal, T., et al., Open-source, high-throughput ultrasound treatment chamber. *Biomed Tech (Berl)*, **2015**. 60(1): p. 77-87. DOI: 10.1515/bmt-2014-0046.
180. Castle, J., S. Kotopoulos, and F. Forsberg, Sonoporation for Augmenting Chemotherapy of Pancreatic Ductal Adenocarcinoma. *Methods Mol Biol*, **2020**. 2059: p. 191-205. DOI: 10.1007/978-1-4939-9798-5_9.
181. Schneider, M., Characteristics of SonoVue (TM). *Echocardiography-a Journal of Cardiovascular Ultrasound and Allied Techniques*, **1999**. 16(7): p. 743-746. DOI: DOI 10.1111/j.1540-8175.1999.tb00144.x.
182. Sontum, P.C., Physicochemical characteristics of Sonazoid, a new contrast agent for ultrasound imaging. *Ultrasound Med Biol*, **2008**. 34(5): p. 824-33. DOI: 10.1016/j.ultrasmedbio.2007.11.006.
183. Duan, X., A.C.H. Yu, and J.M.F. Wan, Cellular Bioeffect Investigations on Low-Intensity Pulsed Ultrasound and Sonoporation: Platform Design and Flow Cytometry Protocol. *IEEE Trans Ultrason Ferroelectr Freq Control*, **2019**. 66(9): p. 1422-1434. DOI: 10.1109/TUFFC.2019.2923443.
184. *Frequencies of Cell Types in Human Peripheral Blood*. StemCell Technologies: https://www.stemcell.com/media/files/wallchart/WA10006-Frequencies_Cell_Types_Human_Peripheral_Blood.pdf.
185. Leitch, C., et al., Hydroxyurea synergizes with valproic acid in wild-type p53 acute myeloid leukaemia. *Oncotarget*, **2016**. 7(7): p. 8105-18. DOI: 10.18632/oncotarget.6991.
186. Krutzik, P.O. and G.P. Nolan, Intracellular phospho-protein staining techniques for flow cytometry: monitoring single cell signaling events. *Cytometry A*, **2003**. 55(2): p. 61-70. DOI: 10.1002/cyto.a.10072.


187. Gradiz, R., et al., MIA PaCa-2 and PANC-1 - pancreas ductal adenocarcinoma cell lines with neuroendocrine differentiation and somatostatin receptors. *Sci Rep*, **2016**. 6: p. 21648. DOI: 10.1038/srep21648.
188. Deer, E.L., et al., Phenotype and genotype of pancreatic cancer cell lines. *Pancreas*, **2010**. 39(4): p. 425-35. DOI: 10.1097/MPA.0b013e3181c15963.
189. Waters, A.M. and C.J. Der, KRAS: The Critical Driver and Therapeutic Target for Pancreatic Cancer. *Cold Spring Harb Perspect Med*, **2018**. 8(9). DOI: 10.1101/cshperspect.a031435.
190. Escoffre, J.M., et al., Irinotecan delivery by microbubble-assisted ultrasound: in vitro validation and a pilot preclinical study. *Mol Pharm*, **2013**. 10(7): p. 2667-75. DOI: 10.1021/mp400081b.
191. Ren, X.D., et al., Disruption of Rho signal transduction upon cell detachment. *J Cell Sci*, **2004**. 117(Pt 16): p. 3511-8. DOI: 10.1242/jcs.01205.
192. Muz, B., et al., The role of hypoxia in cancer progression, angiogenesis, metastasis, and resistance to therapy. *Hypoxia (Auckl)*, **2015**. 3: p. 83-92. DOI: 10.2147/HP.S93413.
193. Abrahamsen, I. and J.B. Lorens, Evaluating extracellular matrix influence on adherent cell signaling by cold trypsin phosphorylation-specific flow cytometry. *BMC Cell Biol*, **2013**. 14: p. 36. DOI: 10.1186/1471-2121-14-36.
194. Belham, C.M., et al., Trypsin stimulates proteinase-activated receptor-2-dependent and -independent activation of mitogen-activated protein kinases. *Biochem J*, **1996**. 320 (Pt 3): p. 939-46.
195. *Annexin V staining of adherent cells for flow cytometry*, B. Bioscience, Editor. 2013.
196. Maciorowski, Z., P.K. Chattopadhyay, and P. Jain, Basic Multicolor Flow Cytometry. *Curr Protoc Immunol*, **2017**. 117: p. 5 4 1-5 4 38. DOI: 10.1002/cpim.26.
197. Cossarizza, A., et al., Guidelines for the use of flow cytometry and cell sorting in immunological studies (second edition). *Eur J Immunol*, **2019**. 49(10): p. 1457-1973. DOI: 10.1002/eji.201970107.
198. Krutzik, P.O., et al., High-content single-cell drug screening with phosphospecific flow cytometry. *Nat Chem Biol*, **2008**. 4(2): p. 132-42. DOI: 10.1038/nchembio.2007.59.
199. Krutzik, P.O., et al., Analysis of protein phosphorylation and cellular signaling events by flow cytometry: techniques and clinical applications. *Clin Immunol*, **2004**. 110(3): p. 206-21. DOI: 10.1016/j.clim.2003.11.009.
200. Bonnevier, J., C. Hammerbeck, and C. Goetz, Flow Cytometry: Definition, History, and Uses in Biological Research, in *Flow Cytometry Basics for the Non-Expert*. 2018, Springer Nature Switzerland AG: Cham, Switzerland.
201. Krutzik, P.O. and G.P. Nolan, Fluorescent cell barcoding in flow cytometry allows high-throughput drug screening and signaling profiling. *Nat Methods*, **2006**. 3(5): p. 361-8. DOI: 10.1038/nmeth872.
202. Krutzik, P.O., et al., Fluorescent cell barcoding for multiplex flow cytometry. *Curr Protoc Cytom*, **2011**. Chapter 6: p. Unit 6 31. DOI: 10.1002/0471142956.cy0631s55.
203. Bibby, M.C., Orthotopic models of cancer for preclinical drug evaluation: advantages and disadvantages. *Eur J Cancer*, **2004**. 40(6): p. 852-7. DOI: 10.1016/j.ejca.2003.11.021.
204. Lejbkiewicz, F. and S. Salzberg, Distinct sensitivity of normal and malignant cells to ultrasound in vitro. *Environ Health Perspect*, **1997**. 105 Suppl 6: p. 1575-8. DOI: 10.1289/ehp.97105s61575.
205. Trendowski, M., et al., Preferential enlargement of leukemia cells using cytoskeletal-directed agents and cell cycle growth control parameters to induce sensitivity to low frequency ultrasound. *Cancer Lett*, **2015**. 360(2): p. 160-70. DOI: 10.1016/j.canlet.2015.02.001.
206. Qu, N., et al., Breast Cancer Cell Line Phenotype Affects Sonoporation Efficiency Under Optimal Ultrasound Microbubble Conditions. *Med Sci Monit*, **2018**. 24: p. 9054-9062. DOI: 10.12659/MSM.910790.
207. Fan, P., et al., Cell-cycle-specific Cellular Responses to Sonoporation. *Theranostics*, **2017**. 7(19): p. 4894-4908. DOI: 10.7150/thno.20820.
208. Macintosh, I.J. and D.A. Davey, Chromosome aberrations induced by an ultrasonic fetal pulse detector. *Br Med J*, **1970**. 4(5727): p. 92-3. DOI: 10.1136/bmj.4.5727.92.

209. Cabezas, S., et al., Damage of eukaryotic cells by the pore-forming toxin sticholysin II: Consequences of the potassium efflux. *Biochim Biophys Acta Biomembr*, **2017**. 1859(5): p. 982-992. DOI: 10.1016/j.bbmem.2017.02.001.
210. Porta, H., et al., Role of MAPK p38 in the cellular responses to pore-forming toxins. *Peptides*, **2011**. 32(3): p. 601-6. DOI: 10.1016/j.peptides.2010.06.012.
211. Morotomi-Yano, K., H. Akiyama, and K. Yano, Nanosecond pulsed electric fields activate MAPK pathways in human cells. *Arch Biochem Biophys*, **2011**. 515(1-2): p. 99-106. DOI: 10.1016/j.abb.2011.09.002.
212. Horn, A. and J.K. Jaiswal, Cellular mechanisms and signals that coordinate plasma membrane repair. *Cell Mol Life Sci*, **2018**. 75(20): p. 3751-3770. DOI: 10.1007/s00018-018-2888-7.
213. Babychuk, E.B., et al., Intracellular Ca(2+) operates a switch between repair and lysis of streptolysin O-perforated cells. *Cell Death Differ*, **2009**. 16(8): p. 1126-34. DOI: 10.1038/cdd.2009.30.
214. Tyagi, R., et al., Rheb Inhibits Protein Synthesis by Activating the PERK-eIF2alpha Signaling Cascade. *Cell Rep*, **2015**. 10(5): p. 684-693. DOI: 10.1016/j.celrep.2015.01.014.
215. Preston, A.M. and L.M. Hendershot, Examination of a second node of translational control in the unfolded protein response. *J Cell Sci*, **2013**. 126(Pt 18): p. 4253-61. DOI: 10.1242/jcs.130336.
216. Bischof, L.J., et al., Activation of the unfolded protein response is required for defenses against bacterial pore-forming toxin in vivo. *PLoS Pathog*, **2008**. 4(10): p. e1000176. DOI: 10.1371/journal.ppat.1000176.
217. Morotomi-Yano, K., et al., Nanosecond pulsed electric fields act as a novel cellular stress that induces translational suppression accompanied by eIF2alpha phosphorylation and 4E-BP1 dephosphorylation. *Exp Cell Res*, **2012**. 318(14): p. 1733-44. DOI: 10.1016/j.yexcr.2012.04.016.
218. Hauge, R., et al., Intracellular Signaling in Key Pathways Is Induced by Treatment with Ultrasound and Microbubbles in a Leukemia Cell Line, but Not in Healthy Peripheral Blood Mononuclear Cells. *Pharmaceutics*, **2019**. 11(7). DOI: 10.3390/pharmaceutics11070319.
219. Koul, H.K., M. Pal, and S. Koul, Role of p38 MAP Kinase Signal Transduction in Solid Tumors. *Genes Cancer*, **2013**. 4(9-10): p. 342-59. DOI: 10.1177/1947601913507951.
220. Kopechek, J.A., et al., Ultrasound Targeted Microbubble Destruction-Mediated Delivery of a Transcription Factor Decoy Inhibits STAT3 Signaling and Tumor Growth. *Theranostics*, **2015**. 5(12): p. 1378-87. DOI: 10.7150/thno.12822.
221. Duluc, C., et al., Pharmacological targeting of the protein synthesis mTOR/4E-BP1 pathway in cancer-associated fibroblasts abrogates pancreatic tumour chemoresistance. *EMBO Mol Med*, **2015**. 7(6): p. 735-53. DOI: 10.15252/emmm.201404346.
222. Alassaf, A., A. Aleid, and V. Frenkel, In vitro methods for evaluating therapeutic ultrasound exposures: present-day models and future innovations. *J Ther Ultrasound*, **2013**. 1: p. 21. DOI: 10.1186/2050-5736-1-21.
223. Kaur, G. and J.M. Dufour, Cell lines: Valuable tools or useless artifacts. *Spermatogenesis*, **2012**. 2(1): p. 1-5. DOI: 10.4161/spmg.19885.
224. Sulen, A., et al., Elevated monocyte phosphorylated p38 in nearby employees after a chemical explosion. *Sci Rep*, **2016**. 6: p. 29060. DOI: 10.1038/srep29060.
225. Spitzer, M.H. and G.P. Nolan, Mass Cytometry: Single Cells, Many Features. *Cell*, **2016**. 165(4): p. 780-91. DOI: 10.1016/j.cell.2016.04.019.
226. Kleinmanns, K., *Rethinking High-Grade Serous Ovarian Carcinoma: Development of New Preclinical Animal Models for Evaluation of Image-guided Surgery and Immunotherapy*. 2019, University of Bergen: Bergen, Norway.
227. Kooiman, K., et al., Ultrasound-Responsive Cavitation Nuclei for Therapy and Drug Delivery. *Ultrasound Med Biol*, **2020**. DOI: 10.1016/j.ultrasmedbio.2020.01.002.

I

Article

Intracellular Signaling in Key Pathways Is Induced by Treatment with Ultrasound and Microbubbles in a Leukemia Cell Line, but Not in Healthy Peripheral Blood Mononuclear Cells

Ragnhild Haugse ^{1,2,3} , Anika Langer ^{1,3}, Stein-Erik Gullaksen ^{3,4}, Silje Maria Sundøy ¹, Bjørn Tore Gjertsen ^{3,4}, Spiros Kotopoulos ^{5,6,7,*} and Emmet McCormack ^{1,3,*}

¹ Department of Clinical Science, The University of Bergen, Jonas Lies vei 65, 5021 Bergen, Norway

² Department of Quality and Development, Hospital Pharmacies Enterprise in Western Norway, Møllendalsbakken 9, 5021 Bergen, Norway

³ Centre for Cancer Biomarkers CCBIO, Department of Clinical Science, The University of Bergen, Jonas Lies vei 65, Bergen 5021, Norway

⁴ Department of Internal Medicine, Hematology Section, Haukeland University Hospital, Jonas Lies vei 65, 5021 Bergen, Norway

⁵ Phoenix Solutions AS, Ullernchausseen 64, 0379 Oslo, Norway

⁶ Department of Clinical Medicine, The University of Bergen, Jonas Lies vei 65, 5021 Bergen, Norway

⁷ National Centre for Ultrasound in Gastroenterology, Haukeland University Hospital, Jonas Lies vei 65, 5021 Bergen, Norway

* Correspondence: Spiros.Kotopoulos@uib.no (S.K.); Emmet.Mc.Cormack@uib.no (E.M.);

Tel.: +47-450-80-085 (S.K.); +47-55-97-46-28 (E.M.)

Received: 5 June 2019; Accepted: 4 July 2019; Published: 6 July 2019



Abstract: Treatment with ultrasound and microbubbles (sonoporation) to enhance therapeutic efficacy in cancer therapy is rapidly expanding, but there is still very little consensus as to why it works. Despite the original assumption that pore formation in the cell membrane is responsible for increased uptake of drugs, the molecular mechanisms behind this phenomenon are largely unknown. We treated cancer cells (MOLM-13) and healthy peripheral blood mononuclear cells (PBMCs) with ultrasound at three acoustic intensities (74, 501, 2079 mW/cm²) ± microbubbles. We subsequently monitored the intracellular response of a number of key signaling pathways using flow cytometry or western blotting 5 min, 30 min and 2 h post-treatment. This was complemented by studies on uptake of a cell impermeable dye (calcein) and investigations of cell viability (cell count, Hoechst staining and colony forming assay). Ultrasound + microbubbles resulted in both early changes (p38 (Arcsinh ratio at high ultrasound + microbubbles: +0.5), ERK1/2 (+0.7), CREB (+1.3), STAT3 (+0.7) and AKT (+0.5)) and late changes (ribosomal protein S6 (Arcsinh ratio at low ultrasound: +0.6) and eIF2α in protein phosphorylation). Observed changes in protein phosphorylation corresponded to changes in sonoporation efficiency and in viability, predominantly in cancer cells. Sonoporation induced protein phosphorylation in healthy cells was pronounced (p38 (+0.03), ERK1/2 (−0.03), CREB (+0.0), STAT3 (−0.1) and AKT (+0.04) and S6 (+0.2)). This supports the hypothesis that sonoporation may enhance therapeutic efficacy of cancer treatment, without causing damage to healthy cells.

Keywords: sonoporation; microbubbles; ultrasound; intracellular signaling; phosphorylation; ultrasound contrast agents; drug delivery; cellular stress

1. Introduction

The use of microbubbles (MB), such as ultrasound contrast agents, together with ultrasound (US) to improve therapeutic efficacy has a multitude of applications, ranging from enhancing drug penetration through tissue, opening of the blood brain barrier, to sonothrombolysis [1]. The term “sonoporation” has been commonly used to describe the formation of pores in cells using US + MB, derived from the term “electroporation”, and is commonly used to describe the pore formation phenomenon observed in cell culture experiments. The therapeutic effects of US + MB enhanced therapy have shown great potential over the last 20 years. It can be used to increase the delivery and resulting efficacy of drugs and is therefore particularly useful in cancer therapy, where poor uptake of drugs is one of the factors limiting therapeutic effect [2]. The therapeutic benefits of US + MB enhanced therapy in cancer have been demonstrated in numerous preclinical trials [3–6]. Furthermore, a Phase I clinical trial [7] showed that US + MB enhanced therapy in combination with chemotherapy is safe and may increase survival of patients suffering from pancreatic ductal adenocarcinoma, and is being followed by clinical trials in other cancers [8–10].

Numerous *in vitro* studies have demonstrated that the combined use of ultrasound and microbubbles forms pores in the membranes of cancer cells [11]. The improved chemotherapeutic efficacy was subsequently assumed to be due to passive diffusion of the drugs through the pores. Nevertheless, despite substantial research in this field, it is not fully understood if the mechanical stresses induced by the microbubbles contribute to additional molecular mechanisms. It has been suggested that cellular stress induced by sonoporation may contribute to the enhancement of cancer therapy [12]. These additional therapeutic effects, which are induced by the biophysical stimuli of the microbubbles interacting with cells, must involve activation of intracellular signaling pathways. However, it is still not known how protein phosphorylation in intracellular signaling pathways changes in response to sonoporation. Low intensity ultrasound used to accelerate bone and joint healing, has been found to induce integrin/mechanotransduction signaling that include proteins like p38, ERK1/2 and JNK (Mitogen-activated protein (MAP)-kinase pathway) and focal adhesion kinase (FAK), in chondrocytes [13] and synovial cells [14]. Additionally, low intensity ultrasound has been described to stimulate cell growth through the integrin/FAK/phosphoinositide-3-kinase-protein kinase (PI3K) pathway, including Akt, in chondrocytes [15] and osteoblasts [16]. As sonoporation also includes the use of microbubbles, knowledge on how addition of microbubbles influences the cellular responses is needed. In respect to the clinical application of this approach, it would further be of great importance to understand how sonoporation influences different cell types. Specifically, to contrast the effects induced on cancer cells or healthy cells, of which both will inevitably be exposed during cancer therapy.

To gain more insight into the molecular mechanisms of sonoporation, our aim was to analyze phosphorylation changes in intracellular signaling networks following treatment with ultrasound with and without the addition of microbubbles. Uptake of a cell impermeable dye and cell viability assays were used to determine the efficacy of sonoporation. We have investigated the intracellular signaling responses of increasing ultrasound intensity and addition of microbubbles using two commercially available ultrasound contrast agents in both a cancer cell line and healthy peripheral blood mononuclear cells (PBMCs).

2. Materials and Methods

2.1. Chemicals

All chemicals were purchased from Merck KGaA (Darmstadt, Germany) unless otherwise stated.

2.2. Microbubbles

Sonazoid™ (GE Healthcare, Little Chalfont, UK) was reconstituted™ by adding 2 mL NaCl 9 mg/mL (Fresenius Kabi, Bad Homburg vor der Höhe, Germany) and gently agitating for 30 s. The bubbles were aspirated via a 19 G needle, and a 19 G venting needle was used to avoid a pressure drop in

the vial. Bubbles were diluted in NaCl 9 mg/mL immediately before addition to cells. SonoVue® (Bracco S.p.A., Milan, Italy) was prepared following manufacturer specifications. To ensure that the reconstituted bubbles were stable, Sonazoid™ bubbles were used within 1 h of reconstitution, and SonoVue® bubbles within 30 min.

2.3. Cell Culture

The leukemic cell-line MOLM-13 (DSMZ, Braunschweig, Germany) was cultured in RPMI 1640 medium supplemented with 10% fetal bovine serum and 1% L-glutamine. Peripheral blood mononuclear cells (PBMCs) were isolated from concentrated leukocyte suspensions of healthy donors, generated from whole blood by centrifugation. Blood was supplied from healthy volunteers, from the Department of Immunology at Haukeland University Hospital, Bergen, Norway. PBMCs were isolated using density gradient separation (Lymphoprep™, Abbott Laboratories, Chicago, IL, USA), followed by red blood cell lysis performed in Red Cell lysis buffer (155 mM NH₄Cl, 10 mM NaHCO₃, 0.1 mM EDTA and distilled water). PBMCs were cultured in RPMI 1640 supplemented with 10% FBS and 1% L-glutamine. All cells were cultured in a 5% CO₂ humidified atmosphere at 37 °C.

2.4. In Vitro Treatment with Ultrasound and Microbubbles

MOLM-13 cell suspension was seeded into six wells of a 24-well plate (TPP Techno Plastic Products AG, Trasadingen, Switzerland). A total of 1×10^6 cells/well in 2.5 mL supplemented RPMI 1640 culture media were seeded (0.4×10^6 cells/mL) and rested for approximately 1–2 h prior to sonication. The MOLM-13 cell line was exposed to ultrasound whilst in exponential growth. The PBMCs were treated directly following separation from blood. A total of 8×10^6 cells/well in 2.5 mL supplemented RPMI 1640 culture media (3.2×10^6 cell/mL) were seeded and rested for approximately 30–60 min prior to sonication. As MOLM-13 cells are larger than PBMC cells, the PMBC cell concentration was increased to match the total cell volume of the MOLM-13 experiments (Figure S1). Microbubbles were added at a final concentration of 0.4×10^6 bubbles/mL (1×10^6 bubbles per well), based on an a priori dose-response study (Figure S2). This microbubble dose correlates to a clinical dose of 1.7 mL of Sonazoid™, and 10.0 mL of SonoVue®. Both doses are above clinical imaging and diagnostic recommendations from the manufactures. Immediately following bubble addition, a self-adhering membrane (TopSeal™-A, Perkin Elmer, Waltham, MA, USA) was stuck on the top surface of the 24-well plate to create a watertight seal. This membrane was used as the acoustic propagation interface and the acoustic amplitude was compensated for the membrane attenuation (measured to be <1% at 1.0 MHz). The plate was inverted, placed in the ultrasound treatment chamber [17] and ultrasound was applied. Figure 1 shows a schematic of the ultrasound treatment chamber. In short, the ultrasound chamber consisted of 6 single element, unfocused, disc transducers (PZ26, 2 mm thickness, 15 mm diameter). A 3D printed chamber was used to accurately align the transducers and 6 wells within the 24 well plate. The center of the water volume in the cell culture wells was aligned with the axial acoustic focus. Three different US conditions were used (Table 1), referred to as “Low”, “Medium”, or “High”. All samples were sonicated for 10 min. In all experiments the Mechanical Index (MI) was kept below 0.4, which is generally considered safe [18]. Only the “High” acoustic condition was above the clinical diagnostic imaging guidelines in terms of the I_{SPTA} value. Nevertheless, much higher values are already used in therapeutic ultrasound clinical trials.

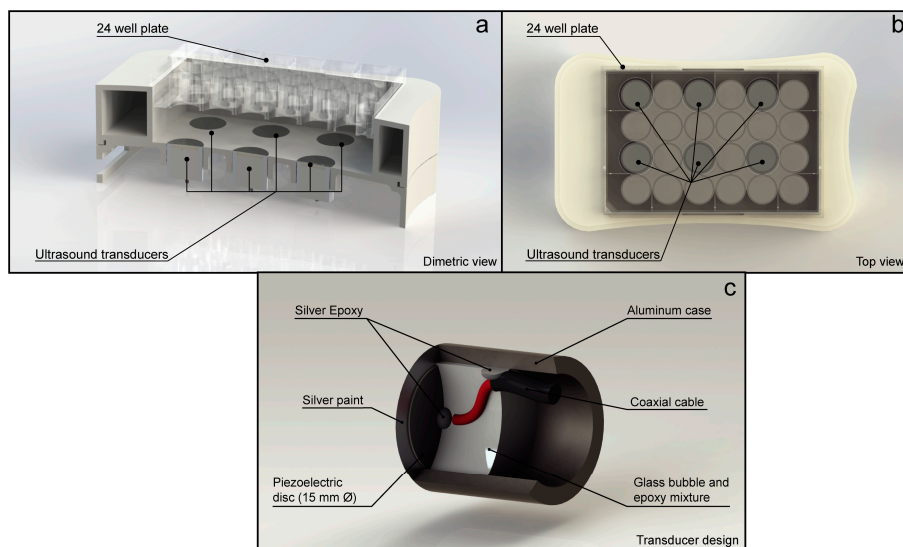


Figure 1. Ultrasound treatment chamber and transducer design used to treat the cells. (a) Cutaway of the dimetric view of ultrasound treatment chamber showing the distance. (b) Top view of the chamber showing which cell culture wells were exposed to ultrasound. (c) Cutaway of the transducer design used in the ultrasound treatment chamber.

Table 1. Ultrasound conditions used to treat the cells.

Name	Frequency (MHz)	No. of Cycles	Duty Cycle (%)	Pulse Repetition Frequency (kHz)	MI	Intensity	
						I_{SPTA} (mW/cm ²)	I_{SPPA} (W/cm ²)
Low	1.108	4	4	10	0.2	74	0.66
Medium	1.108	18	16	10	0.3	501	2.31
High	1.108	41	37	10	0.4	2079	5.0

2.5. Uptake of Cell Impermeable Dye

To measure sonoporation efficiency calcein, a non-toxic, cell impermeable fluorescent dye, was added during treatment with ultrasound \pm microbubbles. Calcein was dissolved in 1 M NaOH to a stock solution of 50 mg/mL and protected from light at 2–8 °C. For each experiment, a fresh solution of 2.5 mg/mL in 9 mg/mL NaCl (Fresenius Kabi, Bad Homburg vor der Höhe, Germany) was prepared. Calcein was added to the cell suspension to a concentration of 5 μ M immediately before sonication. After ultrasound treatment, the cells were incubated for 40–60 min, washed twice in PBS, and subsequently analyzed using an Accuri C6 flow cytometer (BD Bioscience, Franklin Lakes, NJ, USA). Incubation time was evaluated prior to experiments (Figure S3). A duration of 40 min or more was required due to experimental feasibility constraints. An incubation time of 60 min was chosen as this was an indicated pore re-sealing time [19]. A minimum of three replicates were analyzed per experiment, and all experiments were performed three times.

2.6. Viability Analysis

In separate experiments without calcein, cells were treated with ultrasound \pm microbubbles and samples were harvested for both viability assays and studies on intracellular signaling. Cell concentration was determined by manual counting using a haemocytometer. This was done immediately after treatment with ultrasound and after 24 h of culture. Apoptotic cell death was

assessed by adding 0.01 mg/mL Hoechst 33342 (Merck KGaA, Darmstadt, Germany) to cells after 24 h of culturing. Cells were fixed in 4% formaldehyde and imaged by fluorescence microscopy. The total number of cells was determined in Fiji [20] by adjusting the image brightness and contrast followed by a manual threshold then using the “Analyze particles” function. Apoptotic cells were counted manually using the “Cell counter” plugin in Fiji. Colony forming assay (Methocult™ Classic H4434; Stemcell™ Technologies, Vancouver, BC, Canada) was used to evaluate the proliferation of the MOLM-13 cells. Cells were seeded immediately after treatment and colonies were counted after 7–10 days incubation. All experiments were performed in triplicate.

2.7. Sample Preparation for Phosphospecific Flow Cytometry

Samples for intracellular signaling studies were taken at three different time points: immediately after sonoporation (approximately 5 min), after 30 min, and 2 h of incubation. Cells were fixed by adding 16% paraformaldehyde (Alfa Aesar, Haverhill, MA, USA) to a final concentration of 2% and incubating for 15 min at room temperature, washed in cold PBS and permeabilized in ice-cold methanol, following a modified protocol [21,22]. As positive controls for intracellular signaling, MOLM-13 cells were treated with either 1 μ M A23187 (Calcimycin; calcium ionophore) for 4 h, 100 ng/mL TNF- α for 15 min, or 1 μ M A23187 + 100 nM phorbol myristate acetate (PMA; PKC activator) for 30 min. PBMCs were treated with 1 μ M A23187 + 100 nM PMA for 30 min as positive control. Variation in response to A23187 + PMA between cells from 3 different donors and MOLM-13 are shown in Figure S6.

2.8. Barcoding and Antibody Staining

Fluorescent cell barcoding was used to perform multiplex flow cytometry. Individual cell samples were stained with unique signatures of succinidylesters of Pacific Blue (0.05 μ g/mL, 0.5 μ g/mL, 5 μ g/mL) and Pacific Orange (0 μ g/mL, 2.5 μ g/mL and 20 μ g/mL). After barcode staining, the samples were pooled prior to antibody staining [23]. A graphical depiction of barcoding/sample preparation for phospho-flow cytometry is shown in Figure S4. One barcode represents all samples from one timepoint in each experiment. Barcoded cells were split into staining panels and each panel was stained separately with a combination of antibodies conjugated to either Alexa Fluor® 488 or 647 (Table S1). PBMC samples were incubated with FcR-blocking reagent (Miltenyi Biotec, Bergisch Gladbach, Germany) prior to antibody staining. Samples were analyzed on an LSR Fortessa flow cytometer (BDBioscience, Franklin Lakes, NJ, USA). After flow cytometric analysis the samples were de-barcoded and the arcinhratio for each treated sample to the untreated cells, harvested at the same timepoint, was calculated.

2.9. Western Blots

Samples for western blot were harvested 2 h post sonoporation, washed twice in PBS and lysed in RIPA buffer containing protease- and phosphatase inhibitor (Thermo Fisher Scientific, Waltham, MA, USA). Protein concentration was quantified in accordance with Bio-Rad DC protein assay instruction manual for microtiter plates. For the western blots 10% SDS-polyacrylamide gels were loaded with 20–30 μ g protein per well. Proteins were separated at 100–120 V and transferred to a nitrocellulose membrane (240 mA, 150 min, 4 °C), followed by 1 h blocking using 5% skim milk powder in Tris-buffered saline (TBS) + 1% Tween 20. Primary antibodies were diluted in 5% skim milk in TBS-Tween and incubated over night at 4 °C. Primary antibodies used were p-eIF2 α Ser-51 (Abcam, Cambridge, UK) and eIF2 α (Abcam). COX IV (Abcam) was used as loading control. Secondary antibodies were diluted in 5% skim milk powder in TBS-Tween 20 and incubated for 1 h at room temperature. Membranes were developed using SuperSignal® West Pico or SuperSignal® West Femto Chemiluminescence Substrate (Thermo Fischer Scientific) in accordance with manufacturers recommendations.

2.10. Data Analysis/Statistical Analysis

Data collected from the Accuri C6 flow cytometer was analyzed in FlowJo® (BDBioscience, Franklin Lakes, NJ, USA). Data collected from LSR Fortessa on barcoded samples were de-barcoded

and gated in FlowJo®. Gating strategy is shown in Supplemental Figure S5. Further analysis was performed in Cytobank (Cytobank Inc., Santa Clara, CA, USA). Arcsinh ratio ($\text{arsinh}(\text{treated}/5) - \text{arsinh}(\text{control}/5)$) was used to calculate changes in phosphorylation. Statistical comparisons were performed in Prism 6 (GraphPad Software, San Diego, CA, USA) using unpaired two-tailed *t*-tests. Significance level was set at *p*-value 0.05. All *p*-values are shown in Tables S2–S6.

3. Results

3.1. Efficiency of Sonoporation Was Increased by Addition of Microbubbles and High Ultrasound Intensity

3.1.1. Percentage of Cells Taking Up Calcein (Permeabilization Efficiency)

We investigated sonoporation efficiency by measuring uptake of the cell impermeable dye calcein into the cells, a measure of cell permeabilization. Figure 2 shows the percentage of cells positive for calcein after ultrasound treatment ± microbubbles. Increasing ultrasound intensity increased the percentage of calcein-positive cells (Figure 2a,b). In the absence of microbubbles, only high ultrasound intensity induced a significant increase in calcein-positive MOLM-13 cells. The addition of either SonoVue® or Sonazoid™ microbubbles resulted in a significantly increased number of calcein-positive cells at medium or high ultrasound intensity (No bubbles: 1.5% and 1.5%; SonoVue®: 6.4% and 29%; Sonazoid™: 14% and 35%, at medium and high ultrasound respectively) (Figure 2a, Tables S2 and S3). Sonazoid™ induced a significantly higher percentage of calcein-positive cells than SonoVue® (Table S4) and based on these results we used Sonazoid™ for subsequent experiments. In PBMCs, the addition of Sonazoid™ increased the number of calcein-positive cells to 6% at medium ultrasound and to 20% at high ultrasound intensity, while no significant difference was observed without the use of microbubbles (Figure 2b). Figure 2c compares the efficacy of each ultrasound condition + Sonazoid™ for MOLM-13 cells and PBMCs. At medium and high ultrasound intensities, a significantly larger population of the MOLM-13 cells vs. PBMCs were calcein-positive (Table S5).

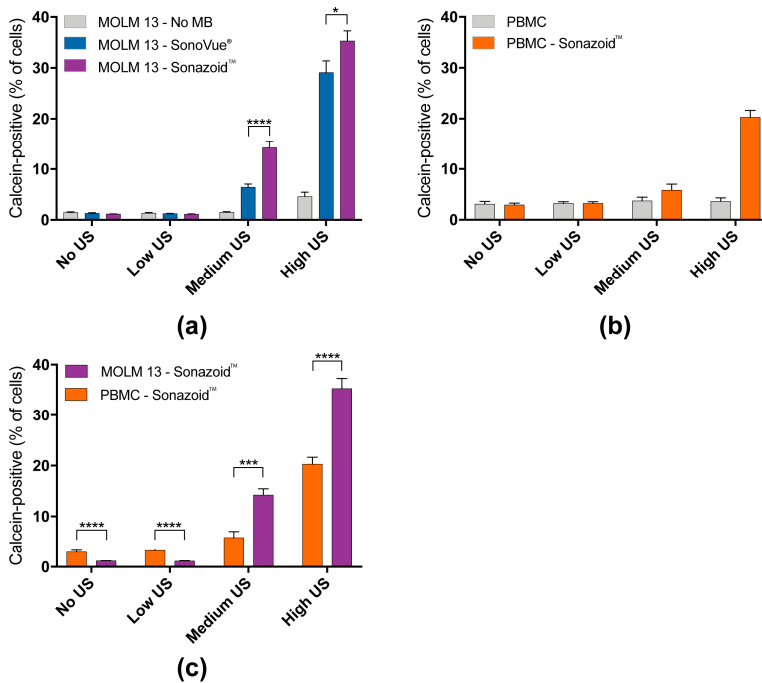


Figure 2. Increasing the ultrasound intensity and the addition of microbubbles significantly increased the percentage of calcein-positive cells. (a) Percentage of calcein-positive MOLM-13 cells versus ultrasound intensity. Increasing the ultrasound intensity correlated to an increase in calcein positive cells. The addition of microbubbles significantly increased the calcein-positive population. At medium and high ultrasound intensities Sonazoid™ was significantly better than SonoVue®. (b) Percentage of calcein positive peripheral blood mononuclear cells (PBMCs) versus ultrasound intensity. Ultrasound alone did not increase the calcein-positive population. The addition of Sonazoid™ significantly increased the calcein-positive population at medium and high ultrasound intensities. (c) Comparison of calcein-positive population between MOLM-13 cells and PBMCs. At medium and high ultrasound intensities a significantly larger population of the MOLM-13 cells were calcein positive. * = $p < 0.05$, ** = $p < 0.01$, *** = $p < 0.001$, **** = $p < 0.0001$ (Significance depicted for Sonazoid™ vs. SonoVue®, and MOLM-13 vs. PBMC. All p -values can be found in Tables S2–S5).

3.1.2. Quantified Uptake of Calcein

The median fluorescence intensity (MFI) was used as an estimate of calcein uptake and is depicted as fold change of controls not treated with ultrasound or microbubbles (Figure 3). As for the percentage of calcein-positive cells (Figure 2c) the effect of increasing ultrasound intensity alone was only significant at high ultrasound intensity, while the addition of microbubbles increased calcein uptake at all ultrasound intensities in MOLM-13 cells (Figure 3a, Tables S2 and S3). The uptake enhancement by using Sonazoid™ vs. SonoVue® was confirmed (SonoVue®: 8-fold and 14-fold increase at increase at medium and high ultrasound intensity respectively; Sonazoid™: 12-fold and 22-fold) at all three ultrasound intensities (Table S4). In PBMCs a significant increase in calcein uptake was observed at medium and high ultrasound intensity + Sonazoid™ (Figure 3b). The uptake was significantly higher in MOLM-13 cells than PBMCs at all 3 ultrasound intensities (Figure 3c, Table S5).

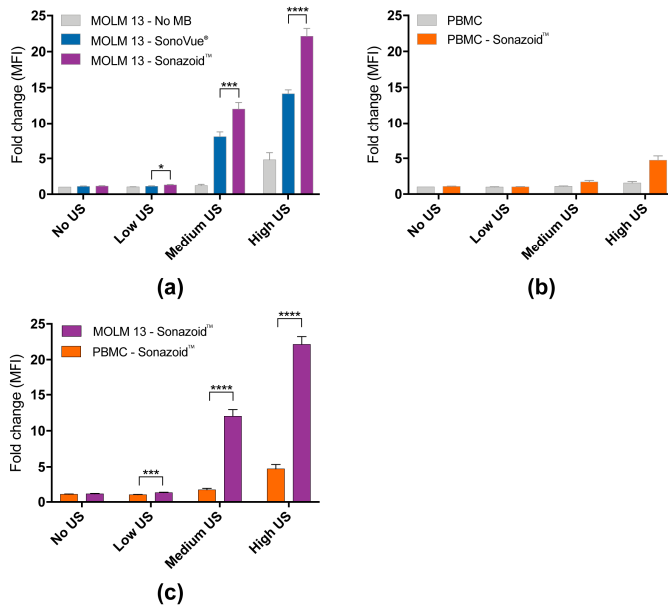


Figure 3. Sonoporation induced significant increase in uptake of model drug calcein in sonoporated cells measured by median fluorescence intensity. (a) Fold change of median fluorescence intensity (MFI) in MOLM-13 cells affected by sonoporation (=calcein-positive cells). The increase in calcein uptake depended on addition of microbubbles and ultrasound intensity. Use of Sonozaoid resulted in significantly higher increase in uptake than SonoVue at all three ultrasound intensities. (b) Fold change of median fluorescence intensity (MFI) in calcein-positive PBMC. The uptake is significantly dependent on addition of microbubbles and ultrasound intensity (significant increase in uptake only seen at high ultrasound intensity). (c) Comparison of calcein uptake between MOLM-13 and PBMC. A significantly higher percentage of cancerous MOLM-13 cells were affected than healthy PBMC at all 3 ultrasound intensities. * $p < 0.05$, ** $p < 0.01$, *** $p < 0.001$, **** $p < 0.0001$ (Significance depicted for Sonozaoid™ vs. SonoVue®, and MOLM-13 vs. PBMC. All p -values can be found in Tables S2–S5).

3.2. Decreased Viability in Cancerous MOLM-13 Cells after Sonoporation

The cell count was measured immediately after sonoporation to determine if the mechanical forces lead to any immediate cell damages from the treatment. Cell lysis or immediate necrosis was only observed at much higher acoustic intensities than those evaluated in this study, (i.e., $MI = 0.6$, $I_{SPTA} = 2673 \text{ mW/cm}^2$, Duty Cycle = 20%). No significant changes in total cell counts were observed for either MOLM-13 or PBMCs at any of the ultrasound intensities when compared to controls not treated with ultrasound (Figure 4a,d, Tables S2 and S3). However, a small increase in cell count was observed using low ultrasound without microbubbles at both 0 and 24 h compared to untreated cells. After 24 h a significantly lower cell count was observed in MOLM-13 cells treated with medium and high ultrasound with the addition of microbubbles (Figure 4b, Tables S2 and S3). In PBMCs a modest, but statistically significant, decrease in cell count after 24 h was observed at medium ultrasound with microbubbles ($p < 0.05$) (94% and 99% cells relative to untreated cells, respectively). To elucidate if the reduced cell count of MOLM-13 was a result of increased cell death or reduced proliferative ability, Hoechst 33342 staining and colony forming assay were performed. The addition of microbubbles and application of medium or high US increased the percentage of apoptotic MOLM-13 cells to 6% and 13% respectively (Figure 4c, Tables S2 and S3). Upon Hoechst staining of PBMCs, no significant change in apoptotic cells was observed at any treatment regime. Colony forming assays (Figure 4d,

Tables S2 and S3) demonstrated that MOLM-13 cells formed significantly less colonies at medium and high ultrasound intensity + microbubbles (77% and 50% fewer colonies, respectively).

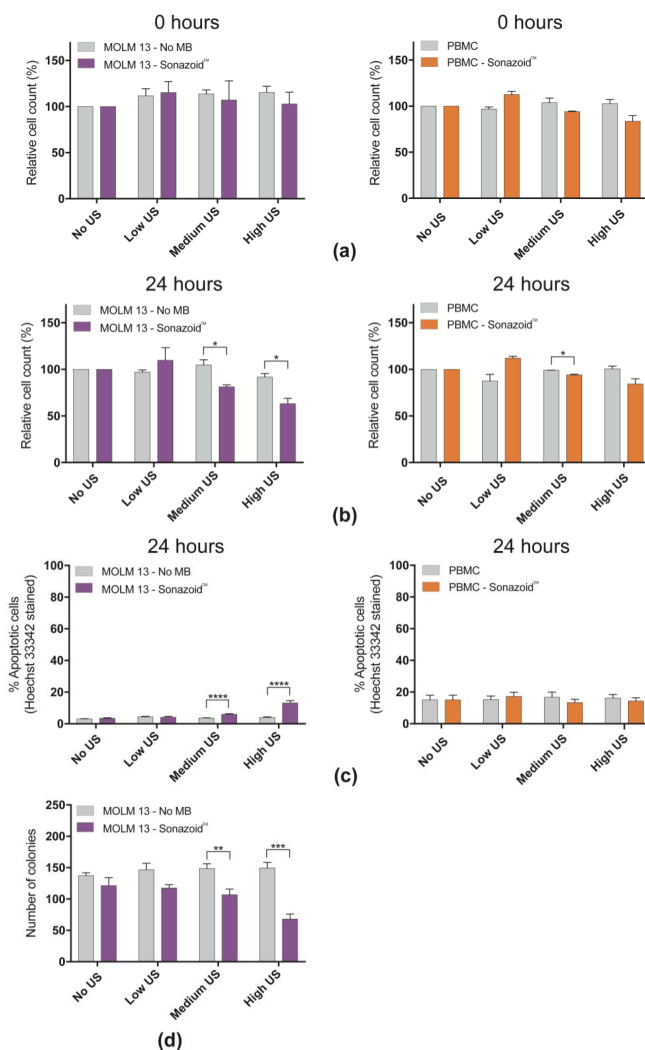


Figure 4. Viability of cells in response to ultrasound \pm Sonazoid™ microbubbles (a) Normalized cell count at different ultrasound intensities \pm Sonazoid™ microbubbles (normalized to cells not treated with ultrasound), of cells harvested immediately after sonoporation (0 h). No significant change in cell count due to sonoporation was observed (b) Normalized cell count of cells harvested 24 h after sonoporation. After 24 h the cell count was significantly lower in samples treated with medium ($p < 0.05$) and high ($p < 0.05$) ultrasound intensity. The cell count of PBMCs did not change much after 24 h in any of the samples. A small increase in cell count was observed in the samples treated with the lowest ultrasound intensity, but this effect is not significant. A small, but significant, decrease in cell count was observed in the sample treated with medium ultrasound intensity. (c) Apoptotic cells 24 h post sonoporation by Hoechst 33342 staining in MOLM-13 and PBMC (d) Number of colonies of MOLM-13 formed post sonoporation (colony forming assay). * $p < 0.05$, ** $p < 0.01$, *** $p < 0.001$, **** $p < 0.001$.

3.3. Sonoporation Induced Changes in Intracellular Signaling-Profiles

In line with the results observed from calcein uptake experiments (Figures 2 and 3) the changes in intracellular signaling were more pronounced in MOLM-13 cells (Figure 5a) compared to PBMCs (Figure 5b). Significantly increased signaling was observed at medium and high ultrasound intensity and when microbubbles were added during sonication (Figure 5a, Table S6). Increased phosphorylation from untreated cells was observed for p-38 T180/Y182, ERK1/2 T202/Y204, CREB S133/ATF-1, Akt S473 and STAT3 S727 in the MOLM-13 cell line. Sonoporation altered STAT3 phosphorylation specifically at the Ser727 epitope, and there was no change in phosphorylation status on the Tyr 705 epitope. STAT5 phosphorylation level was not affected by sonoporation. Phosphorylation status of FAK, NF-kB, Src, PDPK1 or p53 did not change.

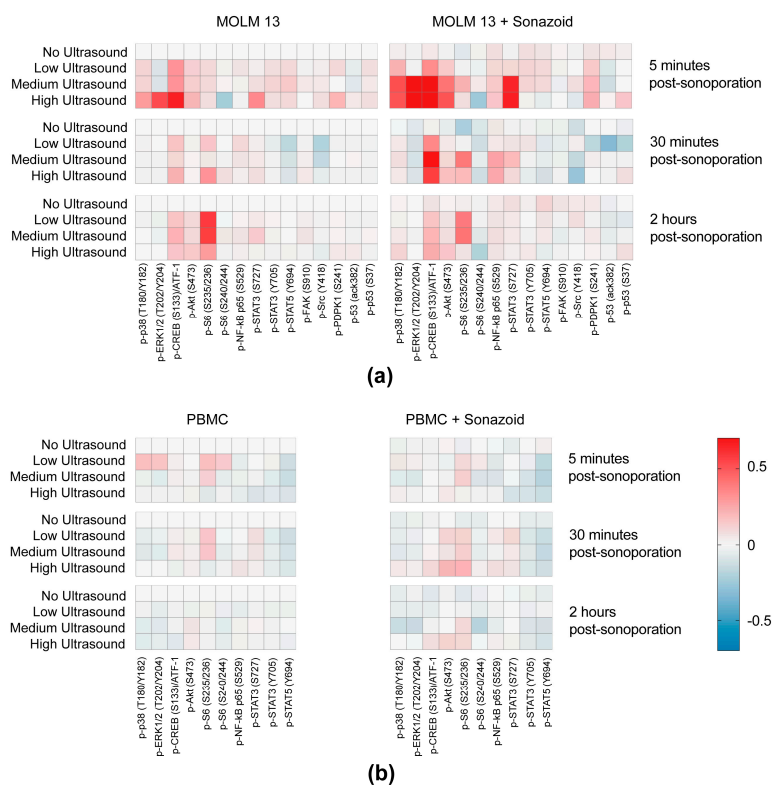


Figure 5. Intracellular signaling profiles of sonoporated cells. (a) Heatmaps displaying changes in phosphorylation status in MOLM-13 of the chosen range of proteins in response to treatment with ultrasound with and without Sonazoid™ microbubbles. Phosphorylation status was detected 5 min, 30 min and 2 h post sonoporation (mean of Arcsinh ratios) (b) Heatmaps displaying changes in phosphorylation status in PBMC of the chosen range of proteins in response to treatment with ultrasound with and without Sonazoid™ microbubbles. Phosphorylation status was detected 5 min, 30 min and 2 h post sonoporation (mean of Arcsinh ratios).

3.3.1. Immediate Effects of Sonoporation

Changes in intracellular signaling by sonoporation in MOLM-13 were mostly observed immediately after treatment (Figure 5a). Phosphorylation of p38 T180/Y182, ERK1/2 T202/Y204, Akt S473, and STAT3 S727 (Figure 6a, Table S5) was significantly increased 5 min after sonoporation.

Phosphorylation generally decayed rapidly and the difference from controls was either lower or not detected 30 min after sonoporation. Changes in phosphorylation were primarily observed when cells were treated with medium and high ultrasound intensity with microbubbles. Only phosphorylation of p38 was significantly increased without microbubbles, and only at high ultrasound intensity. A significant increase in phosphorylation immediately after sonoporation with microbubbles was also observed for CREB S133/ATF-1. However, this was sustained for a longer time period. Phosphorylation of CREB S133/ATF-1 was significant increased for up to 2 h when using medium or high US + MB (Figure 6b, Table S5). Furthermore, the changes in phosphorylation of p38 T180/Y182, ERK1/2 T202/Y204, CREB S133/ATF-1, Akt S473 and STAT3 S727 are predominantly seen when increasing ultrasound from low to medium intensity (+ microbubbles). No significant differences were found when increasing from medium to high ultrasound intensity (Figure 6, Table S6).

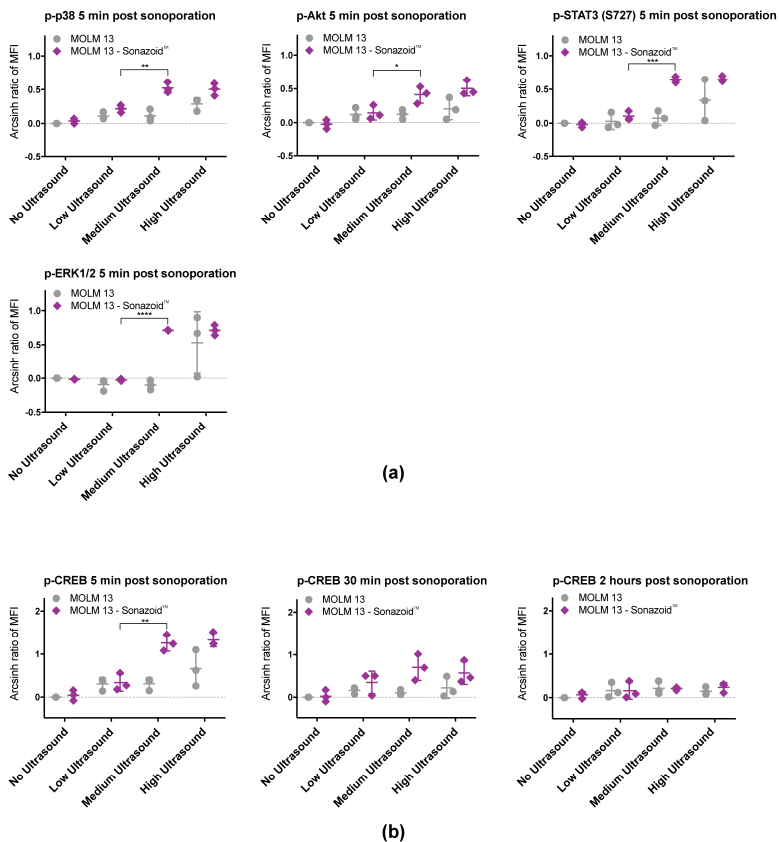


Figure 6. Significant changes in phosphorylation were observed for p38, ERK1/2, CREB, Akt and STAT3 (S727) in MOLM-13 cells. The increases in phosphorylation primarily occurred when increasing ultrasound from low to medium. (a) Scatter plots of results 5 min post sonoporation from 3 individual experiments. Phosphorylation status of p38, ERK1/2, Akt and STAT3 (S727) were transiently altered from untreated controls at medium and high ultrasound intensity in the presence of microbubbles. (b) Scatter plots of results at 5 min, 30 min and 2 h from 3 individual experiments. Phosphorylation status of CREB was altered by sonoporation for up to 2 h. * $p < 0.05$, ** $p < 0.01$, *** $p < 0.001$, **** $p < 0.001$ (Significance depicted for Low ultrasound vs. Medium ultrasound. All p -values can be found in Tables S2–S5).

3.3.2. Downstream Effects of Sonoporation—Ribosomal Protein S6

Not all the effects of sonoporation on intracellular signaling were observed immediately after treatment. A difference in phosphorylation status of ribosomal protein S6, specifically on the S235/236 epitope, was seen 2 h after sonoporation (Figure 7). At high ultrasound, phosphorylation was lower than at the lower ultrasound intensities and in particular at high ultrasound with addition of microbubbles there is almost no difference in phosphorylation compared to untreated controls. At low and medium ultrasound intensity the phosphorylation is higher than untreated controls both with and without microbubbles. A similar yet very weak response was also detected in PBMCs (Figure 5b). However, none of the observed changes in phosphorylation of ribosomal protein S6 were statistically significant. No changes from untreated controls in phosphorylation were observed at the S240 epitope on ribosomal protein S6.

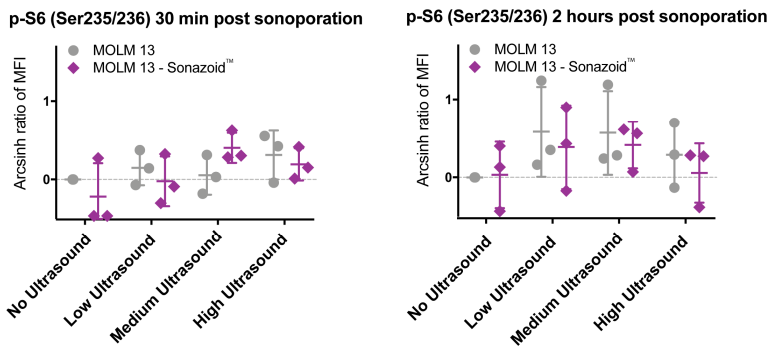


Figure 7. Changes in phosphorylation as observed for ribosomal protein S6 in MOLM-13 cells, shown as scatter plots of results at 30 min and 2 h from three individual experiments. The trend is an increase in phosphorylation at low and medium ultrasound intensity both with and without microbubbles, which is reduced at high ultrasound intensity. Changes in phosphorylation of ribosomal protein S6 at Ser 235/236 were not significant. This is probably due to high variation in results between experiments.

3.3.3. Downstream Effects of Sonoporation—Eukaryotic Initiation Factor 2 α

Eukaryotic initiation factor 2 alpha (eIF2 α) signaling may have an inverse relationship to mTOR/S6 signaling [24], and to elucidate the downstream mechanism the phosphorylation status of eIF2 α was investigated. The Western blot in Figure 8 shows that eIF2 α was phosphorylated 2 h post sonoporation in MOLM-13 when exposed to medium and high ultrasound intensity with addition of microbubbles. The phosphorylation of eIF2 α was increasing from medium to high ultrasound (+ microbubbles).

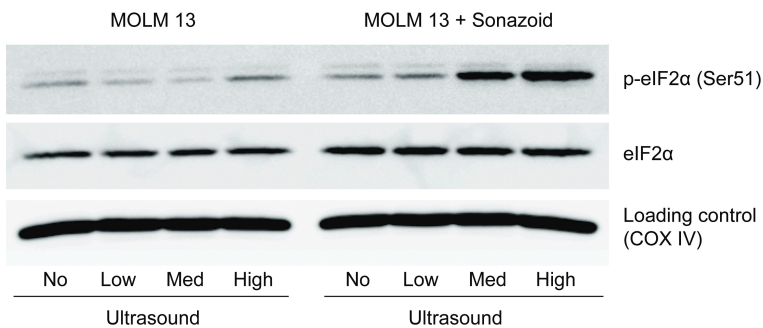


Figure 8. Phosphorylation of eIF2 α in MOLM-13 (Western blot) when treated with medium and high ultrasound in the presence of microbubbles 2 h post sonoporation.

4. Discussion

In this study we present a new insight in the cellular responses following sonoporation, by an extensive screen of phosphorylation changes in intracellular signaling pathways. Although a range of bioeffects in response to sonoporation is already known [25,26], the intracellular signaling responses have so far been overlooked. We found that sonoporation activates key signaling pathways, such as the MAP-kinase pathway and PI3K-pathway, and both transcription and translation factors. The use of our high-throughput ultrasound treatment chamber [17] enabled us to relate these new findings with more commonly used measures of sonoporation efficiency: uptake of a cell-impermeable dye [19,27–31] (permeabilization) and cell viability [19,27,31–33]. Interestingly, there is a shift in the phosphorylation profile of the cells at the acoustic/microbubble conditions in which calcein uptake is increased and viability is decreased, and this trend corresponds with increasing ultrasound intensity and was significantly enhanced by addition of microbubbles during US treatment. The results on calcein uptake and viability are in agreement with the existing literature, although an important observation is the higher sensitivity to sonoporation of the cancerous MOLM-13 compared to healthy PBMCs. Also, in the PBMCs, only minor changes in intracellular signaling are detected. The increased susceptibility of cancer cells to ultrasound has previously been observed [34,35], and suggested to be a result of different cell size, morphology or faster growth rate of cancer cells. While the MOLM-13 cells used in this study are indeed larger in size than PBMCs (Figure S1) further work will be required to verify this hypothesis.

Our calcein uptake experiments indicated that Sonazoid™ microbubbles are more effective than SonoVue® microbubbles at the chosen treatment conditions. Whilst both agents are lipid-shell based they have different responses to ultrasound (e.g., different resonant frequencies), gas content, shell stiffness, stability, size distribution, and polydispersity [36,37]. The improved effectiveness of Sonazoid™ could be due to any of these physicochemical properties or behaviors at the chosen ultrasound parameters and concentrations. Changing the acoustic frequencies, concentration, or selecting a specific bubble size population could result in SonoVue® or any other microbubble being more effective.

The effect of sonoporation on intracellular phosphorylation patterns in MOLM-13 can be divided into immediate effects and more long-lasting effects. An immediate and transient increase of phosphorylation was observed for proteins of the MAP-Kinase (ERK, p38) and PI3K (Akt) pathway. Activation of p38, ERK and Akt by ultrasound alone was also observed in previous studies in other cell types [13,14,16]. In contrast to our results, these previous studies showed increased cell growth. The activation of these proteins is known to be involved in increased proliferation of cells, but the broad range of effects of those proteins is not only limited to the regulation of cell growth and differentiation. They also involve transmission of stress stimuli (p38 [38]), cell cycle regulation and proliferation (ERK [39]) and cell survival (Akt [40]). We further observe an increase in phosphorylation of transcription factors CREB and STAT3, which may be activated downstream of MAP-kinases [41–43]. For STAT3, this is supported by the fact that it is phosphorylated on the serine 727 epitope only, and there is no change in phosphorylation status on the Tyr705 epitope which is phosphorylated downstream of JAK in the JAK/STAT pathway [41,42].

The downstream effects of sonoporation in MOLM-13 that we have observed are changes in phosphorylation of eIF2 α and ribosomal protein S6. The phosphorylation of ribosomal protein S6, specifically at the Ser235/236 epitope, followed the inverse trend of immediate signaling events, and was induced by low and medium ultrasound \pm microbubbles. This activation was not observed when high ultrasound + microbubbles was used. Ribosomal protein S6 is linked to an increase in cell growth whilst phosphorylation of eIF2 α may reduce cell growth [24]. Both eIF2 α and ribosomal protein S6 are involved in protein translation, the final step in expression of genes into proteins and a part of biosynthesis that is tightly connected to cell growth. Therefore, these signaling events are in line with our observed decrease in viability at the higher ultrasound plus microbubble conditions. Phosphorylation of eIF2 α inhibit general protein translation and cell proliferation in response to cellular stresses, among them endoplasmic reticulum (ER-) stress—a known bioeffect in response to

sonoporation [33]. Activation of ribosomal protein S6 Ser235/236, on the other hand, may simulate cap-dependent protein translation, downstream of ERK [44]. The observed signaling events suggest that sonoporation may influence protein translation.

These results, performed on the same validated experimental platform, indicate that sonoporation may in fact induce both signals, promoting and decreasing viability of cells, depending on ultrasound intensity and the addition of microbubbles. In clinical use, ultrasound parameters, microbubbles and drugs must be chosen carefully, and protein phosphorylation can potentially be used as biomarkers to guide the choice of therapeutic parameters. Furthermore, a reason that the sonoporation mechanisms are still debated is the diversity of experimental parameters, experimental systems and cell types used in the *in vitro* studies [25,45]. This study also highlights that differences in ultrasound parameters and treatment of different cell types may result in variable, maybe even opposing, biological responses.

Throughout this study, an increase in acoustic intensity induced increased responses. This increased intensity was achieved by increasing both the number of acoustic cycles, *i.e.*, the duty cycle, and peak-negative acoustic pressure, which makes it impossible to correlate the effects specifically to an increase in either MI or duty cycle. Due to thermal and design limitations in the experimental setup, it was not possible to use a single MI value or duty cycle to achieve the given range of acoustic intensities. Further work should be performed to determine which of the two parameters is more critical. Nevertheless, taking into account that microbubble stability is very low after 10–20 continuous ultrasound cycles, we can conjecture that the MI is the dominant factor and a similar response could be observed at clinically relevant acoustic intensities.

Whilst the results in this study signify that each cell type may respond differently to the same treatment conditions, it is important to note that this work was performed in an *in vitro* configuration that does not accurately mimic the human physiology. Specifically, this experimental configuration used hard plastics that results in acoustic aberrations, there was no flow or temperature and gas saturation regulation, the treatment fluids had a different viscosity to blood, and they were performed in a large open chamber instead of vessel mimicking setup. To validate the results, these experiments should be repeated in a more physiologically relevant model. It should also be noted that even though ultrasound enhanced therapies has been suggested for leukemia [46], the main focus is on solid tumors and the repeated experiments should be performed using cell types constituting solid tumors.

5. Conclusions

Our results show that the treatment with ultrasound and microbubbles alone affect viability and intracellular signaling in cells, and this may be relevant for the efficacy of sonoporation to enhance cancer therapy. The cancerous MOLM-13 cells were more susceptible to sonoporation when compared to the healthy blood cells. Ultrasound alone at clinical diagnostic conditions had no significant effect on cell permeabilization, cell viability, or intracellular protein phosphorylation. The addition of microbubbles, or surpassing clinical diagnostic intensities resulted in increased permeabilization efficiency, reduced cell viability and a change in phosphorylation status of p38, ERK1/2, CREB, Akt, STAT3, ribosomal protein S6 and eIF2 α in the cancer cells.

Supplementary Materials: The following are available online at <http://www.mdpi.com/1999-4923/11/7/319/s1>. Figure S1: Volume normalisation of cell concentration. Figure S2: (a) Percentage calcein-positive cells by increasing concentration of SonazoidTM (b) Calcein uptake (fold change of mean fluorescence intensity) of cells by increasing concentration of SonazoidTM. Figure S3: Optimisation of incubation time post treatment ($n = 1$). Increasing the incubation time results in minor increases in the number of calcein positive cells. Figure S4: Sample processing for phospho-flow cytometry. After sonoporation cells were fixed and permeabilised, barcoded, stained with phosphorylation specific antibodies and analysed by flow cytometry. Barcoding of cells allows for reduced analytical variation. Samples harvested after 5 min, 30 min and 2 h after sonoporation at low medium and high ultrasound intensity were barcoded and pooled in to one sample per timepoint. All treated samples were normalized to untreated cells in the same barcode. Pooled samples were divided in tubes for antibody staining with panels consisting of 2 phosphospecific antibodies conjugated to respectively Alexa 488 and Alexa 647. Figure S5: Gating strategy of flow cytometric data. After identification of the populations the median fluorescence intensity of each sample of cells treated with ultrasound \pm microbubbles was compared to the median fluorescence intensity of the untreated cells. Figure S6: Change in phosphorylation status in response to positive controls

(A23187 + PMA), represented as arcinhratio normalised to untreated cells. Some variation in response is observed between peripheral blood mononuclear cells (PBMC) from 3 different donors. PBMCs exhibit a stronger response to this stimuli compared to cell line MOLM-13. Table S1: Phospho-proteins investigated using flow cytometry. Table S2: The effect of increasing ultrasound intensity on uptake of calcein and viability (Ultrasound treatment vs untreated sample). Table S3: The effect of adding microbubbles on uptake of calcein and viability (Treatment without microbubbles vs treatment with microbubbles). Table S4: The effect of using different bubbles on calcein uptake (SonoVue® vs Sonazoid™). Table S5: The different response in different cell types on calcein uptake (MOLM-13 vs PBMCs). Table S6: The effect of increasing ultrasound intensity and microbubbles on protein phosphorylation (Ultrasound treatment vs untreated sample). Table S7: The effect of increasing ultrasound intensity protein phosphorylation (Ultrasound treatment X vs Ultrasound treatment Y).

Author Contributions: The experiments were designed by R.H., B.T.G., S.K. and E.M.; R.H., A.L., S.M.S. and S.K. performed the experimental work; R.H. and S.-E.G. performed flow cytometry data analysis; R.H. prepared the figures; R.H., A.L. and S.K. prepared the manuscript; all authors reviewed the manuscript; E.M. and S.K. provided the equipment and funding for the experiments.

Funding: This study was funded by the Western Health Board of Norway (Grant numbers 911779, 911182 and 912035), by the Norwegian Cancer Society (6833652, 182735) and by the Norwegian Research Council (SonoCURE grant no. 250317). This work was supported in part by National Institutes of Health grant R01CA199646.

Acknowledgments: We want to thank Brith Bergum at the Core facility for flow cytometry at the University of Bergen for technical assistance and valuable discussions on flow cytometry. We also want to thank Elisa Thodesen Murvold for her technical assistance.

Conflicts of Interest: The authors declare no conflict of interest. Spiros Kotopoulos is currently a full time employee of Phoenix Solutions AS. Phoenix Solutions AS did not participate in any section of this article but provided Sonazoid® as a generous gift.

References

1. Escoffre, J.M.; Bouakaz, A. *Therapeutic Ultrasound*; Springer International Publishing: Cham, Switzerland, 2016.
2. Qin, J.; Wang, T.Y.; Willmann, J.K. Sonoporation: Applications for Cancer Therapy. *Adv. Exp. Med. Biol.* **2016**, *880*, 263–291. [[CrossRef](#)] [[PubMed](#)]
3. Kotopoulos, S.; Delalande, A.; Popa, M.; Mamaeva, V.; Dimcevski, G.; Gilja, O.H.; Postema, M.; Gjertsen, B.T.; McCormack, E. Sonoporation-enhanced chemotherapy significantly reduces primary tumour burden in an orthotopic pancreatic cancer xenograft. *Mol. Imaging Biol.* **2014**, *16*, 53–62. [[CrossRef](#)] [[PubMed](#)]
4. Kotopoulos, S.; Stigen, E.; Popa, M.; Safont, M.M.; Healey, A.; Kvåle, S.; Sontum, P.; Gjertsen, B.T.; Gilja, O.H.; McCormack, E. Sonoporation with Acoustic Cluster Therapy (ACT®) induces transient tumour volume reduction in a subcutaneous xenograft model of pancreatic ductal adenocarcinoma. *J. Control. Release* **2017**, *245*, 70–80. [[CrossRef](#)] [[PubMed](#)]
5. Escoffre, J.M.; Novell, A.; Serrière, S.; LeComte, T.; Bouakaz, A. Irinotecan Delivery by Microbubble-Assisted Ultrasound: In Vitro Validation and a Pilot Preclinical Study. *Mol. Pharm.* **2013**, *10*, 2667–2675. [[CrossRef](#)] [[PubMed](#)]
6. Matsuo, M.; Yamaguchi, K.; Feril, L.B.; Endo, H.; Ogawa, K.; Tachibana, K.; Nakayama, J. Synergistic inhibition of malignant melanoma proliferation by melphalan combined with ultrasound and microbubbles. *Ultrason. Sonochem.* **2011**, *18*, 1218–1224. [[CrossRef](#)] [[PubMed](#)]
7. Dimcevski, G.; Kotopoulos, S.; Bjånes, T.; Hoem, D.; Schjøtt, J.; Gjertsen, B.T.; Biermann, M.; Molven, A.; Sorbye, H.; McCormack, E.; et al. A human clinical trial using ultrasound and microbubbles to enhance gemcitabine treatment of inoperable pancreatic cancer. *J. Control. Release* **2016**, *243*, 172–181. [[CrossRef](#)] [[PubMed](#)]
8. Targeted Delivery of Chemotherapy with Ultrasound and Microbubbles. Available online: <https://ClinicalTrials.gov/show/NCT03458975> (accessed on 29 March 2018).
9. Ultrasound-enhanced Delivery of Chemotherapy to Patients with Liver Metastasis from Breast- and Colorectal Cancer. Available online: <https://ClinicalTrials.gov/show/NCT03477019> (accessed on 14 November 2018).
10. KVUS at Neoadjuvant CTx of Breast Cancer. Available online: <https://ClinicalTrials.gov/show/NCT03385200> (accessed on 28 December 2017).
11. Postema, M.; Spiros, K.; Anthony, D.; Odd, H.G. Sonoporation: Why Microbubbles Create Pores. *Ultraschall Med.* **2012**, *11*, 97–98.
12. Chen, X.; Wan, J.M.; Yu, A.C. Sonoporation as a Cellular Stress: Induction of Morphological Repression and Developmental Delays. *Ultrasound Med. Biol.* **2013**, *39*, 1075–1086. [[CrossRef](#)]

13. Whitney, N.P.; Lamb, A.C.; Louw, T.M.; Subramanian, A. Integrin-Mediated Mechanotransduction Pathway of Low-Intensity Continuous Ultrasound in Human Chondrocytes. *Ultrasound Med. Biol.* **2012**, *38*, 1734–1743. [[CrossRef](#)]
14. Sato, M.; Nagata, K.; Kuroda, S.; Horiuchi, S.; Nakamura, T.; Karima, M.; Inubushi, T.; Tanaka, E. Low-Intensity Pulsed Ultrasound Activates Integrin-Mediated Mechanotransduction Pathway in Synovial Cells. *Ann. Biomed. Eng.* **2014**, *42*, 2156–2163. [[CrossRef](#)]
15. Takeuchi, R.; Ryo, A.; Komitsu, N.; Mikuni-Takagaki, Y.; Fukui, A.; Takagi, Y.; Shiraishi, T.; Morishita, S.; Yamazaki, Y.; Kumagai, K.; et al. Low-intensity pulsed ultrasound activates the phosphatidylinositol 3 kinase/Akt pathway and stimulates the growth of chondrocytes in three-dimensional cultures: A basic science study. *Arthritis Res. Ther.* **2008**, *10*, R77. [[CrossRef](#)] [[PubMed](#)]
16. Huang, T.F.; Tang, C.H.; Yang, R.S.; Huang, T.H.; Lu, D.Y.; Chuang, W.J.; Fu, W.M. Ultrasound Stimulates Cyclooxygenase-2 Expression and Increases Bone Formation through Integrin, Focal Adhesion Kinase, Phosphatidylinositol 3-Kinase, and Akt Pathway in Osteoblasts. *Mol. Pharmacol.* **2006**, *69*, 2047–2057. [[CrossRef](#)]
17. Kotopoulos, S.; Yddal, T.; Cochran, S.; Gilja, O.H.; Postema, M. Open-source, high-throughput ultrasound treatment chamber. *Biomed. Tech. Eng.* **2015**, *60*, 77–87. [[CrossRef](#)]
18. Ter Haar, G. Safety and bio-effects of ultrasound contrast agents. *Med. Biol. Eng. Comput.* **2009**, *47*, 893–900. [[CrossRef](#)] [[PubMed](#)]
19. Zeghimi, A.; Escoffre, J.M.; Bouakaz, A. Role of endocytosis in sonoporation-mediated membrane permeabilization and uptake of small molecules: A electron microscopy study. *Phys. Biol.* **2015**, *12*, 066007. [[CrossRef](#)] [[PubMed](#)]
20. Schindelin, J.; Arganda-Carreras, I.; Frise, E.; Kaynig, V.; Longair, M.; Pietzsch, T.; Preibisch, S.; Rueden, C.; Saalfeld, S.; Schmid, B.; et al. Fiji: An open-source platform for biological-image analysis. *Nat. Methods* **2012**, *9*, 676–682. [[CrossRef](#)] [[PubMed](#)]
21. Krutzik, P.O.; Nolan, G.P. Intracellular phospho-protein staining techniques for flow cytometry: Monitoring single cell signaling events. *Cytometry* **2003**, *55*, 61–70. [[CrossRef](#)] [[PubMed](#)]
22. Sulen, A.; Gullaksen, S.E.; Bader, L.; McClymont, D.W.; Skavland, J.; Gavasso, S.; Gjertsen, B.T. Signaling effects of sodium hydrosulfide in healthy donor peripheral blood mononuclear cells. *Pharmacol. Res.* **2016**, *113*, 216–227. [[CrossRef](#)]
23. Krutzik, P.; Nolan, G.P. Fluorescent cell barcoding in flow cytometry allows high-throughput drug screening and signaling profiling. *Nat. Methods* **2006**, *3*, 361–368. [[CrossRef](#)]
24. Tyagi, R.; Shahani, N.; Gorgen, L.; Ferretti, M.; Pryor, W.; Chen, P.Y.; Swarnkar, S.; Worley, P.F.; Karbstein, K.; Snyder, S.H.; et al. Rheb Inhibits Protein Synthesis by Activating the PERK-eIF2 α Signaling Cascade. *Cell Rep.* **2015**, *10*, 684–693. [[CrossRef](#)]
25. Lentacker, I.; De Cock, I.; Deckers, R.; De Smedt, S.; Moonen, C. Understanding ultrasound induced sonoporation: Definitions and underlying mechanisms. *Adv. Drug Deliv. Rev.* **2014**, *72*, 49–64. [[CrossRef](#)] [[PubMed](#)]
26. Qin, P.; Han, T.; Yu, A.C.; Xu, L. Mechanistic understanding the bioeffects of ultrasound-driven microbubbles to enhance macromolecule delivery. *J. Control. Release* **2018**, *272*, 169–181. [[CrossRef](#)] [[PubMed](#)]
27. Nguyen, D.X.; Guzmán, H.R.; Khan, S.; Prausnitz, M.R. Ultrasound-mediated disruption of cell membranes. I. Quantification of molecular uptake and cell viability. *J. Acoust. Soc. Am.* **2001**, *110*, 588–596.
28. Guzman, H.R.; Nguyen, D.X.; Khan, S.; Prausnitz, M.R. Ultrasound-mediated disruption of cell membranes. II. Heterogeneous effects on cells. *J. Acoust. Soc. Am.* **2001**, *110*, 597–606. [[CrossRef](#)] [[PubMed](#)]
29. Guzmán, H.R.; McNamara, A.J.; Nguyen, D.X.; Prausnitz, M.R. Bioeffects caused by changes in acoustic cavitation bubble density and cell concentration: A unified explanation based on cell-to-bubble ratio and blast radius. *Ultrasound Med. Biol.* **2003**, *29*, 1211–1222. [[CrossRef](#)]
30. Lammertink, B.H.; Bos, C.; Van Der Wurff-Jacobs, K.M.; Storm, G.; Moonen, C.T.; Deckers, R. Increase of intracellular cisplatin levels and radiosensitization by ultrasound in combination with microbubbles. *J. Control. Release* **2016**, *238*, 157–165. [[CrossRef](#)] [[PubMed](#)]
31. Karshafian, R.; Bevan, P.D.; Williams, R.; Samac, S.; Burns, P.N. Sonoporation by Ultrasound-Activated Microbubble Contrast Agents: Effect of Acoustic Exposure Parameters on Cell Membrane Permeability and Cell Viability. *Ultrasound Med. Biol.* **2009**, *35*, 847–860. [[CrossRef](#)] [[PubMed](#)]

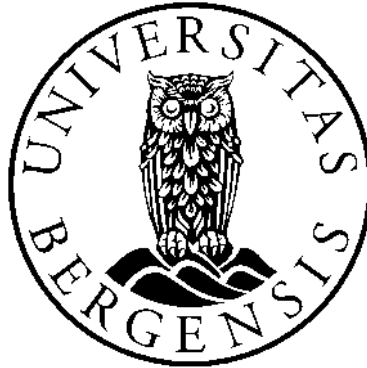
32. Kinoshita, M.; Hynynen, K. Key Factors That Affect Sonoporation Efficiency in in vitro Settings; The Importance of Standing Wave in Sonoporation. *Biochem. Biophys. Res. Commun.* **2007**, *359*, 860–865. [[CrossRef](#)] [[PubMed](#)]
33. Zhong, W.; Chen, X.; Jiang, P.; Wan, J.M.; Qin, P.; Yu, A.C. Induction of Endoplasmic Reticulum Stress by Sonoporation: Linkage to Mitochondria-Mediated Apoptosis Initiation. *Ultrasound Med. Biol.* **2013**, *39*, 2382–2392. [[CrossRef](#)]
34. Lejbkowitz, F.; Salzberg, S. Distinct sensitivity of normal and malignant cells to ultrasound in vitro. *Environ. Health Perspect.* **1997**, *105*, 1575–1578. [[CrossRef](#)]
35. Trendowski, M.; Wong, V.; Zoino, J.N.; Christen, T.D.; Gadeberg, L.; Sansky, M.; Fondy, T.P. Preferential enlargement of leukemia cells using cytoskeletal-directed agents and cell cycle growth control parameters to induce sensitivity to low frequency ultrasound. *Cancer Lett.* **2015**, *360*, 160–170. [[CrossRef](#)] [[PubMed](#)]
36. Sontum, P.C. Physicochemical Characteristics of Sonazoid™, A New Contrast Agent for Ultrasound Imaging. *Ultrasound Med. Biol.* **2008**, *34*, 824–833. [[CrossRef](#)] [[PubMed](#)]
37. Schneider, M. Characteristics of SonoVue (TM). *Echocardiography* **1999**, *16*, 743–746. [[CrossRef](#)] [[PubMed](#)]
38. Cuenda, A.; Rousseau, S. p38 MAP-Kinases pathway regulation, function and role in human diseases. *Biochim. Biophys. Acta* **2007**, *1773*, 1358–1375. [[CrossRef](#)] [[PubMed](#)]
39. Chambard, J.C.; Lefloch, R.; Pouysségur, J.; Lenormand, P. ERK implication in cell cycle regulation. *Biochim. Biophys. Acta* **2007**, *1773*, 1299–1310. [[CrossRef](#)] [[PubMed](#)]
40. Song, G.; Ouyang, G.; Bao, S. The activation of Akt/PKB signaling pathway and cell survival. *J. Cell. Mol. Med.* **2005**, *9*, 59–71. [[CrossRef](#)] [[PubMed](#)]
41. Tkach, M.; Rosemblyt, C.; A Rivas, M.; Proietti, C.J.; Flaqué, M.C.D.; Mercogliano, M.F.; Beguelin, W.; Maronna, E.; Guzmán, P.; Gercovich, F.G.; et al. p42/p44 MAPK-mediated Stat3Ser727 phosphorylation is required for progestin-induced full activation of Stat3 and breast cancer growth. *Endocr. Relat. Cancer* **2013**, *20*, 197–212. [[CrossRef](#)]
42. Sakaguchi, M.; Oka, M.; Iwasaki, T.; Fukami, Y.; Nishigori, C. Role and Regulation of STAT3 Phosphorylation at Ser727 in Melanocytes and Melanoma Cells. *J. Investig. Dermatol.* **2012**, *132*, 1877–1885. [[CrossRef](#)]
43. Naqvi, S.; Martin, K.J.; Arthur, J.S.C. CREB phosphorylation at Ser133 regulates transcription via distinct mechanisms downstream of cAMP and MAPK signalling. *Biochem. J.* **2014**, *458*, 469–479. [[CrossRef](#)]
44. Roux, P.P.; Shahbazian, D.; Vu, H.; Holz, M.K.; Cohen, M.S.; Taunton, J.; Sonenberg, N.; Blenis, J. RAS/ERK Signaling Promotes Site-specific Ribosomal Protein S6 Phosphorylation via RSK and Stimulates Cap-dependent Translation. *J. Biol. Chem.* **2007**, *282*, 14056–14064. [[CrossRef](#)]
45. Yu, H.; Xu, L. Cell experimental studies on sonoporation: State of the art and remaining problems. *J. Control. Release* **2014**, *174*, 151–160. [[CrossRef](#)] [[PubMed](#)]
46. Trendowski, M. Using the Promise of Sonodynamic Therapy in the Clinical Setting against Disseminated Cancers. *Chemother. Res. Prat.* **2015**, *2015*, 1–16. [[CrossRef](#)] [[PubMed](#)]



**Errata for
Molecular mechanisms of sonoporation in cancer
therapy**

Optimization of sonoporation parameters and investigations of intracellular
signalling

Ragnhild Hauge



Thesis for the degree philosophiae doctor (PhD)
at the University of Bergen

(date and sign. of candidate)

(date and sign. of faculty)

Errata

- p. 0 “Haguse” is corrected to “Haugse”
- p. 7 and p. 46 “Photonmultiplier” is corrected to “Photomultiplier”
- p. 7 DC = Duty Cycle is added to the list of abbreviations
- p. 23 “The overall intensity limit is $I_{SPTA} = 720 \text{ mW/cm}^2$ ” is corrected to “The overall intensity limit for diagnostic applications is $I_{SPTA} = 720 \text{ mW/cm}^2$ ”
- p. 23 “...continuous US is not suitable for use in humans because of energy accumulation, which leads to the overheating and destruction of tissue” is corrected to “...continuous US may not be suitable for use in humans at higher acoustic amplitudes because of energy accumulation and deposition, which may cause tissue damage”
- p. 26 Luamson is corrected to Lumason
- p. 26 “... less solubility and lower diffusion...” is corrected to “... less solubility in blood and lower diffusion...”
- p. 28 “Bubble liposome” is corrected to “echogenic “bubble liposomes” ”.
- p. 32 “actual tissue” is corrected to “living tissue”
- p. 38 “first published in [179]” is corrected to “CC BY 4.0 (Paper 1)” in figure legend of Figure 4.
- p. 45 Tryphan Blue is corrected to Trypan Blue
- p. 67 Eventhough is corrected to Even though



Graphic design: Communication Division, UIB / Print: Skjipes Kommunikasjon AS



uib.no

ISBN: 9788230856123 (print)
9788230865842 (PDF)